

Pathophysiological Mechanisms of Neuropathic and Cancer Pain

Pathofysiologische Mechanismen van Neuropathische Pijn en Kankerpijn

Proefschrift

ter verkrijging van de graad van doctor aan de

Erasmus Universiteit Rotterdam

op gezag van de

rector magnificus

Prof.Dr. R.C.M.E. Engels

en volgens besluit van het College voor Promoties.

De openbare verdediging zal plaatsvinden op

woensdag 21 oktober 2020 om 13:30 uur

door

Malik Bechakra

geboren te Metz (Frankrijk)

Promotiecommissie:

Promotoren:

Prof. Dr. P. A. van Doorn

Prof. Dr. C. I. de Zeeuw

Overige leden:

Dr. J. C. Holstege

Prof. Dr. C. G. Faber

Prof. Dr. F. J. P. M. Huygen

Copromotor:

Dr. J. L. M. Jongen

Pour Mylene,

Table of contents

CHAPTER I

General introduction and outline of the thesis 9

SECTION 1 Central Pain and Itch processing

CHAPTER II

Spinal autofluorescent flavoprotein imaging in a rat model of nerve injury-induced pain and the effect of spinal cord stimulation . . . 27

CHAPTER III

Pruritus in anti-DPPX encephalitis 41

SECTION 2 Cutaneous innervation, behavioral changes and pain quality in

experimental animals and humans with neuropathic pain

CHAPTER IV

The reduction of intraepidermal P2X3 nerve fiber density correlates with behavioral hyperalgesia in a rat model of nerve injury induced pain 47

CHAPTER V

Clinical, electrophysiological, and cutaneous innervation changes in patients with bortezomib-induced peripheral neuropathy reveal insight into mechanisms of neuropathic pain 67

CHAPTER VI

Pain-related changes in cutaneous innervation of patients suffering from
bortezomib-induced, diabetic or chronic idiopathic axonal
polyneuropathy 87

SECTION 3 The efficacy of opioids in cancer pain patients

CHAPTER VII

Opioid responsiveness of nociceptive versus mixed pain in
clinical cancer patients 103

CHAPTER VIII

Summary, discussion and future perspectives 117

APPENDICES

General summary 125
Nederlandse samenvatting 126
Reference list 127
Portfolio 137
List of publications 138
Acknowledgements 139
Curriculum vitae 141

CHAPTER I

General introduction and outline of the thesis

1. Organization of the somatosensory system

The somatosensory system signals changes in the external environment through touch and temperature (exteroception), tissue damage (nociception), limb position (proprioception) and the physiological condition of the entire body (interoception). The information processed by the somatosensory system relays along specific anatomical pathways depending on the information carried. The posterior column-medial lemniscal pathway carries discriminative touch and proprioceptive information from the body, and the principal sensory trigeminal pathway carries this information from the face. The spinothalamic pathways carries nociceptive and temperature information from the body, and the spinal trigeminal pathway carries this information from the face (Figure 1).

There are two classes of primary afferent fibers that detect nociceptive and thermal input: peptidergic and non-peptidergic nerve fibers. These two classes of fibers target specific neurons in the spinal dorsal horn (1), are modality-specific (2) and supposedly may each convey specific information about pain along labeled lines to the spinal cord and brain (3-6). Peptidergic nerve fibers can be labeled by CGRP-ir, substance P-ir, but also contain the TrkA receptor for Nerve Growth Factor and the TRPV1 receptor for capsaicin. Non-peptidergic nerve fibers can be labeled with P2X3-ir, Isolectin B4, Mrgprd-ir and contain the RET receptor for glial cell line-derived neurotrophic factor (GDNF) (7). While these two classes of neurons are for the greatest part mutually exclusive, there is some overlap depending on the markers used to label them (5, 8). Thus, peptidergic and non-peptidergic nerve fibers may be considered complementary, because they serve different functions and are more or less mutually exclusive.

Pain is a vital function of the nervous system to protect the body from injury. Melzack and Wall (9) hypothesized that before this information is transmitted to the brain, nociceptive stimuli encounter “nerve gates” that control whether these signals are allowed to pass through to the brain. In some instances, nociceptive signals are passed along more readily and pain is experienced more intensely, i.e. pain is facilitated (10). In other instances, these signals are attenuated or even prevented from reaching the brain, i.e. pain is inhibited.

Furthermore, acute pain and chronic pain have distinct underlying mechanisms: acute pain serves as a warning signal and as such is a physiological reaction of the

normal nervous system, whereas chronic pain may be considered a maladaptive response of the nervous system (11). The underlying mechanisms leading to chronic pain and mechanisms of pain inhibition will be discussed later in the introduction.

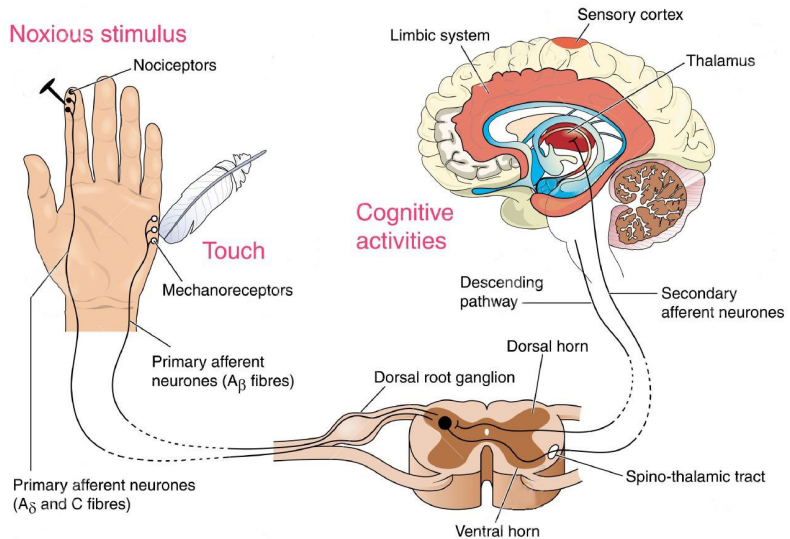


Figure 1: Nociceptive and non-nociceptive stimuli are transmitted through specific classes of nerve fibers to the brain where the sensory information is processed by specific structures, such as the thalamus, the limbic system and the sensory cortex leading to the perception and interpretation of the context of sensory stimuli. (copyright permission granted)

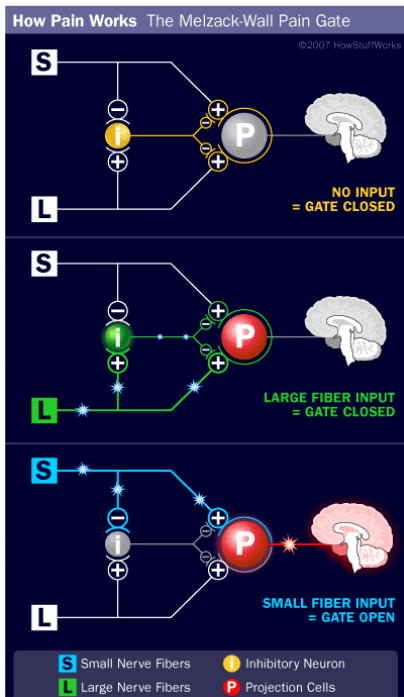


Figure 2: A gating mechanism exists within the dorsal horn of the spinal cord. Small diameter nerve fibers (C and Adelta fibers) and large diameter nerve fibers (Aalpha and Abeta fibers) synapse on projection cells (P), which ascend along the spinothalamic tract to the brain, and on inhibitory interneurons (I) within the dorsal horn. The “gate control theory of pain proposed by Ronald Melzack and Patrick Wall” explains why rubbing of the skin may decrease pain sensation (9) (copyright permission granted).

2. The epidemiology, pathology and pathophysiology of neuropathic and cancer pain

Neuropathic pain is defined as a direct consequence of a lesion or a disease affecting the somatosensory system (12, 13), which may involve the peripheral or the central nervous system. Lesions of the peripheral nervous system may be caused by trauma such as a surgical transection, malignant invasion and metabolic/toxic factors causing nerve fiber degeneration, the latter causing (painful) polyneuropathy.

Cancer pain causes activation of many of the same adaptive pathways as neuropathic pain, since it is also a kind of chronic pain. Cancer pain

may have a nociceptive component mediated by tissue damage and the associated inflammation, as well as a neuropathic component caused by compression or destruction of nerves. Cancer patients may also experience purely neuropathic pain that is usually treatment related, like chemotherapy-induced peripheral neuropathies and post-radiation plexopathies.

a. The epidemiology and pathology of neuropathic pain

Lesions of the nervous system causing neuropathic pain always involve nociceptive pathways. Once neuropathic pain appears, the syndrome usually persists for an extended period of time (i.e. months, years) and can even progress if the damage to the nervous system remains. Neuropathic pain of various origins is very common with an estimated prevalence of 5-8% in the general population, based upon telephone interviews or mailed questionnaires within the general population (14). For a majority of patients, acute neural damage does not progress to chronic neuropathic pain. However, some diseases are associated with a higher than average prevalence of neuropathic pain. For instance, a clinical study with five years follow-up showed that 41% of patients with spinal cord injury had neuropathic pain at the level of the injury (15). The incidence of postherpetic neuralgia (PHN) three months after rash onset in patients affected by herpes zoster ranges from 27-50% (16, 17). A prevalence of painful diabetic peripheral neuropathy (PDN) was found to be 40-60% in patients with type 1 or type 2 diabetes (11, 18, 19).

b. The epidemiology and pathology of cancer pain

Pain (caused by the cancer itself as well as treatment-induced cancer pain) is one of the most serious and feared symptoms in cancer patients, ranging from 25% to 85% depending on the stage of the disease, i.e. early versus advanced cancer. (18)

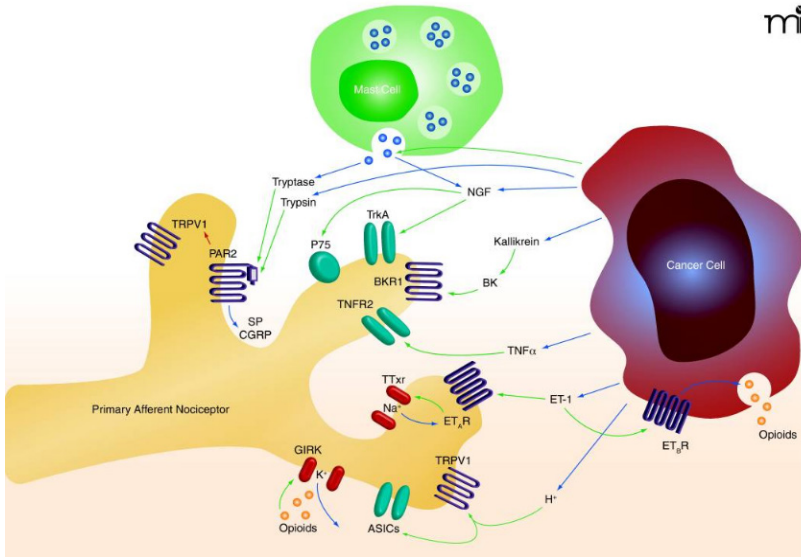


Figure 3: Cancer cells and immune cells release mediators into the cancer microenvironment. Mediators such as $\text{TNF}\alpha$, NGF, trypsin and opioids may directly or indirectly stimulate specific receptors on primary afferent nociceptors (copyright permission granted).

c. Peripheral and central sensitization in neuropathic and cancer pain

Peripheral sensitization is described by the International Association for the Study of Pain (IASP) as an “increased responsiveness and a reduced threshold of peripheral nociceptive neurons to stimulation within their receptive fields.” (20) This occurs after prolonged exposure of nociceptors terminals to noxious stimuli, such as physical stimuli, chemicals and inflammatory mediators. Peripheral sensitization is always localized to the site of the injury (21).

The IASP describes central sensitization as an “increased responsiveness of nociceptive neurons in the central nervous system to their normal or subthreshold afferent input” (22) (23). Two specific mechanisms of central sensitization need to be mentioned here. Following ongoing inflammation, the so-called “wind-up” phenomenon occurs, which is caused by continuous nociceptor

excitation that induces a hyperexcitability response from spinal dorsal horn neurons which bear the N-methyl-D-aspartate (NMDA) receptor and that can last for minutes up to an hour. (24). Another mechanism of central sensitization is long-term potentiation (LTP). LTP is an even longer lasting phenomenon than wind-up, in which C-fiber input produces hours of hyperexcitability that persists even after the input has come to an end. (25). Long-term potentiation of the nociceptive system may occur both in the spinal cord and brain.

Central sensitization mechanisms have been studied at the cellular level *in vitro*, in *ex-vivo* dorsal root-spinal cord experiments, using *in vivo* electrophysiology and finally using functional imaging, mostly fMRI in humans. What is not known is the exact spatio-temporal cascade of events that take place in the superficial spinal dorsal horn in neuropathic pain. We have previously used autofluorescent flavoprotein imaging (AFI), which has a much higher spatial and temporal resolution than any of the aforementioned techniques, to study spinal central sensitization mechanisms induced by capsaicin-induced hyperalgesia, a form of nociceptive pain (26). What is not known is the exact spatio-temporal cascade of events that take place in the superficial spinal dorsal horn in neuropathic pain.

Although central mechanisms such as wind-up and long-term potentiation may explain decreased thresholds and evoked pain, patients mostly complain about pain manifested without an attributable stimulus, *i.e.* spontaneous pain (27). Spontaneous pain appears as a result of ectopic action potential generation in primary sensory neurons, *i.e.* peripheral sensitization (28). After nerve injury, neuronal intrinsic excitability or inflammation may increase resulting in spontaneous pain (29).

d. Pain inhibition

The first pain modulatory mechanism called the “gate control theory” (Figure 2) was proposed by Melzack and Wall in 1962 (30). The idea behind the gate control theory is that non-painful input closes the gates to painful input, which results in a blockade of painful stimuli from entering the CNS, *i.e.*, non-noxious input suppresses pain. More specifically, the gate control theory implies that non-noxious stimulation will produce presynaptic inhibition of dorsal root nociceptor fibers that synapse on nociceptive spinal projection

neurons and that this presynaptic inhibition will block incoming noxious information from reaching the CNS (21). Non-noxious input thus suppresses pain or “closes the gate” to noxious input. The gate control theory was the rationale behind the use of spinal cord stimulation (SCS) for pain relief (31). However, there are many unresolved questions regarding the exact mode and location of action of spinal cord stimulation in neuropathic pain conditions (31).

Apart from the above mentioned propriospinal pain modulatory mechanism, nociceptive input may also be modulated by supraspinal inhibitory mechanisms. These involve amongst others the release of enkephalin from periaqueductal grey (PAG) neurons in the midbrain, acting upon raphe nuclei in the rostral ventromedial medulla (RVM), from where 5-hydroxytryptophan/serotonin containing descending pathways project to the substantia gelatinosa (i.e. lamina II) of the spinal dorsal horn. (32)

3. Neuropathic pain and cancer pain models

Most experimental models of neuropathic pain rely on nerve (usually sciatic) injuries and metabolic or toxic polyneuropathies. In these models, various forms of hyperalgesia to noxious thermal and mechanical stimuli are generally used as outcome measures.

a. Peripheral nerve injury models

The four most commonly used peripheral nerve injury models are the chronic constriction injury (CCI) of the sciatic nerve (33), the partial sciatic nerve ligation model (PNL) (34), the spared nerve-injury model (35) and the spinal nerve ligation model (SNL) (36).

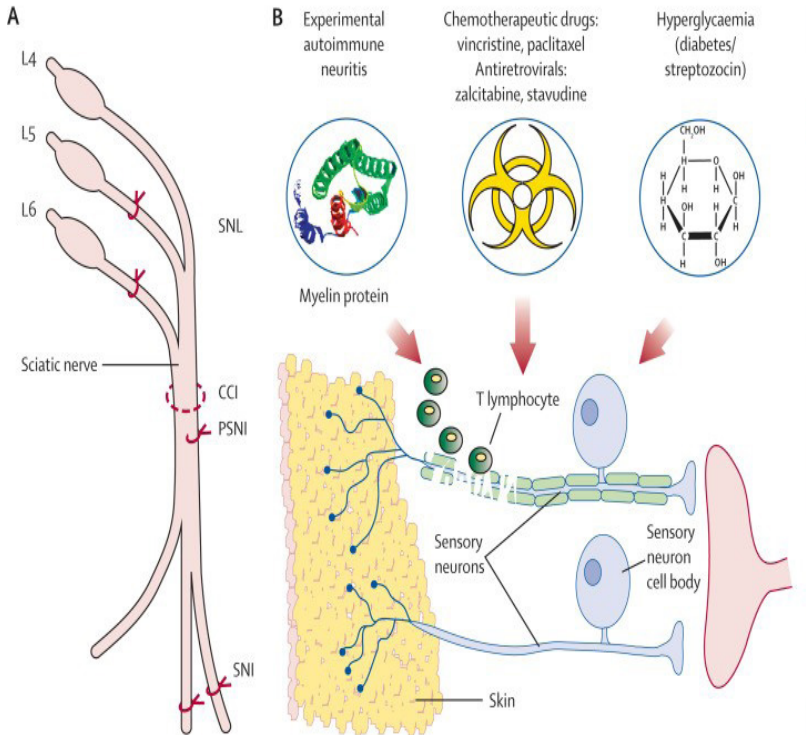
Bennet and Xie (37) demonstrated that a loose ligature of the sciatic nerve (CCI) can induce pain-like behaviors similar to those observed in humans with neuropathic pain. It was shown that an immune reaction to the ligature induces nerve edema, which consequently led to nerve compression and axotomy. The PNL model of Seltzer et al. consists of a tight ligation encompassing 30-50% of the sciatic nerve (34). This model is postulated to have fewer inflammatory

effects than the CCI model. The actual number of ligated axons varies from animal to animal, although it was demonstrated that behavioral changes, i.e. hyperalgesia and allodynia, were evenly distributed across the entire surface of the sole of the foot. Finally, the SNL model consists of an injury of the L5 and L6 spinal nerves, which project to the sciatic nerve (36). All of the aforementioned neuropathic pain animal models are characterized by the development of allodynia and hyperalgesia. Animals also develop spontaneous pain-like behavior, but this is much harder to measure than evoked pain (38).

b. Drug-induced neuropathy models

Neuropathic pain is one of the most common dose-limiting complications of chemotherapy-induced peripheral neuropathy (CIPN). Neurotoxic chemotherapies include platinum compounds (like cis-platinum), vinca-alkaloids (like vincristine), taxanes (like paclitaxel and docetaxel), immunomodulatory drugs (like thalidomide) and proteasome inhibitors (like bortezomib). These drugs cause neuropathy via a variety of mechanisms, like DNA damage in the dorsal root ganglion, microtubule inhibition and mitochondrial damage. Bortezomib is a mainstay of therapy for multiple myeloma, frequently complicated by painful neuropathy. It is unknown which subclass of nociceptors (i.e. peptidergic or non-peptidergic nerve fibers) contribute to the various components of neuropathic pain in BiPN, i.e. the sensory-discriminative versus the affective/evaluative component.

The first animal models of CIPN consisted of local, subperineural injections of the drug (39). They demonstrated demyelination and axonal swelling at the injection site. However, these CIPN models were clearly not very representative of human CiPN. Other studies used repeated intraperitoneal administrations to rats to better mimic clinical CiPN, which is usually characterized by dose-dependent, cumulative toxicity. These animal models were characterized by the development of spontaneous pain-like behavior, allodynia and hyperalgesia (40-42). In contrast to the first CIPN animal models that used a single injection of a chemotherapeutic compound, the administration of repetitive intraperitoneal injections led to the development of axonal



swellings, containing swollen and vacuolated mitochondria (43, 44) and reduced epidermal innervation, the latter as a result of Wallerian degeneration.

Figure 4: (A) Peripheral nerve injury models used in rodents, SNL=spinal nerve ligation. CCI=chronic constriction injury. PSNI=partial sciatic nerve injury. SNI=spared nerve injury. (B) Inflammatory, toxic and metabolic models of painful peripheral neuropathy, e.g. systemic administration of the neurotoxic drugs vincristine or paclitaxel (copyright permission granted).

e. Limitations of animal pain models

The main outcome measure in animal models of neuropathic pain usually is any kind of evoked pain, i.e. mechanical or thermal hypersensitivity. However, it is generally known from clinical practice, that neuropathic pain patients mostly complain about spontaneous pain, not evoked pain. As

previously outlined, spontaneous pain is hard to measure in animal models, mainly because animals “don’t talk”. Although attempts have been made to gauge spontaneous neuropathic pain in experimental animals using grimace scales, even then it is impossible to distinguish distinctive neuropathic pain components, like the sensory-discriminative, the affective and the evaluative component of neuropathic pain in experimental animals. It is thought that this is one of the reasons why new analgesic drugs that have been developed in animals are rarely effective in patients with neuropathic pain.

4. Clinical aspects of neuropathic and cancer pain

a. Peripheral versus central neuropathic pain

Depending upon the anatomical side of the nerve injury, neuropathic pain is classified as central (originating from damage to the brain or spinal cord) or peripheral (originating from damage to the peripheral nerve, plexus, or dorsal root ganglion) neuropathic pain. In this thesis, research is mostly focused on peripheral neuropathic pain (chapter 3) (45, 46).

b. A clinical diagnosis of neuropathic pain

i. Medical History

In contrast to “regular” or nociceptive pain (e.g. acute traumatic pain, inflammatory pain or cancer pain), in which peripheral nociceptors are excited by high-intensity or nociceptive stimuli caused by tissue injury, nerve injury-induced pain is caused by structural damage to the (peripheral or central) nociceptive system (12), which results in a decreased threshold for stimuli and sometimes even spontaneous depolarization of nociceptive system neurons, which is perceived as pain. Unlike “normal” or nociceptive pain, patients with neuropathic pain usually use a lot of adjectives to describe their pain, e.g. burning, deep, tingling, drilling, annoying, tiring etc. Some of these adjectives may have a sensory-discriminative connotation, while others have an affective-evaluative connotation. The McGill pain Questionnaire was the first instrument specifically designed to discern these two neuropathic pain

components. This instrument should not be confused with instruments like the douleur neuropathic 4 scale (DN4) (47), the PainDETECT (48) or the Leeds Assessment of Neuropathic Symptoms Scale (LANSS) (49), which were designed as screening instruments for neuropathic pain, to aid non-pain specialist in screening for patients with neuropathic pain (50). The relevance of the McGill Pain Questionnaire was recently highlighted by the hypothesis that sensory-discriminative and affective neuropathic pain components may be conveyed along specific anatomical pathways. Since the MPQ is not practical for clinical use, we suggest that apart from an NRS for neuropathic pain intensity (through which the sensory discriminative component can be quantified), using an NRS to rate the unpleasantness of pain may be an alternative for the affective-evaluative part of the MPQ.

In addition to typical characteristics from the history, neuropathic pain should also have a distribution that is anatomically plausible (like a stocking and glove-like distribution for painful neuropathy, or hemibody pain following a thalamic stroke) and history should suggest a condition that is associated with the development of neuropathic pain (like diabetes or multiple sclerosis) (12)

ii. Clinical examination and ancillary investigations of patients with neuropathic pain

A thorough neurological examination demonstrating negative (like anesthesia or hypesthesia) or positive sensory phenomena (like hyperalgesia or allodynia) in the area innervated by damaged nociceptive pathways may confirm a working hypothesis of neuropathic pain. Two types of positive sensory phenomena can be distinguished. Firstly, allodynia is defined as pain in response to a non-nociceptive stimulus. In cases of mechanical allodynia, even gentle mechanical stimuli such as a slight bending of hairs can evoke severe pain. Secondly, hyperalgesia is defined as a lowered threshold to a nociceptive stimulus. Another characteristic neuropathic pain feature is temporal summation, which is the progressive worsening of pain evoked by slow repetitive stimulation (51).

Quantitative sensory testing (QST) potentially is a valuable addition to the neurological examination, especially since sensory modalities may be quantified

and more precisely monitored over time (52, 53). QST essentially determines the detection and pain thresholds for cold and warm temperatures, and the vibration sensation threshold by stimulating the skin and comparing the results to normative values. More recently, the QST-methodology has been standardized in a clinical study of 1236 patients with neuropathic pain (54). Besides, this study defined 5 specific patterns of gain and loss of mechanical/thermal functions in patients with various neuropathic pain etiologies. This may have therapeutic consequences, since oxcarbazepine seemed to be more effective in patients with an “irritable nociceptor phenotype” as opposed to one of the other QST sensory profiles (55). However, QST still is subjective and besides it is very time consuming.

Nerve conduction studies/electromyography on the other hand is a very objective and reliable method, but it primarily measures A-alpha and A-beta fiber (dys) function and is not very sensitive to pathology of unmyelinated or thinly myelinated nerve fibers, which fibers are most frequently affected in neuropathic pain conditions (6). Laser-evoked potentials and microneurography may circumvent this issue, but these techniques are limited to a few highly specialized centers.

A final, minimally invasive, ancillary investigation used in neuropathic pain patients especially those suspected of small fiber neuropathy, is intra-epidermal nerve fiber quantification in skin biopsies. Skin biopsies from patients with neuropathic pain often show changes in epidermal innervation, although it remains to be elucidated to what extent such changes can be linked to a particular subgroup of nerve fibers and how these changes are correlated with pain intensity/behavioral abnormalities.

c. A clinical diagnosis of cancer pain

Cancer pain may be caused by the cancer itself or by the treatment against cancer. In the former, purely nociceptive pain, e.g. pain from a metastasis to the hip, should be distinguished from mixed nociceptive pain, e.g. a vertebral metastasis with nerve root compression. A diagnosis of purely nociceptive pain and mixed nociceptive-neuropathic pain is again based on a thorough history and neurological examination with the addition of ancillary imaging, using the same grading system as designed for (purely) neuropathic pain (4). It is a

widely held believe that mixed nociceptive-neuropathic pain is opioid resistant, although this is merely based on single-dose or dose- titrating opioid studies in humans (56). Secondly, pain caused by the treatment against cancer mostly concerns purely neuropathic pain, e.g. painful chemotherapy-induced peripheral neuropathies, post-dissection pain and radiation-induced neuropathic pain.

d. A clinical diagnosis of itch

Itch is a sensory experience that is conveyed along primary afferent fibers that also carry nociceptive information, specifically those who respond to chemical stimuli. Itch may be induced by chemical irritants, degranulation of mast cells caused by allergy and skin diseases like eczema and psoriasis. Chronic itch may also be caused by damage to the nerve fibers that convey the itch-signal and is then called neuropathic itch (57). Similar to pain, sensitization mechanisms may occur in itch. Thus, anatomical pathways and clinical manifestations of itch resemble pain in many ways. Like pain, itch is a subjective finding, for which no objective tests exists (58). It is paramount to (try to) establish the underlying condition that causes itch and treat that condition, since symptomatic treatment is often unsatisfactory, with a unfavorable effect-side effect profile of (chronic) anti-histaminic and anti-inflammatory drugs. Severe itch is a cardinal symptom of Morvan's syndrome, a clinical entity associated with anti-DPPX antibodies. It is not known how exactly (the titers of) those antibodies are associated with clinical symptoms and furthermore, whether the itch is centrally or peripherally mediated.

e. Pain management

i. Medical therapy for cancer pain

Cancer pain is an especially severe form of nociceptive pain, for which a treatment strategy was developed in the 1970s, according to the so-called WHO-pain ladder (59). The original WHO-pain ladder consisted of three steps: step 1) paracetamol alone, or the combination of paracetamol with non-steroidal anti-inflammatory drugs (NSAIDs) or cyclo-oxygenase-2 inhibitors (Coxib's),

step 2) opioids for mild to moderate pain, i.e. tramadol, codeine and step 3) opioids for moderate to severe pain, like morphine, oxycodone, fentanyl, hydromorphone and methadone. These opioids appear in two formulas: long-acting opioids and short-acting or rapid-onset opioids. The former are intended to provide round-the-clock analgesia, while the latter are intended to treat bouts of pain that break through a long-acting analgesic regimen (i.e. breakthrough pain). Later on, a fourth step was added to the original WHO-analgesic ladder, including intravenous, subcutaneous, intrathecal and epidural pain medication and invasive treatments like nerve(root) blocks and spinal tract transections.

Strong-acting opioids are the mainstay of treatment for cancer pain patients. Although all currently clinically available opioids act on the mu-opioid receptor, this receptor has multiple subtypes and receptor affinities of morphine, oxycodone, hydromorphone and fentanyl vary greatly and can be expressed as equianalgesic ratios. Although the WHO analgesic ladder typically relates to purely nociceptive cancer pain, in about 1/3 of cancer patients pain is of mixed nociceptive-neuropathic pathology. Although it has been suggested that this “mixed-pain” is more or less resistant to the analgesic effect of opioids, this hypothesis is mainly based on animal studies and single-dose opioid studies in humans but has not been confirmed in clinical practice. In addition to opioids, adjuvant analgesics (see below) may be added in mixed cancer pain patients.

ii. Medical therapy for neuropathic pain

Neuropathic pain is different from nociceptive pain, in that neuropathic pain is not induced by supra-threshold stimulation of nerve terminals, but by a damaged nervous structure with a pathologically decreased threshold for excitation. Neuropathic pain medication is aimed at restoring/stabilizing the membrane potential of nociceptors and enhancing descending and propriospinal pain inhibition. Tricyclic antidepressants, anti-epileptic drugs and serotonergic and noradrenergic reuptake inhibitors have been used for this purpose and all of these have been found superior to placebo, mainly in randomized controlled clinical trials in patients with painful diabetic neuropathy, post-herpetic neuralgia and trigeminal neuralgia (60). Much less clinical evidence is available in patients suffering from other

causes of neuropathic pain, like painful chemotherapy-induced peripheral and chronic idiopathic axonal neuropathy, although it is assumed that the aforementioned drugs may have similar efficacy in these conditions (61).

iii. Spinal cord stimulation

When chronic (neuropathic) pain is refractory to medical therapy, spinal cord stimulation may be an effective second line of treatment. The most common indications include complex regional pain syndrome (CRPS) (62, 63), failed back surgery syndrome (64-66) and painful diabetic neuropathy (67-69). Spinal cord stimulation is based upon the “gate-control theory”, but it’s exact site of action, i.e. spinal or supraspinal or both is not known (70).

5. Scope of the thesis

This thesis is about the central and peripheral mechanisms that contribute to nerve-injury induced pain and itch, pain in cancer patients and the clinical consequences of these mechanisms. Both nerve-injury induced and cancer pain are examples of chronic pain conditions, although each of them is driven by distinct pathology and has distinctive clinical features.

Aim 1 (Section 1) was to study central pain- and itch processing. We used spinal cord AFI in an animal model of nerve injury-induced pain and a custom made mini-neurostimulator to study spatio-temporal changes in spinal metabolic activity in neuropathic pain and how these changes are affected by SCS (Chapter 2). Secondly, we collected consecutive serum and cerebrospinal fluid samples from a single patient with severe (neuropathic) itch and we collected skin biopsies from the dorsal ankle and trunk, to quantify intraepidermal nerve fiber densities to study the association between anti-DPPX antibody titers and clinical symptoms and to study changes in cutaneous innervation to confirm or rule-out a peripheral etiology of (neuropathic) itch (Chapter 3).

Aim 2 (Section 2) was to study cutaneous innervation, behavioral changes and pain quality in experimental animals and humans with neuropathic pain. We used a model of nerve injury-induced pain, we validated measures of

epidermal innervation and we studied changes in epidermal innervation and correlations between epidermal innervation changes of PGP9.5, CGRP and P2X3-ir fibers and two measures of hyperalgesia, to investigate to what extent behavioral signs of hyperalgesia are correlated with peptidergic and non-peptidergic epidermal nerve fibers in rats (Chapter 4). Secondly, we collected clinical, EMG and skin biopsy data from 22 patients with BiPN to describe the demographic, clinical, electrophysiological and pathological characteristics of BiPN in detail and to study correlations between pathological changes in subsets of unmyelinated nerve fibers in skin biopsies and neuropathic pain descriptors (Chapter 5). Finally, as an extension of the BiPN study, we studied the pathology and pain perception among 22 BiPN, 16 PDN and 16 CIAP patients, again correlating measures of cutaneous with neuropathic pain descriptors, to explore the hypothesis that selective degeneration of nociceptors in neuropathic pain syndromes in general can be associated with distinctive pain qualities, by comparing the pathology and pain perception (Chapter 6).

Finally, Aim 3 (Section 3) was to investigate whether clinical cancer patients with nociceptive cancer pain differ in opioid responsiveness from patients with mixed nociceptive-neuropathic cancer pain. Clinical data including pain intensities, morphine-equianalgesic dose and type of pain were collected from 240 clinical cancer pain patients using opioids. Multiple linear regression was used for assessing the associations between the relative change in morphine equivalent dose and type of pain (nociceptive versus mixed pain), using correction for confounding factors (Chapter 7).

Together, these aims should elucidate mechanisms of nerve-injury induced pain and itch, expose the relation between cutaneous innervation changes and the perception of pain, and finally establish opioid sensitivity in nociceptive versus mixed cancer pain patients.

CHAPTER II

Spinal Autofluorescent Flavoprotein Imaging in a Rat Model of Nerve Injury-Induced Pain and the Effect of Spinal Cord Stimulation¹

Joost L. M. Jongen, Helwin Smits, Tiziana Pederzani, Malik Bechakra, Mehdi Hossaini, Sebastiaan K. Koekkoek, Frank J. P. M. Huygen, Chris I. De Zeeuw, Jan C. Holstege, Elbert A. J. Joosten

¹This chapter has been published in PLoS One. 2014; 9(10): e109029.

Abstract

Nerve injury may cause neuropathic pain, which involves hyperexcitability of spinal dorsal horn neurons. The mechanisms of action of spinal cord stimulation (SCS), an established treatment for intractable neuropathic pain, are only partially understood. We used Autofluorescent Flavoprotein Imaging (AFI) to study changes in spinal dorsal horn metabolic activity. In the Seltzer model of nerve-injury induced pain, hypersensitivity was confirmed using the von Frey and hotplate test. 14 Days after nerve-injury, rats were anesthetized, a bipolar electrode was placed around the affected sciatic nerve and the spinal cord was exposed by a laminectomy at T13. AFI recordings were obtained in neuropathic rats and a control group of naïve rats following 10 seconds of electrical stimulation of the sciatic nerve at C-fiber strength, or following non-noxious palpation. Neuropathic rats were then treated with 30 minutes of SCS or sham stimulation and AFI recordings were obtained for up to 60 minutes after cessation of SCS/sham. Although AFI responses to noxious electrical stimulation were similar in neuropathic and naïve rats, only neuropathic rats demonstrated an AFI-response to palpation. Secondly, an immediate, short-lasting, but strong reduction in AFI intensity and area of excitation occurred following SCS, but not following sham stimulation. Our data confirm that AFI can be used to directly visualize changes in spinal metabolic activity following nerve injury and they imply that SCS acts through rapid modulation of nociceptive processing at the spinal level.

Introduction

Flavoproteins are involved in a wide array of biological processes, among which adenosine triphosphate production via the mitochondrial electron transport chain. During this process the flavoprotein moieties of respiratory chain complexes I and II are oxidized, resulting in green fluorescence when illuminated with blue-spectrum light. This oxidation is followed by a reduction when the energy demand of a cell has been met, overall resulting in a bi-phasic fluorescence response. The light phase of flavoprotein autofluorescence may be used as a marker for neuronal (metabolic) activity (Renert, 2007). We and others have demonstrated a linear relationship between the intensity of the neuronal stimulus and flavoprotein autofluorescence (Renert, 2007 ; Jongen, 2010). Since autofluorescent flavoprotein imaging (AFI) is an optical method, it is suitable to monitor activity in superficial areas of the nervous system such as the somatosensory cortex (Shibuki, 2003 ; Murakami, 2004 ; Weber, 2004 ; Komagata, 2011 ; Yamashita, 2012), auditory cortex (Takashita, 2012 ; Kubota, 2008), visual cortex (Thomi, 2009 ; Husson, 2007), cerebellar cortex (Barnes, 2011 ; Wang, 2011) and superficial dorsal horn of the spinal cord (Jongen, 2010). A major advantage is that it enables imaging of large areas at high-resolution in both the spatial (down to 10610 mm) and temporal (up to 100 frames/ second) domain simultaneously. Furthermore, AFI directly represents neuronal metabolic activity, in contrast to intrinsic optical imaging (Sasaki, 2002) or fMRI using the BOLD signal (Jongen, 2012). AFI, however, does not allow imaging of deep structures like the deep dorsal horn of the spinal cord and has a relatively low signal-to-noise ratio (Jongen, 2010). Peripheral nerve injury often induces pain, which is, among others, driven by sensitization mechanisms within the spinal cord (Latremoliere, 2009). These sensitization mechanisms may be accurately monitored using autofluorescent flavoprotein imaging of the superficial spinal dorsal horn, as was shown previously using intraplantar capsaicin injection (Jongen, 2010 ; Latremoliere, 2010). The Seltzer model consists of partial ligation of the proximal part of the sciatic nerve, which generates pain behavior in rats, closely resembling the clinical condition of Complex regional Pain Syndrome (CRPS) type 2 in humans (Seltzer, 1990).

CRPS type 2 in turn has many characteristics of painful neuropathy, including spontaneous and evoked pain (Shir 1991 ; Oaklander, 2006). Therefore, the

Seltzer model may be considered a relevant model of nerve injury induced pain (Doth, 2010). Painful neuropathy and CRPS are frequently refractory to pharmacological treatment and physical therapy. Spinal cord stimulation (SCS) is a generally accepted therapy in patients with CRPS (Kemler, 2000 ; Cruccu, 2007) and recently SCS has yielded promising results in patients with painful diabetic neuropathy (de Vos, 2009 ; Pluijms, 2012). SCS is based on the gate-control theory from the 1960's (Moayed, 2013), although the exact mechanism of action is still only partially clarified (Geurts, 2013). Probably, GABA-ergic interneurons, situated in the substantia gelatinosa, are of major importance in SCS treatment of chronic neuropathic pain (Smits, 2012). It should be stressed, however, that the latter evidence is based on data obtained after dialysis of the spinal dorsal horn (Cui, 1997) or immunohistochemical visualization (Janssen, 2012). Hence, these data present only indirect evidence on the exact spatial and temporal changes of SCS in the spinal superficial dorsal horn. We first set out experiments to study the mechanisms of sensitization in the superficial spinal dorsal horn by applying AFI to the Seltzer model. Subsequently, changes in nociceptive transmission in the superficial dorsal horn of chronic neuropathic rats brought about by SCS were visualized at a high spatial and temporal resolution using the same AFI imaging technology.

Materials and Methods

Animal preparation All animal experimentation conformed to the guidelines laid out in the Guide for the Care and Use of Laboratory Animals (National Academy of Sciences) and was approved by the Institutional Animal Ethics Committee of Erasmus MC Rotterdam (EMCnr. 115-08-26). Recordings were obtained from a total number of 18 young adult male Sprague Dawley rats from Harlan or Charles River, the Netherlands, weighing 250–300 g. Neuropathic pain was induced by partial ligation of the sciatic nerve as described by Seltzer et al (Seltzer, 1990). Recordings from 20 Wistar rats with similar age/weight from previous experiments (Jongen, 2010) were used as controls.

Behavioral tests Behavioral testing took place before the Seltzer operation and at post-operative days 10, 12 and 14. Every time before behavioral testing, rats were habituated to the experimenter (T.P. or M.B.), the room in which

the behavioral experiments took place and the transparent chamber used for von Frey testing, for at least half an hour. Mechanical sensitivity was assessed by testing the withdrawal response to increasing in thickness von Frey filaments (Stoelting Co., Wood Dale, IL). The threshold was set at three out of five withdrawal responses. After testing for mechanical sensitivity, thermal thresholds were assessed by the hotplate test. The surface of the hot plate was heated to a constant temperature of 51°C. Rats were placed on the hot plate (25.4 cm×25.4 cm) (Ugo Basile Srl., Comerio, VA, Italy), which was surrounded by a transparent plexiglas chamber with an open top, and the latency to respond with either a hind paw lick or hind paw flick was measured. Immediately after a response rats were removed from the hotplate. Rats were also removed if they did not respond after 30 seconds, to prevent tissue injury.

Autofluorescent Flavoprotein Imaging in rats with nerve injury After behavioral testing at day 14, rats were anesthetized and surgery and image acquisition for autofluorescent flavoprotein imaging of the spinal cord was performed as previously described (Jongen, 2010), using a high speed 16-bit CCD camera with 512×6512 pixel resolution (Roper Scientific, Evry, France). A silicon cuff containing a bipolar electrode was placed around the left sciatic nerve proximal to the knee, i.e. just distal to the suture from the partial nerve ligation. As a measure of fluorescence, generally DF/F is used. DF/F represents the change in fluorescence intensity of each pixel during registration relative to the mean fluorescence intensity of these pixels in frames preceding electrical stimulation (see also Jongen, 2010). AFI responses were expressed as the maximal DF/F change in fluorescence following stimulation (AFI intensity), or as the area with an AFI intensity above a predefined DF/F level (area of excitation). This predefined DF/F level was always kept constant. Recordings using 2.5 mA, 10 Hz electrical stimulation of the left sciatic nerve lasting 10 seconds were obtained in 13 Sprague Dawley rats that had undergone partial sciatic nerve ligation and compared with recordings from 20 naïve Wistar rats from previous experiments (Jongen, 2010), using the same electrical stimulus. A similar experiment was carried out in rats ($n=5+5$) using a 10 seconds lasting 1 Hz innocuous palpation of the plantar surface of the left hind paw (Jongen, 2010).

Autofluorescent Flavoprotein Imaging in rats with nerve injury undergoing SCS or sham stimulation Following “before treatment” AFI recordings in

neuropathic Sprague Dawley rats (see above), a monopolar stimulation system with a 3.061.060.1 mm platinum-iridium rectangular plate micro cathode was placed in the dorsal epidural space at the T12-T13 vertebral level, while the anode was placed in a subcutaneous pocket on the back, and rats underwent 50 Hz, amplitude 2/3 of motor threshold SCS (n=7) or no electrical stimulation (sham; n=6) for 30 minutes, as previously described (Smits, 2006). Immediately following SCS or sham the micro cathode was removed and AFI responses to left sciatic nerve electrical stimulation (same stimulus as baseline) were recorded at T=0 after SCS or sham and then every 5 minutes for up to an hour. Both the intensity of the AFI response (expressed as DF/F of the light phase) and the area with an AFI intensity above a predefined DF/F level was calculated and expressed as a percentage of DF/F before treatment. At the end of the experiment, rats were euthanized with an overdose of intraperitoneal urethane.

Statistical analysis and presentation of the figures Statistical analyses were performed using GraphPad Prism version 6.0e and SPSS statistics version 21 software. For a comparison of means of behavioral responses, a repeated-measures ANOVA was used. For an overall comparison of means of AFI intensities and areas of excitation between naïve and neuropathic rats and between sides, two-way ANOVAs were used. For a comparison of means of AFI intensities following nonnoxious palpation in naïve and neuropathic rats, an unpaired t-test was used. For comparing the effect of SCS versus sham on AFI intensities and area of excitation, paired t-tests were used, Pearson's correlation coefficients were calculated and a linear regression analysis was performed. The data in the figures are expressed as mean \pm SEM. Figures were composed in Photoshop CS6 software version 13.0.6. Adjustments were made only to brightness and contrast and applied evenly to all panels of a figure.

Results

Following partial ligation of the left sciatic nerve in the thigh, all 18 Sprague Dawley rats used in this study developed mechanical and thermal hypersensitivity characteristic of the Seltzer model (Table S1) (Seltzer, 1990). Repeated-measures ANOVAs (source of variation timepoint) demonstrated that the decrease in von Frey thresholds and hotplate latencies was statistically significant (Fig. 1A; p,

0.01). We then set out to capture AFI responses in these neuropathic Sprague Dawley rats. A typical AFI recording of a 10 s, 2.5 mA, 10 Hz electrical stimulation of the left sciatic nerve showed a steep increase in spinal fluorescence (light phase) immediately after the start of the stimulation, followed by a decrease below baseline (dark phase) (Fig. 2; Movie S1). This pattern of activity is typical of autofluorescent flavoprotein imaging in the brain and spinal cord.

In the rest of this paper we only use the light phase for analysis, since this is the default measure of activity in AFI. Next, we compared mean AFI intensities and areas of excitation following 10 s, 2.5 mA, 10 Hz electrical stimulation of 13 Sprague Dawley rats with partial nerve ligation, with those from 20 naïve Wistar rats from a previous study (Jongen, 2010), that had undergone exactly the same electrical stimulation protocol (Fig. 3; Table S2). The main effects of both type of animal (naïve Wistar versus neuropathic Sprague-Dawley rats) and side (ipsilateral versus contralateral) on AFI intensity and area of excitation were not significantly different, nor were the interactions between type of animal and side on AFI intensity and area of excitation ($p=0.23$; two-way ANOVAs). Since it is known (Latremoliere, 2009 ; Seltzer, 1990) that in neuropathic pain states also innocuous stimuli may elicit nociceptive activity in the superficial dorsal horn, we investigated AFI responses to 10 s, 1 Hz innocuous palpation of the left hind paw. We compared AFI intensities in 5 neuropathic Sprague Dawley rats with those from 5 naïve Wistar rats from our previous study (Fig. 4; Movie S2, Table S3). While we have demonstrated that after innocuous palpation in naïve rats AFI intensity is not different from recordings without stimulation, there was a robust increase in AFI intensity following palpation in neuropathic rats on the ipsilateral side, which was statistically significantly different from naïve rats ($p=0.03$; unpaired t-test). Results on the contralateral side of naïve and neuropathic rats were not statistically significantly different ($p=0.7$; unpaired t-test). Finally, the effect of spinal cord stimulation on AFI responses in neuropathic Sprague Dawley rats was investigated. Prior to stimulation, neuropathic pain behavior was not statistically significantly different between rats that underwent SCS ($n=7$) or sham ($n=6$) stimulation (Fig. 1B and 1C; $p=0.06$; repeatedmeasures ANOVA, source of variation treatment). We then studied relative AFI responses, expressed as a percentage of the “before

treatment” AFI response, in 7 neuropathic rats after 30 minutes 50 Hz spinal cord stimulation, using a platinum cathode at the T12-T13 vertebral level, and in 6 neuropathic rats that underwent sham stimulation, i.e. with cathode placement but without the 50 Hz electrical stimulus (Table S4). In rats with SCS there was a strong and statistically significant reduction in AFI intensity as well as area of activation directly after cessation of SCS on the ipsilateral side (Fig. 5; $p=0.049$ and $p=0.041$ respectively; paired t-test), while in rats that underwent sham stimulation there was no statistically significant reduction ($p=0.8$; paired t-test). In the period from $T=0$ to $T=60$ minutes following cessation of SCS, there was a statistically significant linear increase in AFI intensity on the ipsilateral side in the rats with SCS (slope $0.92\%DF/F \cdot \text{min}^{-1}$; $p=0.021$; Pearson’s correlation coefficient and linear regression analysis), indicating a reducing efficacy of SCS at these later time-points. In the rats with sham stimulation the slope was not statistically significant non-zero (slope $0.19\%DF/F \cdot \text{min}^{-1}$; $p=0.72$; Pearson’s correlation coefficient and linear regression analysis), indicating no treatment effect in the rats that underwent sham stimulation.

Discussion

Nerve injury-induced pain is a complex disorder, which is driven by a multitude of plastic changes, like sensitization of (peripheral) nociceptors (Bennett, 1998 ; Woolf, 2007), increased excitability of spinal cord projection neurons (Schoffnegger, 2008), decreased propriospinal (Hassaini, 2010) and descending (Hossaini, 2012) spinal inhibition, spinal glia activation (Coull, 2005) and changes in the transmission of nociceptive signals in the brainstem and neocortex (Tracey, 2007). In this study we focused on changes following nerve injury in (metabolic) activity in the superficial dorsal horn, a major relay station in the transmission of the nociceptive signal to higher brain centers. Using the Seltzer model of nerve injury-induced pain and AFI, we first demonstrate that although neuropathic rats did not have an increased activation following nociceptive electrical stimulation compared to naive rats, they express a robust ipsilateral response to non-noxious palpation, which is not present in naive rats. Secondly, we used AFI to study the effect of spinal cord stimulation on nociceptive activity in the superficial dorsal horn in neuropathic animals. AFI shows an immediate and pronounced, but short-

lasting reduction in intensity and area of spinal nociceptive activity following SCS, which was not observed following sham stimulation. We have previously put forward, that the spinal cord AFI response following primary afferent stimulation is generated by projection neurons and local interneurons in the superficial laminae of the spinal dorsal horn (Jongen, 2012). Secondly, we have shown that spinal AFI is suitable to study plastic changes in this area following an intraplantar capsaicin injection (Jongen, 2010). In this study we have used a similar approach to study changes in spinal nociceptive activity following nerve-injury. Behavioral studies in experimental animals (Seltzer, 1990 ; Costigan, 2009) and psychophysical studies (Ochoa, 1993 ; Rowbothan, 1996) in humans with nerve injury consistently demonstrate pain (behavior) evoked by stimuli that are not painful under normal conditions, e.g. tactile allodynia. Similarly, in the Seltzer model of nerve injury-induced pain we now demonstrate a strong ipsilateral AFI response to innocuous palpation, which was not present in naïve animals. There were no statistically significant differences between naïve and neuropathic rats following a nociceptive 2.5 mA electrical stimulus. Although hyperalgesia to nociceptive stimuli does exist both in experimental and clinical neuropathic conditions, a strong enough electrical stimulus may saturate metabolic activity of superficial spinal dorsal horn neurons, i.e. the AFI signal. The electrical stimulus intensity that we used here is almost three times C-fiber threshold and generates a response that is close to the maximal AFI intensity that we found previously in naive animals (Jongen, 2010). Although this response could be further enhanced in the acute situation by intraplantar capsaicin injection (Jongen, 2010), the same may not be true in chronic neuropathy. Similarly, c-Fos expression, another marker of spinal nociceptive activity, is not increased in animals with chronic neuropathy compared to naïve animals, following nociceptive stimulation (Catheline, 1990). To reduce the number of experimental animals, we used naïve rats from a previous study (Jongen, 2010) as controls. These animals were Wistar rats, i.e. not the same strain as the Sprague-Dawley rats that were used here because of the Seltzer model. One may therefore argue that the above-described lack of a difference in AFI activity following nociceptive electrical stimulation between naïve and neuropathic rats could be the result of a genetic difference in sensitivity to nociceptive stimuli. However, at least behaviorally Sprague-Dawley rats demonstrate a hyperalgesic phenotype in

comparison to other rat strains, including Wistar rats (Mogil, 1990 ; LaCroix-Fralish, 2005). In addition, it is highly unlikely that non-noxious palpation would induce an AFI response in naïve Sprague-Dawley rats (as opposed to Wistar rats), since metabolic activity solely in the deep dorsal horn cannot be visualized by AFI. We therefore conclude that the strain differences in our study do not affect our conclusions regarding spinal nociceptive processing in nerve injury-induced pain. Regarding our second aim, to study mechanisms of action of SCS, this is the first report directly demonstrating reduced activity in the superficial dorsal horn in vivo following SCS. We used the AFI response to a 2.5 mA electrical stimulus as outcome measure, since in our hands this stimulus generates the most robust and consistent AFI responses. Others have also used nociceptive stimulation to study the effect of SCS (Shechter, 2013). Previous studies measuring peptides involved in antinociception (Cui, 1997 ; Schechtmann, 2008) or using pharmacological approaches (Song, 2011 ; Barchini, 2012) present only indirect evidence of reduced spinal nociceptive activity. Furthermore, studies of electrophysiological activity in wide dynamic range neurons in the deep dorsal horn (Guan, 2010) focus on an area that may not be decisive in generating the neuropathic pain phenotype (Craig, 2003-2004) and that may not be the locus of “gate control”, which instead is postulated to be the substantia gelatinosa in the superficial dorsal horn (Moayedi, 2013). Our finding of decreased activity in the superficial dorsal horn is in line with two reports (Smits, 2009 ; Maeda, 2009) demonstrating a significant increase in c-Fos expression in the superficial dorsal horn following SCS in rats with nerve injury, which was larger than the increase in the deep dorsal horn. These c-Fos expressing neurons presumably represent inhibitory interneurons (Hossaini, 2010), considering the decrease in neuronal metabolic activity in the superficial dorsal horn. Indeed, a double immunohistochemical staining procedure revealed the presence of c-Fos positive GABA-immunoreactive neurons in the superficial dorsal horn of SCS-treated chronic neuropathic rats (Janssen, 2012). The latter report and that of Cui et al. (Cui, 1997) stress the role of GABA-ergic interneurons in the mechanism underlying SCS in chronic neuropathic pain. Nevertheless, so far no direct changes in the spatial and temporal domain related to the effect of SCS on nociceptive transmission in the superficial dorsal horn of chronic neuropathic rats have been studied. Our findings

therefore provide the first direct evidence that SCS acts through modulation of nociceptive processing at the spinal segmental level. The effect of SCS on nociceptive activity in the superficial dorsal horn that we describe here is rather short lasting, as demonstrated by a linear decrease of efficacy from SCS directly following cessation of stimulation (i.e. T=0 min) and a lack of statistical significance between SCS and sham animals at timepoints T=5 minutes or later after SCS. A lack of statistical significance at those later time-points may be caused by a relatively low signal-to-noise ratio and technical challenges of spinal cord AFI that were discussed previously (Jongen, 2010), resulting in large variation between recordings within the same animal and between animals. However, behavioral effects of SCS also do not outlast the duration of SCS [33]. The relatively short duration of an initially significant effect of SCS does not preclude a clinical meaningful effect of SCS in patients with nerve injury-induced pain or CRPS, since in patients spinal cord stimulators deliver continuous stimulation. Continuous stimulation during AFI recording was not feasible due to our experimental setup, as the spinal electrode prevented imaging of the spinal cord. In conclusion, we demonstrated changes in neuronal metabolic activity in the superficial dorsal horn following nerve injury, which may reflect mechanisms of hyperalgesia in patients with neuropathic pain syndromes. Secondly, our study provides a rationale for spinal cord stimulation in neuropathic pain patients.

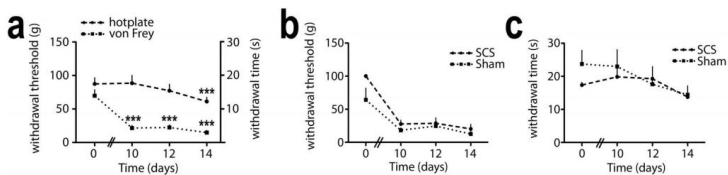


Figure 1. Behavioral data of rats that underwent partial ligation of the proximal sciatic nerve (Seltzer model). (A) Combined results of the von Frey withdrawal thresholds and hotplate latencies, at baseline and 10, 12 and 14 days after nerve ligation, from all 18 rats in the study, demonstrating tactile and thermal hyperalgesia. Error bars indicate SEM. $p < 0.01$; repeated measures ANOVAs, source of variation timepoint; ***, $p < 0.01$; pairwise comparisons of day 0 versus day 10, 12 and 14, using Bonferroni correction. (B,C) Von Frey withdrawal thresholds (B) and hotplate latencies (C) from 7 neuropathic rats that subsequently underwent SCS and 6 neuropathic rats that subsequently underwent sham stimulation, demonstrating a similar degree of

tactile and thermal hyperalgesia in both groups. Error bars indicate SEM. $p < 0.06$; repeated measures ANOVAs, source of variation treatment.

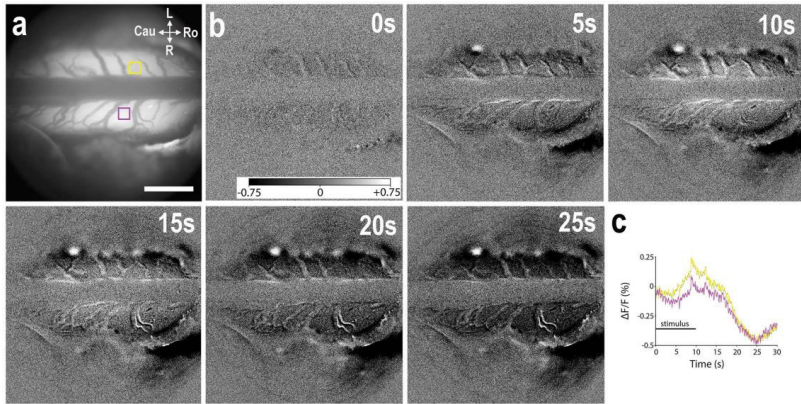


Figure 2. Spinal cord AFI signal following nociceptive electrical stimulation of the sciatic nerve, in a rat with partial ligation of the proximal sciatic nerve (Seltzer model). (A) Image of background fluorescence showing the dorsal surface of the spinal cord at the T13 vertebral level. The upper half is left, the lower half is right, the dark structure in the center is a dural vein. (B) Subtracted DF/F images at various time points after start of electrical stimulation (2.5 mA, 10 Hz) of the left sciatic nerve. (C) Graph showing the time course of DF/F in the yellow (left, i.e. ipsilateral or stimulated side) and purple (right, i.e. contralateral side) 20620 pixel square selections in (A). Scale bar, 1 mm. Gray scale bar ranging from 20.75% (black) to +0.75% (white) of the 16-bit range; Cau = caudal, Ro = rostral, L = left, R = right.

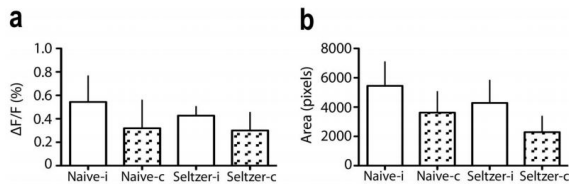


Figure 3. Mean intensity of the AFI signal (A) and area of excitation (B) following nociceptive electrical stimulation of the sciatic nerve, in naïve versus neuropathic rats (Seltzer model), on the ipsilateral (i) and contralateral (c) side of the nerve injury and nerve stimulation. Error bars indicate SEM; $n = 20$ naïve rats, $n = 13$ neuropathic rats

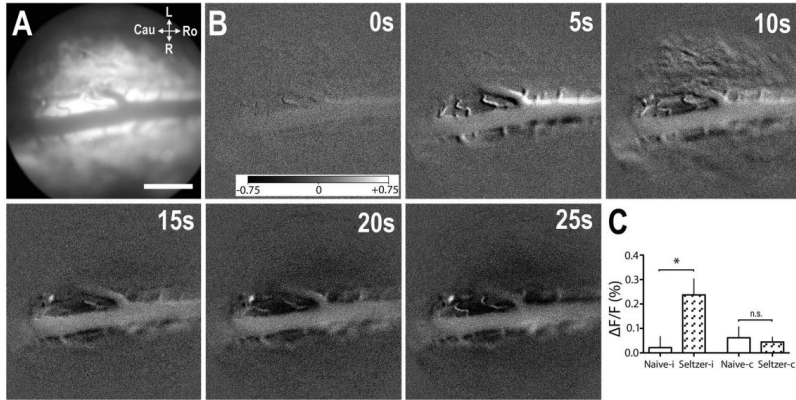


Figure 4. Intensity of the AFI signal, following innocuous palpation in naive rats and rats with partial ligation of the proximal sciatic nerve (Seltzer model). (A) Image of background fluorescence of the dorsal surface of the spinal cord at T13. (B) Subtracted DF/F images at various time points after start of 10 seconds, 1 Hz innocuous palpation of the plantar surface of the left hindpaw. (C) Mean DF/F of the light phase in 20620 pixel square selections on the ipsi-(i) and contralateral (c) side at the L4-6 spinal level, in naive rats from our previous experiments [3] and in rats with partial ligation of the proximal sciatic nerve (Seltzer model). Scale bar, 1 mm. Gray scale bar ranging from 20.75% (black) to +0.75% (white) of the 16-bit range. Error bars indicate SEM; * $p < 0.05$; unpaired t-test; $n = 5$ naive rats, $n = 5$ neuropathic rats.

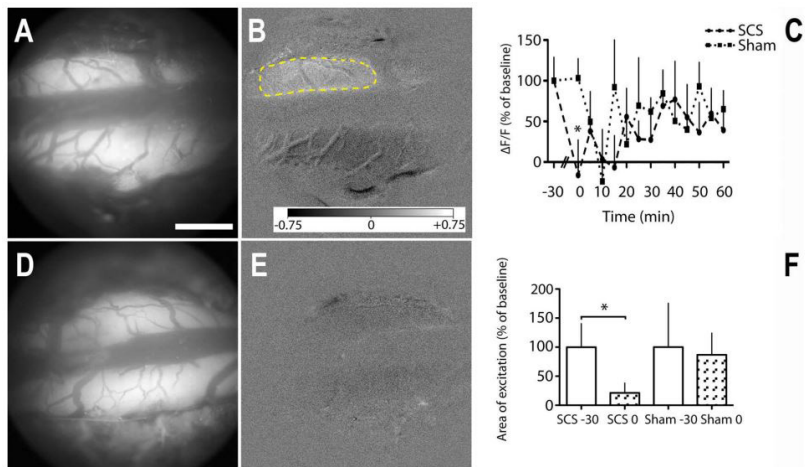


Figure 5. Effect of 30 minutes SCS or sham stimulation on the intensity of the AFI signal and area of excitation in response to sciatic nerve electrical stimulation, in rats with partial ligation of the proximal sciatic nerve (Seltzer model). (A,D) Images of background fluorescence of the dorsal surface of the spinal cord at T13 of a sham (A) and SCS treated rat (D). (B,E) Area of excitation (yellow) on the ipsilateral side, directly after sham stimulation (B); after SCS, in this rat, there is no area exceeding the predefined $\Delta F/F$ level (E). (C) Time course of the intensity of the AFI signal after SCS or sham stimulation ($T = 0$ min), as a percentage of $\Delta F/F$ before treatment ($T = -30$ min), in 20620 pixel square selections on the ipsilateral side at the L4-L6 spinal level. (F) Mean areas of excitation on the ipsilateral side directly after SCS or sham stimulation ($T = 0$ min), as a percentage of the areas before treatment ($T = -30$ min). Scale bar, 1 mm; Grayscale bar ranging from 20.75% (black) to +0.75% (white) of the 16-bit range; Error bars indicate SEM; * $p < 0.05$; paired t-tests; $n = 7$ SCS, $n = 6$ sham stimulation.

CHAPTER III

Pruritus in anti-DPPX encephalitis²

JJuerd Wijntjes, Malik Bechakra, Marco W.J. Schreurs, Joost L.M. Jongen,
Aart Koppenaar, and Maarten J. Titulaer

²This chapter has been published in *Neurol Neuroimmunol Neuroinflamm.*
2018 May; 5(3): e455.

We present a unique case of a patient with anti-dipeptidyl peptidase-like protein 6 (DPPX) encephalitis in which severe pruritus was the cardinal symptom. Anti-DPPX encephalitis is caused by cell surface autoantigens to DPPX, a subunit of the Kv4.2 potassium channel.¹ Most patients had a combination of limbic encephalitis, brainstem dysfunction, diarrhea, and weight loss.^{1–3} We describe a patient with severe pruritus and provide long-term follow-up, offering recommendations for treatment.

Case presentation

A 57-year-old patient presented with a variety of complaints, developing over months. These started with gastrointestinal symptoms (diarrhea and abdominal pain). *Blastocystis hominis* infection was cultured in stool, but without improvement to treatment. Five months later, he developed cognitive decline and severe pruritus with allodynia centered on his trunk. There was severe self-neglect. Our patient was admitted on and off neuropsychiatric wards for 3 years. During progression, he also developed myoclonic jerks, autonomic failure, rigidity, and ataxia. On neurologic examination, his consciousness was clear. The muscle tone was slightly rigid. There was severe rigidity of the trunk muscles, slight rigidity of the extremities, and antecollis. He had action myoclonus and hyperekplexia. His gait was remarkably “marionette-like,” and broad-based, tandem gait was impossible. Deep tendon reflexes of the legs were diminished. He had scratching marks from pruritus centered on his trunk and could not bear clothing. Neurocognitive testing revealed psychomotor slowing on all tasks. Brain MRI showed bilateral temporal lobe atrophy and an aspecific white matter lesion. EEG showed slight background slowing. Routine blood examination was normal. CSF analysis showed mild lymphocytosis (12 cells/ μL), a slightly elevated protein level (0.52 g/L), and matched oligoclonal bands.

Extensive ancillary examinations (among others, CT-thorax/abdomen, bone marrow biopsy, and serologic tests on lues, borrelia, and HIV) were all normal. A diagnosis of progressive encephalomyelitis with rigidity and myoclonus (PERM) was established. Subsequent testing for DPPX antibodies was positive in both serum and CSF cell-based assays and confirmed by neuropil staining on immunohistochemistry. Other autoimmune antibodies were negative. A skin biopsy from the symptomatic lumbar region showed a normal intraepidermal nerve fiber density for this region.

After the start of immunosuppressive therapy, our patient improved, but several relapses followed. Multiple immunosuppressive agents were tried, and only after adequate treatment with cyclophosphamide and rituximab, aiming for complete B-cell depletion, our patient improved markedly without any further relapses to the present (figure). Two and a half years after the diagnosis of PERM, our patient developed B-cell non-Hodgkin lymphoma (NHL).

Discussion

PERM is a syndrome that is believed to result from brain stem and spinal cord dysfunction. Patients with PERM often have glycine receptor antibodies or in a minority anti-GAD65 antibodies.⁴ Only recently, the association with anti-DPPX antibodies and PERM has been described.⁵ These cases were characterized mainly by CNS symptoms and autonomic dysfunction, while pruritus was a minor symptom.² By contrast, in our patient pruritus, that was refractory to dermatological treatments (reviewed elsewhere) was the cardinal symptom.⁶

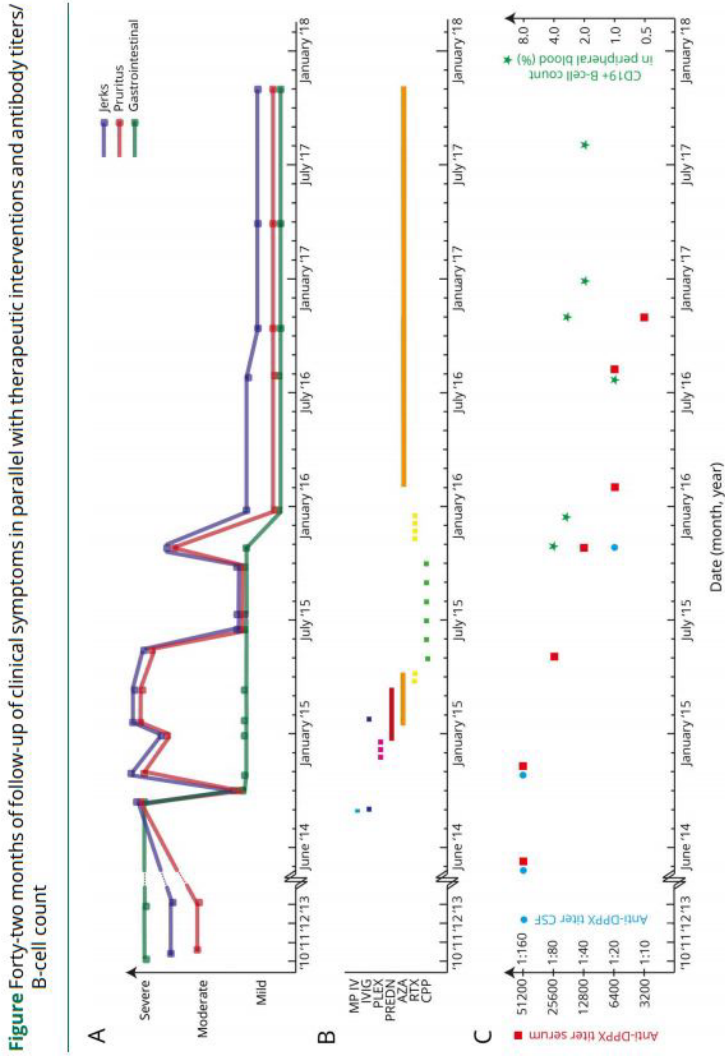
Anatomically, two pruritus-sensitive afferent pathways exist (histamine- and cowhage-stimulated pathways). From the level of the dorsal horn, the pathway travels in the contralateral spinothalamic tract and synapse onto neurons in the thalamus. The role of Kv4.2 in neurogenic pruritus is not exactly known. Genetic elimination of Kv4.2 in mice increased excitability of dorsal horn neurons resulting in enhanced sensitivity to tactile and thermal stimuli and might explain its role in neurogenic itch.⁷

In our patient, the normal intraepidermal nerve fiber density and the absence of an effect from dermatological treatments suggest pruritus was of central origin located at the dorsal horn induced by anti-DPPX antibodies.

In line with other forms of autoimmune encephalitis (AIE), such as anti-Caspr2 encephalitis, anti-DPPX encephalitis is less subacute, resembling a neurodegenerative disease. Fulminant and rapidly progressive (autonomic or sensory) symptoms have been attributed to paraneoplastic neuropathy associated with Hu or amphiphysin antibodies. In contrast to other AIEs, such as anti-NMDA receptor encephalitis, patients with anti-DPPX encephalitis tend to need prolonged immunosuppressive therapy. As illustrated by our case, every attempt to taper immunosuppressive therapy resulted in a very rapid decline. This necessitates the use of chronic immunosuppressive therapy, and complete B-cell depletion seems necessary.

B-cell NHL is associated with chronic immunosuppressive therapy. B-cell neoplasms developed in 3/39 patients with anti-DPPX encephalitis, remitting after rituximab.^{2,3} In our case, the delayed diagnosis of

B-cell NHL could have been masked by treatment (steroids and rituximab). Therefore, it is important to perform diagnostic tests in advance of immunosuppressive therapy and during follow-up, especially during relapses.



(A) Symptom severity; (B) Medication overview; (C) Antibody titers/B-cell counts. AZA = azathioprine; CPP = cyclophosphamide; DPPX = dipeptidyl peptidase-like protein 6; IVIG = IV immunoglobulin; MP IV = IV methylprednisolone; PLEX = plasma exchange; PREDN = prednisone; RTX = rituximab.

CHAPTER IV

The reduction of intraepidermal P2X₃ nerve fiber density correlates with behavioral hyperalgesia in a rat model of nerve injury-induced pain³

Malik Bechakra, Barthold N Schüttenhelm, Tiziana Pederzani, Pieter A van Doorn, Chris I de Zeeuw, Joost L M Jongen

³This chapter has been published in J Comp Neurol. 2017 Dec 1;525(17):3757-3768.

Abstract

Skin biopsies from patients with neuropathic pain often show changes in epidermal innervation, although it remains to be elucidated to what extent such changes can be linked to a particular subgroup of nerve fibers and how these changes are correlated with pain intensity. Here, we investigated to what extent behavioral signs of hyperalgesia are correlated with immunohistochemical changes of peptidergic and non-peptidergic epidermal nerve fibers in a rat model of nerve injury-induced pain. Rats subjected to unilateral partial ligation of the sciatic nerve developed significant mechanical and thermal hyperalgesia as tested by the withdrawal responses of the ipsilateral footpad to von Frey hairs and hotplate stimulation. At day 14, epidermal nerve fiber density and total epidermal nerve fiber length/mm² were significantly and consistently reduced compared to the contralateral side, following testing and re-testing by two blinded observers. The expression of calcitonin gene-related peptide, a marker for peptidergic nerve fibers, was not significantly changed on the ipsilateral side. In contrast, the expression of the P2X₃ receptor, a marker for non-peptidergic nerve fibers, was not only significantly reduced but could also be correlated with behavioral hyperalgesia. When labeling both peptidergic and non-peptidergic nerve fibers with the pan-neuronal marker PGP9.5, the expression was significantly reduced, albeit without a significant correlation with behavioral hyperalgesia. In conjunction, our data suggest that the pathology of the P2X₃ epidermal nerve fibers can be selectively linked to neuropathy, highlighting the possibility that it is the degeneration of these fibers that drives hyperalgesia.

INTRODUCTION

Neuropathic pain is a syndrome caused by a lesion or disease of the somatosensory nervous system, most commonly peripheral neuropathy. In the latter, damage to nociceptors, that is, thinly myelinated (Ad or unmyelinated (C) primary afferent nerve fibers, presumably is the initiating event, since at least clinically selective degeneration of Ab fibers (e.g., in vitamin B12 deficiency [Koike et al., 2015], cis-platinum induced peripheral neuropathy [Jongen, Broijl, & Sonneveld, 2015] or Friedreich's ataxia [Durr et al., 1996]) causes significant neuropathic pain in only a minority of patients, while on the other hand selective small-fiber neuropathies (e.g., in sarcoidosis, HIV, amyloidosis, and Fabry's disease) (Hoeijmakers, Faber, Lauria, Merckies, & Waxman, 2012) are almost invariably painful. Once neuropathic pain has been initiated by damage to nociceptors, it is maintained by adaptive changes in other parts of the sensory system, like increased spontaneous activity of un-injured Ad and C fibers (Hulse, Wynick, & Donaldson, 2010), increased spontaneous activity of Ab fibers (Govrin-Lippmann & Devor, 1978), sprouting of autonomic nerve fibers in the upper dermis (Grelík, Bennett, & Ribeiro-da-Silva, 2005; Taylor, Osikowicz, & Ribeiro-da-Silva, 2012), expression changes in the dorsal root ganglion (Villar et al., 1991; Michael, Averill, Shortland, Yan, & Priestley, 1999; Li, Song, Higuera, & Luo, 2004; Chen et al., 2014) and changes in the spinal cord and brainstem (West, Bannister, Dickenson, & Bennett, 2015).

Skin biopsies, using immunohistochemistry with the pan neuronal marker PGP9.5 (Wang, Hilliges, Jernberg, Wiegleb-Edstrom, & Johansson, 1990), provide an accessible way to study changes in innervation following nerve injury (Lauria et al., 2010). While Ab fibers terminate in specialized end-organs in the dermis (Nolano et al., 2003), Ad and C nociceptors terminate as fine unmyelinated nerve fibers, so-called free nerve endings (Cauna, 1980), in the epidermis. C-fibers, which make-up the majority of nociceptors, can be broadly subdivided into two classes: peptidergic nerve fibers, which contain neuropeptides like calcitonin gene-related peptide (CGRP), and non-peptidergic nerve fibers, which can be identified by expression of the P2X3 receptor (Bradbury, Burnstock, & McMahon, 1998; Burnstock, 2000; Taylor, Peleshok, & Ribeiro-da-Silva, 2009), a ligand gated ion-channel which is responsive

to adenosine triphosphate.

The epidermis is predominantly innervated by non-peptidergic nociceptors (Perry & Lawson, 1998), while the internal organs receive mostly peptidergic innervation (Plenderleith & Snow, 1993; Perry & Lawson, 1998; Taylor et al., 2009; Guedon et al., 2016) or peptidergic and non-peptidergic innervation to an equal degree (Bradbury et al., 1998). At the same time, sensory qualities that are distinct in neuropathic pain, like paresthesias, burning pain and tactile allodynia, are typically experienced in skin, suggesting an important role for the nonpeptidergic subclass of nociceptors in neuropathic pain. No consistent correlation between severity of neuropathic pain (behavior) and (intra) epidermal nerve fiber density (IENFD) exists (Lindenlaub & Sommer, 2002; Kalliomaki et al., 2011; Schley et al., 2012). We hypothesize that neuropathic pain may be initiated and/or maintained by selective degeneration of non-peptidergic subclass of primary afferent nerve fibers.

To test this hypothesis, varying degrees of neuropathy were induced by partial ligation of the proximal sciatic nerve in a rat. This model, which was first described by Seltzer et al., induces hyperalgesia in the rat footpad with various levels of intensity. These levels are unform but graded, depending on the proportion of sciatic nerve fibers contained within the ligation (Seltzer, Dubner, & Shir, 1990). We set out to study correlations between epidermal innervation in skin biopsies from the footpad and mechanical and thermal hyperalgesia in that same area, using PGP9.5, CGRP, and P2X3 immunohistochemistry. The presence of a correlation between P2X3 nerve fiber density and hyperalgesia, that is, neuropathic pain behavior, and the absence of a correlation with CGRP fiber density would support our hypothesis.

MATERIALS AND METHODS

In total, 21 young adult male Sprague Dawley rats from Harlan or Charles River, the Netherlands, weighing 250–350 g, were used for this study. To reduce the number of experimental animals, we used rats that had already participated in another study on spinal imaging of nerve injury-induced pain (Jongen et al., 2014), which experiment was conducted in accordance with the principles of laboratory animal

care (NIH publications no. 8023, revised 1978) and approved by the Institutional Animal Ethics Committee of Erasmus MC Rotterdam (EMCnr. 115–08-26).

Peripheral nerve lesion, behavioral testing and harvesting of skin biopsies

Neuropathic pain was induced by partial ligation of the sciatic nerve as described by Seltzer et al. (1990). Behavioral testing took place before the Seltzer operation and at post-operative days 10, 12, and 14. Every time before behavioral testing, rats were habituated to the experimenter (T.P.), the room in which the behavioral experiments took place and the transparent chamber used for von Frey testing, for at least half an hour. The chamber used for von Frey testing had an opaque, flatsurfaced plastic platform with holes through which von Frey hairs are inserted and applied to the plantar surface of the paw (Pitcher, Ritchie, & Henry, 1999). Mechanical sensitivity was assessed by testing the withdrawal response to von Frey filaments (Stoelting Co, Wood Dale, IL) of increasing thickness. The threshold was set at three out of five withdrawal responses. After testing for mechanical sensitivity, thermal thresholds were assessed by the hotplate test. The surface of the hot plate was heated to a constant temperature of 51 8C. Rats were placed on the hot plate (25.4 cm 3 25.4 cm) (Ugo Basile Srl., Comerio, Italy), which was surrounded by a transparent chamber with an open top, and the response latency to either a hind paw lick or hind paw flick was measured. Immediately after a response rats were removed from the hotplate. Rats were also removed if they did not respond after 30 s, to prevent tissue injury.

After behavioral testing at day 14, rats were anesthetized and spinal imaging of nerve injury-induced pain was performed as described in a previous article. During this experiment rats underwent electrical/sham spinal cord stimulation and trains of 2,5 mA electrical stimulation of the sciatic nerve distal to the site of the Seltzer ligation (Jongen et al., 2014). Skin biopsies were harvested after the above experiment was completed and the rats had been euthanized, that is, were residual material

Skin biopsies, histologic processing, immunohistochemistry and anti-body characterization

The glabrous skin from the left and right footpad, the area that was also targeted during behavioral testing, was biopsied using a 3 mm disposable punch. The skin biopsy was immediately transferred to cold fixative, consisting of 2% paraformaldehyde-lysine periodate in Sorenson's buffer (0.133M Na₂HPO₄ and KH₂PO₄), and post fixed overnight at 4 8C. After several washes and increasing gradients of sucrose in 0.1 M phosphate buffer (PB), tissues were stored at 2808C in a mixture of 20% glycerol and 0.2M PB, until used. Before cutting, skin biopsies were embedded in 12% gelatin, 10% sucrose blocks, which were left in 4% paraformaldehyde for 2.5 hr at room temperature (RT) to harden. The gelatin blocks were then kept overnight at 4 8C in a 30% sucrose solution. Consequently, 50 lm sections were cut perpendicular to the surface on a freezing microtome and processed as free floating sections. Sections from the ipsilateral and contralateral footpad were collected in cryoprotectant solution (37.5% glycerol and 37.5% ethylene glycol in 0.0125M PB) in a 24-well plate, each well containing 8–10 sections (i.e., 6 wells per rat/ side) and stored at 220 8C until start of the immunohistochemical procedure.

At the start of the immunohistochemical procedure sections were washed in 0.05 M phosphate-buffered saline (PBS) (6 times, 10 min each), after which sections were incubated for 10 min in a 3% H₂O₂ solution in PBS at RT to quench endogenous peroxidase activity. Sections were then incubated in a 2.5 mM sodium citrate buffer solution at 80 8C during 40 min, to unmask immunoreactivity (Jongen et al., 2007). Sections were washed 6 3 10 min in PBS between all incubations. Nonspecific binding of the secondary antibody was blocked by pretreating the sections with a 10% Bovine Serum Albumin (BSA) solution in 0.05 M PBS also containing 0.4% Triton X-100, for 90 min at RT. Sections were then incubated in a 0.05 M PBS solution containing 2% BSA and 0.4% Triton X-100 and primary antibodies, for 60 hr at 4 8C. Dilutions of primary antibodies were 1:2,000 for rabbit anti-PGP 9.5 (Catalog# ADI-905–520; Enzo Life Sciences, Farmingdale, NY; RRID: AB_10622540), 1:30.000 for rabbit anti-CGRP (Catalog# PC205L; Millipore, Billerica, MA; RRID: AB_2068524) and 1:100.000 for rabbit anti-P2X3 (Catalog# RA10109; Neuromics, Minneapolis, MN; RRID: AB_2157931) (Table 1).

Omission of the primary antibodies and preabsorbtion of the primary antibodies with a more than 253 molar excess of the protein (PGP9.5) or peptides (CGRP and P2X3) the primary antibodies were raised against were used as negative control experiments. While antiPGP9.5 may be considered as a general marker for unmyelinated nerve fibers in the epidermis, anti-CGRP and anti-P2X3 each recognize specific epitopes. Therefore, in addition, a specific immunohistochemical staining pattern of rabbit anti-CGRP, rabbit anti-P2X3 and a guinea pig anti-P2X3 antibody (kindly donated and characterized by Dr. Vulchanova, University of Minnesota, MN) (Vulchanova et al., 1998) in spinal cord sections and a similar staining pattern of guinea pig anti-P2X3 compared to rabbit anti-P2X3 in skin sections were used as positive control experiments.

After primary antibody incubation, sections were washed for 6 3 10 min in PBS and incubated in biotin-conjugated goat anti-rabbit IgG, diluted 1:400 in PBS also containing 2% BSA and 0.4% Triton X-100, for 90 min at RT. After another 6 3 10 min washes in PBS, sections were processed with the ABC method (Vector Elite, Burlingame, CA) for 90 min at RT and then washed another time for 6 3 10 min in PBS.

In the sections that were incubated with the P2X3-antibody, further signal amplification was achieved by treating these sections with biotin-tyramide (diluted 1:1,000 in imidazole containing 3% H₂O₂) for 12 min at RT (Hopman, Ramaekers, & Speel, 1998). After 6 3 10 min washes in PBS, these sections were then incubated overnight at 4 8C in ABC complex in PBS solution, also containing 2% BSA and 0.5% Triton X-100. Then, following 2 3 10 min washes in PBS and 4 3 10 min washes in 0.05 M PB, sections from all three primary antibodies were reacted with 0.33% diaminobenzidine, containing 0.016% hydrogen peroxide. Sections were mounted on slides, air-dried ove night, dehydrated using absolute ethanol (< 0.01% methanol), transferred to xylene and cover slipped with Permount mounting medium (Fisher, Hampton, NH). One slide contained one primary antibody and one side (i.e., ipsi- or contralateral). All three primary antibodies and ipsilateral and contralateral skins of 4 or 5 animals at a time were processed during the same immunorun. Thus, five immunoruns were performed altogether.

Quantification of epidermal nerve fiber density

For quantification of epidermal nerve fiber density, slides were scanned and digitized using a Hamamatsu NanoZoomer 2.0-HT slide scanner (Hamamatsu Photonics, Hamamatsu City, JP). For unidentified reasons, the scanner did not recognize some slides, resulting in 7.9% missing IENFD, branches/unit or epidermal nerve fiber length (ENFL) data (see below). Sections were analyzed using Leica Aperio ImageScope software (freely available at <http://www.leicabiosystems.com/pathology-imaging/aperio-epathology/integrate/imagescope/>) at 403 magnification. Four sections per slide and six frames per section were sampled. Frames were selected so that they comprised the entire epidermal thickness. Three parameters were manually counted/traced for each primary antibody, by a single, blinded observer (M.B.) (Figure 1):

1. The number of crossings of the dermal–epidermal junction per mm length of dermal–epidermal junction (IENFD). The length of the dermal–epidermal junction was automatically determined by the ImageScope software after tracing.
2. The number of branches within the epidermis per individual nerve fiber (i.e., unit) crossing the dermal–epidermal junction (braches/unit).
3. The total length of the epidermal nerve fibers (ENFL) was determined by the ImageScope software after tracing and expressed as mm fiber length per mm² of the epidermal frame area.

In 24 frames, the above parameters were re-counted by M.B. and also counted by a second blinded observer (B.S.), to calculate intraclass correlation coefficients.

Statistical analysis

For a comparison of means of behavioral responses at day 0, 10, 12, and 14, repeated-measures ANOVAs were used. Three separate paired t-tests were used to compare CGRP and P2X3-labeled epidermal fibers on the unaffected right side. Three individual mixed ANOVAs (for IENFD, branches/unit and ENFL) were used to compare epidermal innervation (PGP9.5, CGRP, and P2X3) of the

ipsilateral (i.e., left) and contralateral (i.e., right) footpad. Bonferroni-correction was always applied for post-hoc analysis. The intraclass correlation coefficient (two-way mixed model) was employed to calculate test–retest and inter-observer reliability of measures of epidermal innervation and of the different immunohistochemical markers. To study the correlation between mean behavioral measures at day 10, 12, and 14 and epidermal innervation, Pearson correlation coefficients were calculated and statistical significance was tested by adding VF and HP at day 0 as a predictor variable to the ratio of left and right footpad nerve fiber measures in a multiple linear regression model. Statistical testing was performed using IBM SPSS Statistics v.21.0.0.0 software (IBM Corp., Armonk, NY) or GraphPad Prism v6.0f (GraphPad Software, Inc., La Jolla, CA).

RESULTS

Behavioral testing

All 21 rats used in this study, developed mechanical and thermal hypersensitivity characteristic of the Seltzer model of neuropathic pain. The decrease in von Frey thresholds and hotplate latencies was statistically highly significant (Figure 2; $p < .001$; repeated-measures ANOVAs).

Immunohistochemistry

In the epidermis of the right hind paw, that is, the non-neuropathic or control side, all three immunohistochemical markers labeled individual fibers and bundles of fibers just below and running parallel to the basement membrane. PGP9.5 and CGRP demonstrated the strongest dermal staining, that was frequently associated with blood vessels. From these bundles in the subepidermis and upper dermis, thin and varicose fibers originated that ran almost perpendicular to their origins, thus penetrating the basement membrane (Petersen, Rice, Farhadi, Reda, & Rowbotham, 2010). Since PGP9.5 labels both peptidergic and nonpeptidergic epidermal nerve fibers, IENFD was highest for this marker, although smaller than the sum of CGRP and P2X3 labeled fibers. P2X3 fibers were more abundant,

longer, reaching almost up to the stratum corneum, and had more branches per unit than CGRP fibers (Figures 3 and 5a; $p < .001$; paired t-tests).

To control for non-specific staining of primary antibodies, the same immunohistochemical protocol was used, except that the primary antibodies were omitted or preabsorbed with the protein or peptide they were raised against, which resulted in a complete abolishment of specific signal for all antibodies used (Figure 4a–f). As a positive control, we also used rat spinal cord, in which rabbit anti-CGRP and rabbit and guinea-pig anti-P2X3 gave specific staining patterns in the superficial dorsal horn as described previously (Figure 4g–h) (Villar et al., 1991; Vulchanova et al., 1998). Rabbit anti-P2X3 and guinea pig anti-P2X3 gave similar staining patterns in spinal cord and skin sections, although rabbit anti-P2X3 showed a better signal to background staining in skin biopsies our hands (Figure 3c, d). Therefore, rabbit anti-P2X3 was used for quantitative analyses.

Measures of peptidergic and non-peptidergic epidermal innervation

Next, the sensitivity for the detection of neuropathy of the three different measurements of epidermal innervation was tested (Figure 5). There was a large and statistically highly significant ipsilateral (i.e., left, the side with the neuropathy) versus contralateral (i.e., right, the unaffected side) overall difference for IENFD and ENFL ($p < .01$; repeated measures ANOVAs, source of variation side and the interaction between side and marker). These differences were accounted for by statistically significant differences in PGP9.5 and P2X3 labeling ($p < .01$; two-way ANOVAs with post-hoc Bonferroni correction), while CGRP labeling was not statistically significantly different between sides. The overall ipsilateral versus contralateral difference in number of branches per unit also reached statistical significance ($p < .01$; two-way ANOVA, source of variation side), although the interaction between side and marker and none of the individual markers appeared statistically significantly different with post-hoc Bonferroni correction. We therefore conclude that PGP9.5- and P2X3-IENFD and -ENFL, but not CGRP-IENFD and -ENFL are sensitive measures of neuropathy.

A reliability analysis was performed, by calculating the intraclass correlation coefficient (ICC) for test-retest reliability and for testing the consistency

between two independent observers (M.B. and B.S.). Data are presented in Table 2. Since ICCs were always 0.7 for IENFD and ENFL, we conclude that these measures are reproducible measures of epidermal innervation.

Correlations between immunohistochemical markers and behavioral hyperalgesia

Finally, we studied correlations between epidermal innervation and behavioral hyperalgesia. Only P2X3 labeled fibers correlated statistically significantly with von Frey withdrawal thresholds and hotplate latencies (with the sole exception of P2X3-branches and hotplate latencies), while PGP9.5 and CGRP labeled fibers did not (Figure 6; $p < .05$, multiple linear regression analysis). Thus, lower von Frey thresholds and hotplate latencies correlated with a stronger reduction in P2X3 innervation as compared to the right or unaffected paw. Generally, correlations between epidermal innervation and mechanical thresholds were stronger than correlations between epidermal innervation and hotplate latencies.

DISCUSSION

We have used a rat model of uniform but graded sciatic neuropathy and three immunohistochemical markers to study changes in epidermal innervation and to investigate a correlation between epidermal innervation and pain behavior. Simultaneously, we have validated three measures of epidermal innervation, that is, IENFD, number of branches/unit and ENFL. IENFD and ENFL obtained with the pan neuronal marker PGP9.5 and with the non-peptidergic fiber marker P2X3 were statistically significantly decreased at 14 days following nerve injury, while this was not the case for the peptidergic fiber marker CGRP. In addition, IENFD and ENFL demonstrated good test–retest and inter-observer reliability. We therefore concluded that PGP9.5 and P2X3 are sensitive and robust markers of neuropathy. Of these, only P2X3 epidermal innervation correlated with von Frey withdrawal thresholds and hotplate latencies.

In the Seltzer model, in which the non-fasciculated sciatic nerve is injured in the thigh, varying degrees of sciatic neuropathy are caused by the propor-

tion (generally varying between 30 and 50%) of sciatic nerve fibers that is actually damaged by ligation (Seltzer et al., 1990). As a result of Wallerian degeneration, the damaged nerve fibers will cause nerve fiber terminal loss in the epidermis of the footpad, which is the innervation area of the sciatic nerve. Although uniform behavioral hyperalgesia of the rat footpad was shown previously in this model (Seltzer et al., 1990), the magnitude of the behavioral changes may depend on the amount of sciatic nerve fiber damage and thus nerve fiber terminal loss in the epidermis. Thus, the Seltzer model of following peripheral axotomy, using the same antibodies and immunohistochemical procedures by others from our lab (Duraku et al., 2012; Kambiz et al., 2015).

To reduce the number of experimental animals we used rats that had already participated in another study on spinal imaging of nerve injury-induced pain (Jongen et al., 2014). Although behavioral testing was not affected by this experiment, skin biopsies were harvested directly following an operation and imaging procedure that included 30 min of 50 Hz low-intensity spinal cord stimulation and repeated 10 sbouts of 10 Hz 2.5 mA electrical stimulation of the left sciatic nerve proximal to the ligation. In the short-term, electrical stimulation of peripheral nerves will result in a depletion of CGRP (Dessem et al., 2010), possibly leading to a decreased number of identified CGRP terminals in the skin. Thus, electrical stimulation cannot explain the absence of a reduction of CGRP in our skins. Besides, other studies involving peripheral nerve damage without electrical stimulation (Ma & Bisby, 2000; Peleshok & Ribeiro-da-Silva, 2011; Duraku et al., 2012) found very similar CGRP innervation densities at 2–5 weeks postnerve injury compared to baseline, suggesting that the absence of a CGRP reduction at 14 days following nerve injury induction indicates a rapid regeneration of CGRP fibers after nerve injury. Similar to CGRP, also P2X3 immunoreactivity might have been influenced by the electrical stimulation preceding the skin biopsy. However, in the study of Dessem et al. already cited above (Dessem et al., 2010), a modest longterm increase of P2X3 immunoreactivity following electrical stimulation was found and a short-term change is not to be expected, since P2X3 is a receptor. Thus, this cannot explain the decreased number of P2X3 nerve terminals in our skins. Besides, Peleshok (Peleshok & Ribeiro-daSilva, 2011) and Duraku et al. (Duraku et al., 2012) found very similar P2X3 innervation densities at 2–5 weeks post-nerve

injury compared to baseline in animals that did not undergo electrical stimulation. We therefore conclude that there are no convincing arguments that the electrical stimulation preceding harvesting of the skin biopsies in this study would affect our conclusions regarding the regulation of CGRP and P2X3 immunohistochemistry in nerve fiber terminals by sciatic nerve neuropathy or regarding the correlation between these terminals and behavioral hyperalgesia.

To correct for between-rat differences, we used the ratio of ipsilateral/contralateral epidermal innervation as a predictor variable in the regression model. Although contralateral changes in epidermal innervation have been described (Koltzenburg, Wall, & McMahon, 1999), these changes were relatively mild (amounting to 30% compared to baseline) at 3 weeks after induction of spared nerve injury (Oaklander & Brown, 2004) and not statistically significantly different from baseline in the loose ligation model (Lindenlaub & Sommer, 2002). We therefore conclude that it is appropriate to use epidermal innervation of the contralateral side to correct for between-rat differences in epidermal innervation. To quantify epidermal nerve fibers, apart from using commonly accepted measurements like IENFD (Lauria et al., 2010) and ENFL (Peleshok & Ribeiro-da-Silva, 2011), we also quantified the number of terminal branches in the epidermis, since it was hypothesized that this measure would be a sensitive marker of reinnervation, especially with respect to CGRP. However, it turned out that counting the number of branches/unit was unreliable, probably because these branches are extremely thin, making them relatively hard to visualize and quantify. Measurement of IENFD and ENFL however had good test–retest and inter-observer reliability in our hands.

This is the first time that a correlation between PGP9.5 and both subgroups of epidermal nerve fibers and pain behavior was systematically studied. We found a linear correlation between epidermal P2X3 innervation and behavioral hyperalgesia, but not for CGRP and PGP9.5.

This was true both for mechanical as well as for thermal stimuli, although correlations between epidermal P2X3 innervation and mechanical thresholds (good correlations of 0.6–0.8) were stronger than correlations between epidermal P2X3 innervation and hotplate latencies (moderate correlations of 0.5–0.6) (Campbell, 1997). Based on mice experiments, it was suggested that non-peptidergic nerve

fibers specifically mediate mechanical hyperalgesia (Scherrer et al., 2009). In rats and higher order primates, however, the heat receptor TRPV1 is expressed on both peptidergic and non-peptidergic nerve fibers (Tominaga et al., 1998), which can explain a role of P2X3 nerve fibers in mediating thermal hyperalgesia as well.

Consistent with our findings, it was shown previously that following an initial decrease epidermal CGRP innervation returns to baseline levels already 14 days after partial sciatic nerve ligation (Ma & Bisby, 2000). Also in other neuropathic pain models, epidermal, and upper dermal CGRP/SubstanceP innervation reached baseline levels much faster than P2X3 fibers did (Peleshok & Ribeiro-da-Silva, 2011; Duraku et al., 2013). Thus, changes in epidermal peptidergic innervation cannot be selectively linked to neuropathy, which is a chronic condition. Results from other studies (Ma & Bisby, 2000; Taylor et al., 2012) also support our finding that selective degeneration of non-peptidergic nerve fibers is correlated with behavioral hyperalgesia in animals with nerve injury. However, the relation between degeneration of nonpeptidergic nerve fibers and the development of hyperalgesia is complex, since selective destruction of non-peptidergic nerve fibers alone, using IB4-saporin, did not result in mechanical hyperalgesia, while IB4-saporin followed by nerve injury did (Taylor et al., 2012). Furthermore, loss of non-peptidergic nerve fibers may induce parasympathetic sprouting in the upper dermis (Taylor et al., 2012), raising the possibility that the hyperalgesia that we observed may rather be an indirect effect from non-peptidergic nerve fiber loss. Finally, since we did not study the correlation between epidermal innervation at different time-points, it is impossible to draw a firm conclusion about the causality between epidermal P2X3 nerve fiber loss and the development of hyperalgesia and neuropathic pain.

We conclude that the selective degeneration of epidermal P2X3 fibers that we observed may be necessary but not sufficient to generate hyperalgesia and possibly the full-spectrum of neuropathic pain, at 14 days following nerve injury. Other factors might include lowered thresholds for the transduction of sensory stimuli to the skin of CGRP fibers, sprouted dermal parasympathetic and myelinated nerve fibers and central mechanisms at the level of the spinal cord. We suggest that further research should be targeted at peripheral nerve regeneration, to develop new treatments for the disabling condition of neuropathic pain.

TABLE 1 Antibodies used

Name	Immunogen	Manufacturer, host and type, catalog No., RRID	Concentration
Anti-PGP _{9.5}	Recombinant full length human PGP9.5 (UCH-L1)	Enzo Life Sciences, rabbit polyclonal, ADI-905-520, AB_10622540	1:10,000
Anti-CGRP	Rat α -calcitonin gene related peptide (α -CGRP)	Millipore, rabbit polyclonal, PC205L, AB_2068524	1:30,000
Anti-P2X ₃	Residues 383-397 of the carboxy-terminus of rat P2X3	Neuromics, rabbit polyclonal, RA10109, AB_2157931	1:100,000

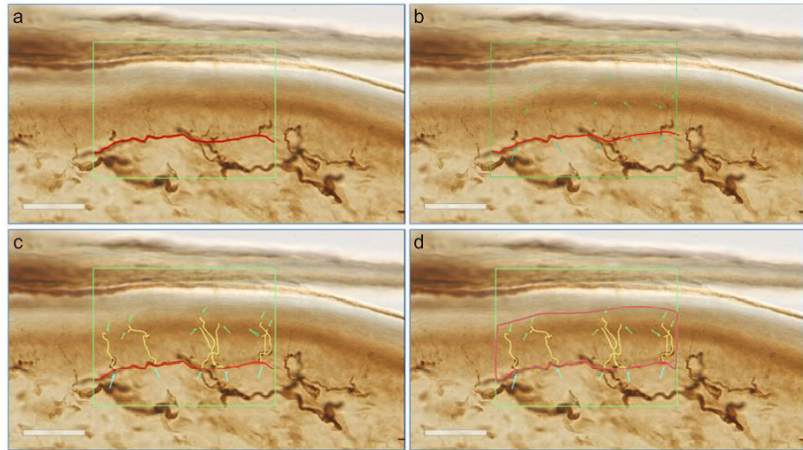


FIGURE 1 Images demonstrating the procedure of digitally analyzing and quantifying the skin biopsies. Firstly, the dermal-epidermal border (red) was drawn for calculating IENFD and a rectangular area in which IENFD and ENFL are calculated was selected using the image analysis software (a). Secondly, crossings of the dermal-epidermal border (blue arrows) and branches (green arrows) were counted (b). Thirdly, epidermal nerve fibers were traced (yellow; c) and finally the epidermal area used to calculate ENFL was delineated (pink; d). The length of the dermal-epidermal border and the surface of the epidermal area are automatically computed by the image analysis software. The white bars represent 50mm

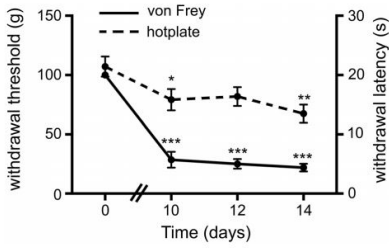
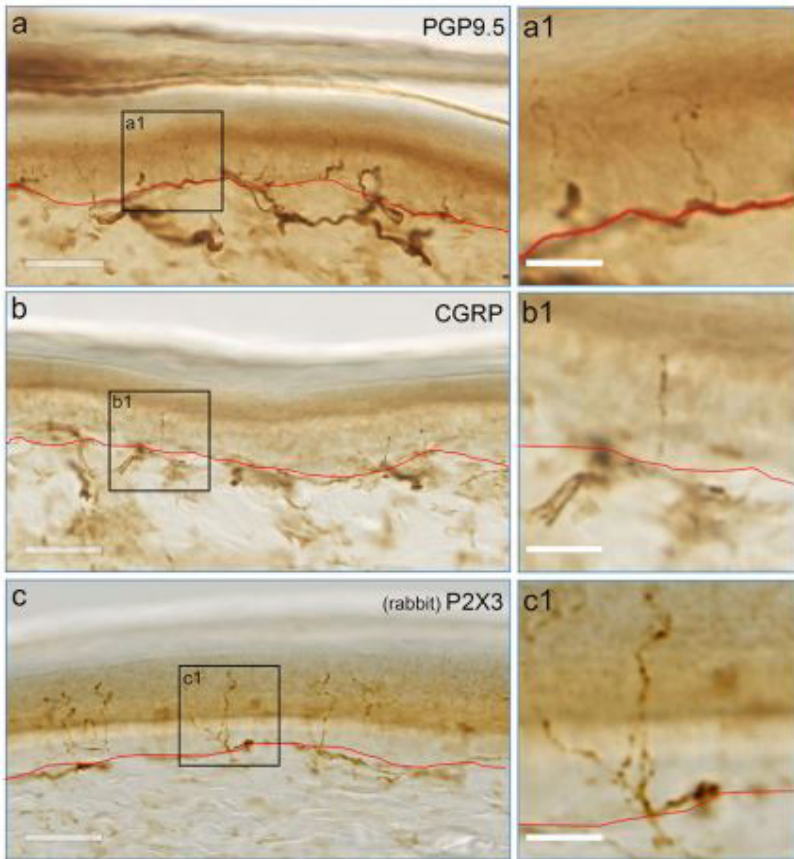


FIGURE 2 Behavioral data of rats that underwent partial ligation of the proximal sciatic nerve (Seltzer model). Combined results of the mean von Frey withdrawal thresholds (grams) and hotplate latencies (seconds), at baseline and 10, 12, and 14 days after nerve ligation, demonstrating tactile and thermal hyperalgesia.

Error bars indicate standard error of the mean (p

$< .001$; repeated measures ANOVAs, source of variation time point; $*p < .05$, $**p < .01$, $***p < .001$; pairwise comparisons of day 0 versus day 10, 12, and 14, using Bonferroni correction; $n = 5$)



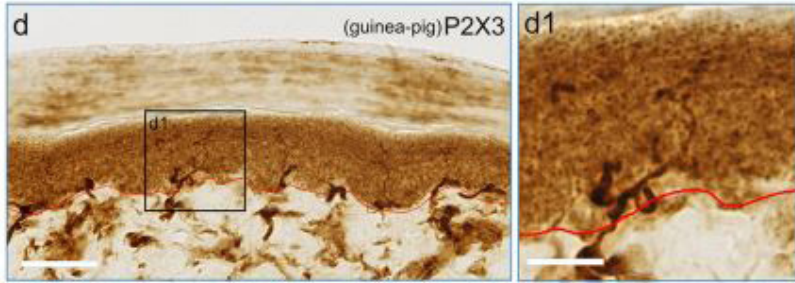


FIGURE 3 Immunohistochemical staining patterns of normal skins. PGP9.5 (a, a1), CGRP (b, b1), P2X3 (rabbit) (c, c1) and P2X3 (guinea pig) (d, d1) immunohistochemistry in skin biopsy sections from the right (normal) hind paw; the red line represents the dermal-epidermal border. The white bars in (a–d) represent 50 mm, the white bars in (a1–d1) represent 10 mm

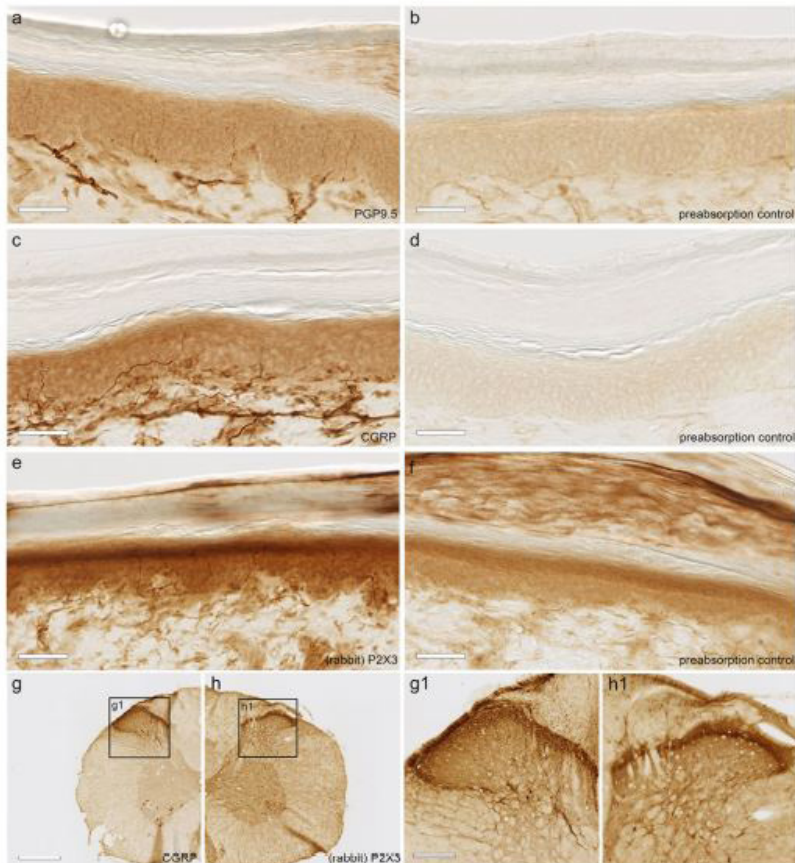


FIGURE 4 Immunohistochemical staining of PGP9.5 (a), CGRP (c) and P2X3 (rabbit) (e) and using pre-absorption controls (b, d, f), in normal skins. Immunohistochemical staining of rat spinal cord, used as a control for the CGRP and P2X3 primary antibodies. (g, h) Immunohistochemical staining of lamina I and II-outer of the dorsal horn with rabbit anti-CGRP (g), of lamina II-inner with rabbit anti-P2X3 (guinea-pig anti-P2X3 gave an identical staining pattern) (h). The white bars in (a–f) represent 1 mm, in (g, h) represent 250 μ m

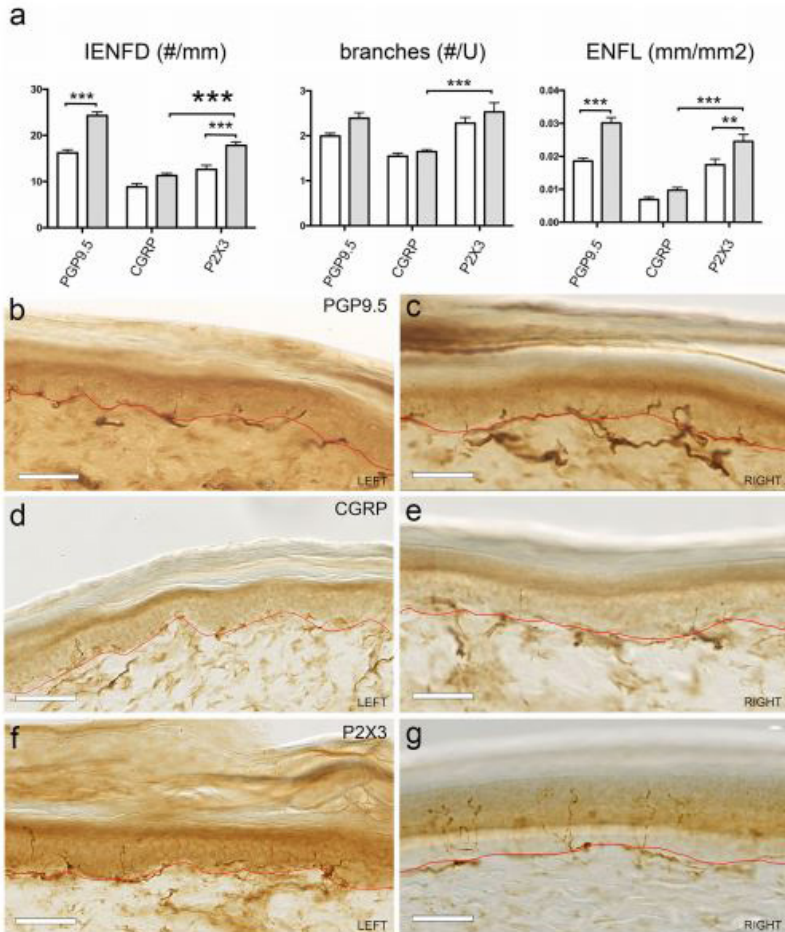


FIGURE 5 Sensitivity of three measures of epidermal innervation for the detection of neuropathy and differences in CGRP and P2X3 innervation in normal skins. (a) Differences in IENFD, number of branches/unit and ENFL between the left (nerve injured; white bars) and the right (normal; grey bars) hind paw (**p < .01, ***p < .001; two-way ANOVAs using Bonferroni correction for multiple testing; n 5 21), and between CGRP and P2X3 labeled fibers on the normal side (***p < .001; paired t-tests; n 5 21). (b–g) The images below the graphs are representative samples of PGP9.5, CGRP and P2X3 immunoreactivity on the left and on the right side. The white bars represent 50 mm

TABLE 2 Reliability analysis

Measure Marker	IENFD		Branches/U		Length	
	Test-retest	Interobserver	Test-retest	Interobserver	Test-retest	Interobserver
PGP _{9.5}	0.72	0.72	0.71	0.67	0.83	0.67
CGRP	0.78	0.98	0.43	0.40	0.83	0.97
P2X ₃	0.79	0.75	0.53	0.06	0.70	0.82

Test-retest reliability and interobserver reliability (intraclass correlation coefficient) for IENFD, number of branches/unit and ENFL for each of the three immunohistochemical markers.

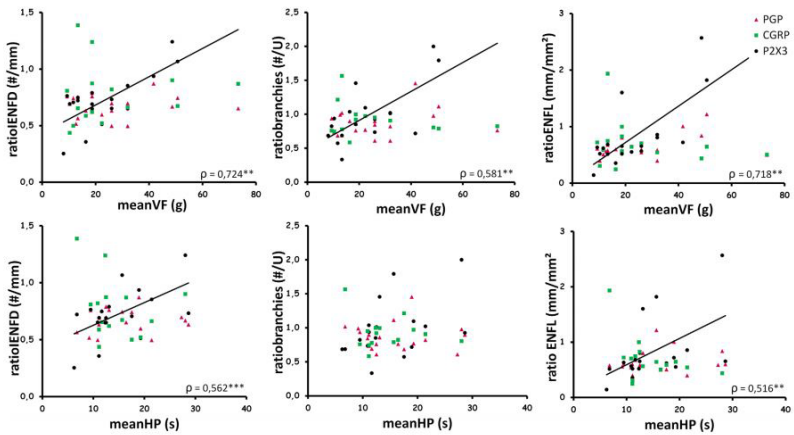


FIGURE 6 Correlations between immunohistochemical markers and behavioral hyperalgesia. The figures represent mean (of day 10, 12, 14) von Frey thresholds and hotplate latencies versus the ratios between left/right IENFD, number of branches/unit and ENFL immunostained with anti-PGP9.5, -CGRP, and -P2X3. Statistically significant correlations between behavior and P2X3-labeled fibers are shown by regression lines (multiple linear regression analysis; q 5 Pearson's correlation coefficients; *p < .05, **p < .01, ***p < .001; n 5 21

CHAPTER V

Clinical, electrophysiological, and cutaneous innervation changes in patients with bortezomib-induced peripheral neuropathy reveal insight into mechanisms of neuropathic pain⁴

Malik Bechakra, Mariska D Nieuwenhoff, Joost van Rosmalen, Geert Jan Groeneveld, Marjan Scheltens-de Boer, Pieter Sonneveld, Pieter A van Doorn, Chris I de Zeeuw and Joost LM Jongen

⁴This chapter has been published in Mol Pain. 2018; 14: 44806918797042.

Abstract

Bortezomib is a mainstay of therapy for multiple myeloma, frequently complicated by painful neuropathy. The objective of this study was to describe clinical, electrophysiological, and pathological changes of bortezomib-induced peripheral neuropathy (BiPN) in detail and to correlate pathological changes with pain descriptors. Clinical data, nerve conduction studies, and lower leg skin biopsies were collected from 22 BiPN patients. Skin sections were immunostained using anti-protein gene product 9.5 (PGP9.5) and calcitonin gene-related peptide (CGRP) antibodies. Cumulative bortezomib dose and clinical assessment scales indicated light-moderate sensory neuropathy. Pain intensity >4 (numerical rating scale) was present in 77% of the patients. Median pain intensity and overall McGill Pain Questionnaire (MPQ) sum scores indicated moderate to severe neuropathic pain. Sural nerve sensory nerve action potentials were abnormal in 86%, while intraepidermal nerve fiber densities of PGP9.5 and CGRP were not significantly different from healthy controls. However, subepidermal nerve fiber density (SENFDF) of PGP9.5 was significantly decreased and the axonal swelling ratio, a predictor of neuropathy, and upper dermis nerve fiber density (UDNFD) of PGP9.5, presumably representing sprouting of parasympathetic fibers, were significantly increased in BiPN patients. Finally, significant correlations between UDNFD of PGP9.5 versus the evaluative Pain Rating Index (PRI) and number of words count (NWC) of the MPQ, and significant inverse correlations between SENFDF/UDNFD of CGRP versus the sensory-discriminative MPQ PRI/NWC were found. BiPN is a sensory neuropathy, in which neuropathic pain is the most striking clinical finding. Bortezomib-induced neuropathic pain may be driven by sprouting of parasympathetic fibers in the upper dermis and impaired regeneration of CGRP fibers in the subepidermal layer.

Introduction

Chemotherapy-induced peripheral neuropathy (CiPN) is a disabling complication, occurring in 10%–50% of patients who are treated for hematological malignancies.^{1,2} Multiple myeloma (MM) is the most common hematological malignancy, with an incidence of 4/100,000/year.³ Although an incurable disease, the life expectancy of MM patients has dramatically increased with the advent of immunomodulatory drugs and proteasome inhibitors about 10 years ago.⁴ Intravenous (i.v.) bortezomib was the first proteasome inhibitor used in clinical practice, firstly in refractory and relapsed MM^{5–7} and later as first-line therapy.^{8,9} Since then, different routes of administration and other proteasome inhibitors have been used in clinical trials, such as subcutaneous (s.c.) bortezomib,¹⁰ i.v. carfilzomib,^{11,12} and oral ixazomib,¹³ often with fewer and/or less severe side effects. However, i.v. bortezomib alone or in combination with other treatment modalities still is a mainstay of therapy for MM.^{14,15}

Bortezomib-induced peripheral neuropathy (BiPN) may occur in up to 50% of patients treated with i.v. bortezomib.^{16–18} The pathological mechanism of BiPN has not been fully elucidated but involves both host, that is, genetic factors,^{19–21} and dose-dependent direct toxicity. Functional and pathological changes in animal models of BiPN are most pronounced in unmyelinated peripheral sensory axons^{22,23} and to a lesser extent present in dorsal roots, dorsal root ganglion cells,^{24,25} and satellite cells.²² It is hypothesized that these changes are mediated through a toxic effect on mitochondria.^{23,26} Clinically, BiPN usually presents as a sensory, often painful, length-dependent (i.e., the longest axons are the earliest and the most affected) axonal peripheral neuropathy,^{8,18,27–29} sometimes with autonomic nerve fiber involvement.^{1,29} Rarely, a demyelinating neuropathy with motor nerve involvement has been described.^{28,30} BiPN, such as most CiPNs, usually has a good prognosis, although some patients develop life-long neuropathic pain or a debilitating sensory neuropathy resulting in ataxia and reduced dexterity.^{1,17,18,29} Because currently there are no evidence-based therapies for the prevention or treatment of BiPN,^{31–33} early recognition is of utmost importance to prevent irreversible neurological damage.¹

Our first aim was therefore to describe the demographic, clinical, electrophysiological, and pathological characteristics of BiPN in detail to aid in the diagnosis of this disabling complication. Pathological changes in nerve fibers were studied in skin biopsies from the lower leg.^{34,35} Since we have previously hypothesized that neuropathic pain may be driven by selective degeneration of subsets of unmyelinated nerve fibers in an animal model of nerve-injury induced pain,³⁶ the second aim of the current study was to use BiPN as a model for nerve-injury induced pain and to study correlations between pathological changes in subsets of unmyelinated nerve fibers in skin biopsies and neuropathic pain descriptors. This way, we aim to test whether the abovementioned hypothesis can be corroborated in humans with neuropathic pain. Thus, BiPN may shed light on mechanisms of neuropathic pain.

Patients and methods

Patients, clinical analyses, nerve conduction studies, and skin biopsies

Between November 2008 and February 2012, 25 patients with a suspected diagnosis of BiPN were referred to the outpatient clinic of the Department of Neurology of Erasmus MC, Rotterdam, the Netherlands. All patients were treated with either bortezomib monotherapy or bortezomib in combination with non-neurotoxic chemo/immunotherapy, that is, hydroxydaunorubicin (n = 8),⁹ lenalidomide (n = 2),³⁷ or rituximab (n = 2). After a diagnosis of BiPN was confirmed on clinical grounds (i.e., a new diagnosis of peripheral neuropathy or a clear deterioration of previously minimally symptomatic peripheral neuropathy following bortezomib), fulfilling the recently published ACTION-APS Pain Taxonomy diagnostic criteria for CiPN³⁸ and the Neuropathic Pain Special Interest Group guidelines for neuropathic pain,³⁹ 22 patients and 17 healthy volunteers who served as controls for the skin biopsy measurements (see subsection “Quantification of nerve fiber densities and swellings”) consented in taking part in the current study. Three patients were excluded because there was no clear temporal relation between bortezomib and the development of neuropathy. The study consisted of the collection of demographic data and clinical data, including pain intensity on a numerical rating scale (NRS) and a sensory sum score that was specifically

designed and validated in our hospital to assess CiPN.⁴⁰ The sensory sum score is a compound measure ranging from 0 to 11 of the presence (1) or absence (0) of paresthesias, numbness, loss of dexterity, unsteadiness of gait, normal (0) or abnormal (1) position sense, vibration sense, pin-prick sensation, Romberg's sign, Romberg's sign with heel-to-toe stand, knee reflex, and ankle reflex. In addition, National Cancer Institute Common Toxicity Criteria of Adverse Events (NCI-CTCAE) v.3.0 for motor neuropathy, sensory neuropathy, and neuralgia/pain (https://ctep.cancer.gov/protocoldevelopment/electronic_applications/docs/ctcae3.pdf); McGill Pain Questionnaires (MPQ; Dutch (n¼ 21) or English (n¼ 1) language versions)^{41,42}; nerve conduction studies (NCS); and 3 mm skin biopsies at the right ankle were performed/collected. For the MPQ, the sum of the sensory-discriminative, affective, and evaluative Pain Rating Indices (PRIs), and the overall sum of PRIs were calculated.^{41,42} In addition, the sum of the number of words count (NWC) for these items were used.^{41,42} NCS consisted of sensory nerve conduction of the sural, ulnar, and median nerve and motor nerve conduction of the peroneal and median nerve. NCS was conducted according to internationally accepted standards,⁴³ and the 3% lower limit of normal of local reference values were used for statistical testing and to determine the percentage of abnormal measurements.

The study was approved by the medical ethical committee of Erasmus MC (MEC-2008-305/NL24284.078.08) and registered at clinicaltrials.gov (NCT00956033).

Histologic processing and immunohistochemistry of skin biopsies

Skin biopsies were taken 10 cm above the right lateral malleolus, under aseptic conditions, and using local anesthesia with 1% lidocaine, using a 3-mm disposable punch. The biopsies were immediately transferred to 2% paraformaldehyde-lysine-sodium metaperiodate fixative and fixed, processed, and stored at 80C according to published guidelines.³⁴ Before cutting, skin biopsies were embedded in 12% gelatin, 10% sucrose blocks, which were left in 4% paraformaldehyde for 2.5 h at room temperature to harden. The gelatin blocks were then kept overnight at 4C in a 30% sucrose solution. Consequently, 50- μ m sections were cut perpendicular to the surface on a freezing microtome and processed as free-floating sections.

The detailed immunohistochemical procedure is described in a recent publication.³⁶ In short, a two-step immunohistochemistry with Streptavidin-Biotin Complex was used for protein gene product 9.5 (PGP9.5), while additional tyramid signal amplification was applied for calcitonin gene-related peptide (CGRP). Concentrations of primary antibodies were 1:10,000 for rabbit anti-PGP 9.5 (Catalog# ADI-905–520; Enzo Life Sciences, Farmingdale, NY), 1:50,000 for guinea pig anti-CGRP (Catalog # 16013; Progen Biotechnik, Heidelberg, DE), and 1:100,000 for rabbit anti-CGRP (Catalog# PC205L; Millipore, Billerica, MA). Omission of the primary antibodies and preabsorbtion of the primary antibodies with a more than 25<?> molar excess of the PGP9.5 protein or CGRP peptide the primary antibodies were raised against were used as negative control experiments.

Since it was impossible to process all sections in one ImmunoRun, sections from 22 BiPN patients, 8 and 9 healthy controls were processed separately, and each primary antibody (anti-PGP9.5 and guinea pig anti-CGRP) was processed separately, although an exactly similar immunohistochemical procedure was followed each time. Thus, six ImmunoRuns were performed altogether. We also attempted to visualize the nonpeptidergic subclass of nociceptors in the skin,³⁶ using a histochemical staining method (i.e., acetylcholinesterase)⁴⁴ and various immunohistochemical markers (i.e., P2X3, IB4, RET, GINIP),^{36,45–47} at varying concentrations and using specific protocols but were unable to obtain reproducible staining patterns allowing for quantification of these fibers.

Quantification of nerve fiber densities and swellings

For quantification of nerve fiber densities and axonal swellings, slides were scanned and digitized using a Hamamatsu NanoZoomer 2.0-HT slide scanner (Hamamatsu Photonics, Hamamatsu City, JP). Sections were analyzed using Leica Aperio ImageScope software (freely available at www.leica-biosystems.com/pathology-imaging/aperio-epathology/integrate/image-scope/) at 40<?> magnification. Four sections per slide and six frames per section were sampled. Frames were selected so that they comprised the entire epidermis, subdermal layer, and at least 50 mm of upper dermis.

The following parameters were manually counted/traced for both PGP9.5 and CGRP, by a single, blinded observer (MB), as previously described³⁶:

1. Intraepidermal nerve fiber density (IENFD) of PGP9.5 and CGRP: the number of crossings of the dermal–epidermal junction per millimeter length of the epidermal surface.³⁴ The length of the epidermal surface was automatically determined by the ImageScope software after tracing.

2. Subepidermal nerve fiber density (SENFDF) of PGP9.5 and CGRP: the number of immunolabeled profiles within the subepidermal layer per millimeter length of epidermal surface.⁴⁸ Branches were not counted as separate profiles.

3. Upper dermis nerve fiber density (UDNFD) of PGP9.5 and CGRP: the number of immunolabeled profiles within the upper dermis per millimeter length of epidermal surface.^{48,49} Branches were not counted as separate profiles.

4. Swelling ratio: the number of axonal swellings of PGP9.5 labeled fibers, with a diameter of at least two to three times the diameter of the axon, divided by the number of intraepidermal nerve fibers, per millimeter length of epidermal surface.^{50,51}

Normative values of IENFD, SENFD, and UDNFD of PGP9.5 and CGRP and axonal swelling ratio were generated from skin biopsies of 17 healthy controls that were processed in our laboratory using exactly the same immunohistochemical and quantification protocol as used for the BiPN skin biopsies.⁵²

As a surrogate for nonpeptidergic innervation, we also calculated IENFD, SENFD, and UDNFD of (PGP9.5 minus CGRP) fibers, since the population of peptidergic and nonpeptidergic nerve fibers are mostly complementary.³⁶

Statistical analysis

Mean and standard deviation (mean SD) of normally distributed continuous variables and median and range (median [range]) of non-normally distributed continuous variables were calculated. The Mann–Whitney test and the chi-square test were used to compare age and sex of healthy volunteers and BiPN patients. One-sample t tests were used to compare nerve conduction velocity results with normative values generated in our laboratory of Clinical Neurophysiology.

Mann–Whitney tests for IENFD, SENFD, and UDNFD were used to compare epidermal innervation of PGP9.5, CGRP, and (PGP9.5-CGRP) and to compare axonal swelling ratios in healthy volunteers and BiPN patients. Bonferroni correction was applied for comparing PGP9.5, CGRP, and (PGP9.5-CGRP) between healthy volunteers and BiPN patients. Mann–Whitney tests, chisquare tests, and independent samples t tests were used to compare demographic data, clinical characteristics, values of NCS, and skin innervation measurements of BiPN patients who had received previous neurotoxic chemotherapy with those of BiPN patients who had not as well as to compare BiPN patients with a duration of neuropathy symptoms 3 months with those with a duration of symptoms >3 months. Spearman’s rank correlation coefficients between pathological changes in subsets of unmyelinated nerve fibers in skin biopsies and neuropathic pain descriptors with p values were determined. The statistical analysis was performed using IBM SPSS Statistics v.21.0.0.0 software (IBM Corp., Armonk, NY). All statistical tests were twosided with a significance level of 0.05.

Results

Clinical, electrophysiological and pathological characteristics of BiPN

Demographic data and clinical and physiological characteristics of the 22 patients with BiPN are listed in Table 1. Patients were predominantly middle-aged men, reflecting the prevalence of MM, which was the most common underlying disorder. Three patients were diagnosed with other plasma cell dyscrasias, that is, Waldenstrom’s disease or plasma cell leukemia and one patient with mantle cell lymphoma. Although 45% of patients had received previous neurotoxic chemotherapy (i.e., vincristine, thalidomide, or a combination of these), only one of the patients had a minimally symptomatic preexisting neuropathy (due to above average alcohol consumption), based on a retrospective review of the medical records. This, however, did not seem to influence our conclusions (see below). The median duration of symptoms until patients were included in the study was two months. Although the duration of symptoms was quite variable ranging from 0.5 to 24 months, findings in patients with a duration of symptoms 3 months were similar to patients with the duration of symptoms >3

months (see below). The age and sex of the 22 patients with BiPN were not statistically significantly different from the 17 healthy volunteers (respective median [range] ages: 63 [39–79] and 63 [27–78] years; male:female ratio of 19:3 and 10:7; $p = 0.305$, Mann–Whitney test; $p = 0.051$, chi-square test).

A mean cumulative bortezomib dose of 15 mg/m², a mean sensory sum score of 6.8, and a median NCICTCAE of 2 for sensory neuropathy and/or pain in our patients indicated light-moderate sensory neuropathy. Pain intensity >4 was present in 77% of the patients, indicating small nerve fiber involvement in the majority of cases, although orthostatic hypotension was present in only 38% of patients. A median pain intensity of 7 [0–9] and a mean overall sum of MPQ PRIs of 19–11 indicated moderate neuropathic pain. In addition, 55% of patients were using adjuvant analgesics (i.e., antidepressants or anticonvulsants), while 27% were using opioids.

In Table 2, the results of NCS are summarized. Only the mean sural nerve sensory nerve action potential (SNAP) amplitude was below the 3% lower limit of normal (LLN; in 19/22 or 86% of patients), based on normative values generated in our laboratory of Clinical Neurophysiology ($p < 0.001$; one-sample t test). In Figure 1, representative PGP9.5 and CGRP immunohistochemical staining patterns in the epidermis, subepidermal layer, and upper dermis are presented, from patients with BiPN (Figure 1(a) and (c)) and from healthy volunteers (Figure 1(b) and (d)). PGP9.5 and CGRP both labeled bundles of fibers just below and running parallel to the basement membrane, which were sometimes associated with blood vessels. From these bundles, thin and varicose fibers originated that ran almost perpendicular to their origins, thus penetrating the basement membrane. In the epidermis, PGP9.5 labeled fibers were more abundant, generally longer, sometimes reaching almost up to the stratum corneum, and had more branches per unit than CGRP fibers. The density of PGP9.5 and CGRP intraepidermal nerve fibers appeared similar in healthy volunteers and BiPN patients, although the density of PGP9.5 fibers appeared lower in the subepidermal layer and higher in the upper dermis in BiPN patients compared to healthy volunteers. Looking in close detail (see insets in Figure 1), PGP9.5-positive intraepidermal nerve fibers also showed axonal swellings, both small (2–3 times

the nerve diameter) and large (>5 times the nerve diameter). These nerve swellings were more abundant in BiPN patients than in healthy volunteers.

To control for nonspecific staining of primary antibodies, the same immunohistochemical protocol was used, except that the primary antibodies were omitted or preabsorbed with the protein or peptide they were raised against, which resulted in a complete abolishment of specific signal for all antibodies used (Figure 2(a)–(d)). Guinea pig anti-CGRP (see also Axelsson et al.53) and rabbit anti-CGRP (see also Bechakra et al.36) gave similar staining patterns in the skin sections, although guinea pig anti-CGRP showed less background staining in our hands (Figure 2(e) and (f)). Therefore, guinea-pig anti-CGRP was used for quantitative analyses. The specificity of anti-PGP9.5 and anti-CGRP antibodies has also been extensively tested on rat skins in previous experiments in our laboratory.36

In Figure 3, the results of IENFD (Figure 3(a)), SENFD (Figure 3(c)), and UDNFD (Figure 3(d)) of PGP9.5, CGRP, and (PGP9.5-CGRP) are summarized, in healthy volunteers and BiPN patients. Swelling ratios of intraepidermal PGP9.5 fibers are presented in Figure 3(b). SENFD of PGP9.5 and (PGP9.5-CGRP) was significantly decreased, while UDNFD of PGP9.5 and (PGP9.5-CGRP) and the axonal swelling ratio were significantly increased in BiPN patients compared to healthy volunteers ($p < 0.001$, $p < 0.001$, $p < 0.001$, $p \approx 0.001$ and $p \approx 0.001$ respectively; Mann–Whitney tests, using Bonferroni correction with an adjusted significance of 0.017).

To control for a potential influence of previous neurotoxic chemotherapy on clinical characteristics, values of NCS and skin innervation measurements, BiPN patients who had received previous neurotoxic chemotherapy ($n \approx 10$) were compared with BiPN patients who had not ($n \approx 12$). None of the 41 outcome measures in

Tables 1 and 2 and Figure 3 were significantly different ($p > 0.05$; uncorrected Mann–Whitney, chi-square tests and independent-samples *t* tests), except that the median age of former group (58 years) was lower than that of the latter (65 years) (uncorrected $p \approx 0.026$; Mann–Whitney test). The age-dependent outcome measures mean sural nerve amplitude was 1.4 mV (9/10 patients below the LLN) in the pretreated group and 1.7 mV (10/12 patients below the LLN) in the nonpretreated group, median IENFD of PGP9.5 was 5.5/mm in

the pretreated group and 5.1/mm in the nonpretreated group (uncorrected $p = 0.88$ and 0.60 , respectively; independent-sample t test, Mann–Whitney test).

To control for a potential influence of the duration of symptoms on clinical characteristics, values of NCS and skin innervation measurements, patients with a duration of symptoms 3 months (i.e., (sub)acute neuropathy; $n = 16$) were compared with patients with a duration of symptoms >3 months (i.e., chronic neuropathy; $n = 6$). None of the 41 outcome measures in Tables 1 and 2 and Figure 3 were significantly different ($p > 0.05$; uncorrected Mann–Whitney, chi-square tests, and independent-samples t tests).

Correlations between pathological changes in subsets of unmyelinated nerve fibers in skin biopsies and descriptors of BiPN-induced neuropathic pain

There were no statistically significant correlations between cumulative bortezomib dose, SSS, NCICTCAE, sural nerve SNAP, IENFD of PGP9.5, and swelling ratio on the one hand, and NRS, MPQ overall sum of PRIs, adjuvant analgesic medication, and morphine equivalent dose on the other hand ($p > 0.05$; Spearman's correlations), except for correlations between NCI-CTCAE sensory neuropathy and neuralgia/pain versus adjuvant analgesic medication (uncorrected $p = 0.047$ and 0.030 ; Spearman's correlations).

In Table 3, correlations between the nerve fiber densities for each immunohistochemical marker versus the sensory-discriminative, affective, and evaluative MPQ PRIs and NWCs are presented, with their respective uncorrected p values. Here, correlations between UDNFD of PGP9.5 versus the evaluative MPQ PRI ($q = 0.447$) and NWC ($q = 0.427$) were found, and inverse correlations between UDNFD of CGRP versus the sensory-discriminative MPQ PRI ($q = 0.422$) and SENFD of CGRP versus the sensory-discriminative MPQ NWC ($q = 0.423$) were found ($p = 0.05$; Spearman's correlations). In addition, p values 0.1 were demonstrated for inverse correlations between IENFD and UDNFD of CGRP versus the sensory discriminative MPQ PRI and NWC and positive correlations between IENFD of PGP9.5

and (PGP9.5-CGRP) versus the affective MPQ PRI ($0.422 < q < 0.413$; $p > 0.1$; Spearman's correlations, for exact values of q and p , see Table 3).

Discussion

Our study reports the clinical, electrophysiological and pathological changes in a cohort of 22 patients with BiPN. The results indicate a light-moderate sensory neuropathy, in which neuropathic pain is the most striking clinical finding. NCS was within the normal range, apart from a significantly reduced mean sural nerve SNAP which was below the lower limit of normal in 86% of patients, consistent with a length-dependent axonal sensory neuropathy. IENFD of PGP9.5 was not significantly decreased compared to healthy volunteers. SENFD of PGP9.5, however, was significantly lower than in healthy volunteers. Furthermore, the axonal swelling ratio and UDNFD of PGP9.5 were significantly increased.

Finally, significant positive correlations between UDNFD of PGP9.5 versus the evaluative PRI and NWC of the MPQ, and significant inverse correlations between SENFD of CGRP versus the sensorydiscriminative MPQ NWC and UDNFD of CGRP versus the sensory-discriminative MPQ PRI were found. Clinical, pathological and electrophysiological characteristics of BiPN

All patients were treated with either bortezomib monochemotherapy or bortezomib in combination with nonneurotoxic chemo/immunotherapy. Although the fact that 45% of the patients had received previous neurotoxic therapy is a potential weakness of this study, outcome measures were not significantly different between BiPN patients who had received previous neurotoxic therapy and patients who had not, except that the median age of the pretreated group was seven years younger. There is no reason to suspect that this relatively small age difference might (indirectly) have influenced our conclusions, since the age-dependent outcome measure sural nerve amplitude was also abnormal in 10/12 of nonpretreated patients and IENFD of PGP9.5 was (not significantly) higher in the pretreated group. Thus, even if baseline data were not systematically assessed, our study population was quite homogeneous and there were no major confounding factors. In addition, the wide range of the duration of symptoms did not seem to affect our conclusions.

In comparison to earlier reports of BiPN, the cumulative bortezomib dose at the presentation of neuropathy was relatively low and the severity of neuropathy in our cohort was rather mild.^{8,9,18,54}

An obvious reason may be the fact that the referring hemato-oncologists in our academic cancer center are very keen on a suspected evolving neuropathy and had sent those patients to our Outpatient Clinic of Neurology for consultation at an early stage. This has to be taken into consideration when comparing our results with the literature.

Since it was previously suggested that predominantly small diameter nerve fibers are affected in BiPN^{27,55,17,18}, skin biopsies were collected and analyzed for innervation densities in all patients, as the epidermis exclusively contains unmyelinated nerve fibers.⁵⁶ Although an immunofluorescent technique may give clearer labeling, less background staining and provide an opportunity for double and triple labeling,^{57,58} bright field immunohistochemistry was used to label nerve fibers in this study, since we have previously validated this technique and reference values were generated in our own lab. Apart from a few cases^{8,55,59} and a small cohort,⁶⁰ systematic skin biopsies in patients with BiPN have not been reported. The aforementioned studies represent highly selected cases or a small series as part of CiPN in general; therefore, it is impossible to draw any conclusions about the validity of IENFD in BiPN from them. Our study is the first that systematically assesses nerve fiber densities of PGP9.5 and CGRP in skin biopsies from BiPN patients. Skin biopsies were obtained from the hairy skin at the ankle and processed and quantified according to published international guidelines.^{34,35} We not only assessed IENFD of PGP9.5, but also SENFD and UDNFD,^{48,49} since these measures may provide additional information on innervation changes in the skin, especially in relation to neuropathic pain indices.⁴⁸

In addition, IENFD, SENFD and UDNFD were determined for CGRP.⁴⁸ CGRP is generally considered a valid marker for the peptidergic subclass of C-fibers,^{36,61} which is localized within sympathetic nerve fibers as well.⁶² Direct staining of the nonpeptidergic subclass of nerve fibers in the skin biopsies was unsuccessful (see Materials and Methods section). As far as we are aware there are no reports in the literature

regarding quantifiable (epi)dermal labeling of nonpeptidergic nerve fibers in humans either. Since it is hypothesized that peptidergic and nonpeptidergic nociceptors are mostly complementary and may each convey specific information about pain along labeled lines to the spinal cord and brain,^{63,64} we decided to use IENFD, SENFD and UDNFD of the difference (PGP9.5-CGRP) as surrogate markers for the number of nonpeptidergic fibers in order to get a complete picture of skin innervation in our cohort of BiPN patients. Finally, since our cohort contained patients with relatively mild BiPN, we also calculated the percentage of axonal swellings in epidermal PGP9.5 fibers, which may be considered an early indicator of nerve degeneration, preceding nerve terminal loss.^{50,51,65}

Contrary to the notion that bortezomib predominantly affects small diameter nerve fibers, we found that the sural nerve SNAP, which only represents large diameter nerve fibers, was significantly decreased, while IENFD of PGP9.5 and CGRP were not. One explanation for this lack of a decrease in IENFD may be the fact that the main symptoms of BiPN are focused in the glabrous skin under the foot while skin biopsies were collected 10 cm above the lateral malleolus (according to international guidelines).³⁴ Furthermore, NCS is a physiological measure to evaluate functional pathology while Wallerian degeneration, that is, structural damage, may only occur at a later stage. A significant increase in the axonal swelling ratio of unmyelinated epidermal nerve fibers is in line with this idea. Secondly, SENFD of PGP9.5 was decreased in our cohort of BiPN patients, as has also been observed in other neuropathies with small nerve fiber involvement.^{48,49} Our observations therefore confirm that bortezomib does affect small diameter nerve fibers indeed.

Correlations between pathological changes in subsets of unmyelinated nerve fibers in skin biopsies and descriptors of BiPN-induced neuropathic pain

Neuropathic pain was the most prevalent symptom in our cohort of BiPN patients, occurring in 77% of patients. No consistent correlation between changes in (epi)dermal innervation and neuropathic pain intensity has been described in patients with neuropathy.^{48,56,66} This may be caused by mixed pathology, for example, in painful diabetic neuropathy, or by the fact that

selective degeneration of a subset of nociceptors, which may not be detected using the pan axonal marker PGP9.5, may drive hyperalgesia and eventually neuropathic pain.³⁶ Our cohort of BiPN-patients was very well suited to study the pathophysiological changes that may lead to neuropathic pain, since there was no mixed pathology and we used both CGRP immunohistochemistry and a (surrogate) marker for nonpeptidergic nerve fibers.

It has previously been demonstrated that sprouting of parasympathetic fibers into the upper dermis occurs due to the loss of nonpeptidergic fibers in the subepidermis, while sprouting of sympathetic fibers into the upper dermis occurs due to the loss of peptidergic fibers.^{45,67,68} We found an increased UDNFD of PGP9.5 and a decreased SENFD of (PGP9.5-CGRP), while UDNFD of CGRP, which is also expressed in sympathetic neurons,⁶² was not increased, and there was no loss of peptidergic fibers in the subepidermis. Therefore, even if we did not provide direct evidence, we suggest that the increased UDNFD of PGP9.5 represents sprouting of parasympathetic fibers. Although less studied than the sympathetic nervous system in mediating chronic pain, acetylcholine from parasympathetic nerve fibers may also sensitize nociceptor terminals in the skin.^{69,70} Furthermore, the apparent sprouting of parasympathetic fibers in the upper dermis appeared to correlate with the evaluative PRI and NWC of the MPQ. Thus, our findings may indicate that parasympathetic fiber sprouting into the upper dermis plays a role in mediating neuropathic pain, specifically the evaluative component.

A second striking finding was that SENFD of CGRP was not significantly reduced, although SENFD of PGP9.5 and (PGP9.5-CGRP) were. This may suggest that CGRP-fiber reinnervation of the subepidermis, which has been shown previously in rats,^{36,71} also occurs in humans. Apparently, this reinnervation was insufficient to salvage normal pain sensation, since SENFD of CGRP was negatively correlated with the sensory-discriminatory NWC of the MPQ, and UDNFD of CGRP was negatively correlated with the sensory-discriminatory PRI. Borderline significant negative correlations of IENFD of CGRP and UDNFD of CGRP versus sensory-discriminative PRI and NWC further support this notion.

In contrast, a borderline significant positive correlation of IENFD of PGP9.5 and (PGP9.5-CGRP) versus the affective PRI of the MPQ was found, highlight-

ing the possibility that reinnervation of nonpeptidergic nerve fibers directly or indirectly (i.e., via parasympathetic sprouting, see above) contributes to the affective component of BiPN-induced neuropathic pain. This component may be further modulated at the spinal level via glutamate receptors.^{72,73}

Taken together, the observed correlations of CGRP nerve fibers with the sensory-discriminative component, of parasympathetic nerve fibers with the evaluative component and possibly nonpeptidergic nerve fibers with the affective component of neuropathic pain fit well with the hypothesis of parallel pain pathways that serve different pain qualities.^{36,63,64} It also fits with the clinical observation that neuropathic pain patients often report relatively mild pain intensities on a NRS scale (the sensorydiscriminative component) in relation to their suffering (the evaluative and affective component), since nonpeptidergic afferents may be more characteristically involved in neuropathic pain.⁷²

In conclusion, BiPN is a sensory neuropathy, in which neuropathic pain is the most striking clinical finding. Since IENFD of PGP9.5 may be normal, NCS and axonal swelling ratios may be more sensitive ancillary investigations. Secondly, nociceptor subset specific changes may (directly or indirectly) contribute to the sensory-discriminative, evaluative, and affective components of neuropathic pain. Although the MPQ is impractical for use in routine clinical practice, we suggest to rate pain intensity as well as pain unpleasantness, using a NRS, to take into account both the sensorydiscriminative and the and affective components of neuropathic pain in BiPN patients. Furthermore, selective targeting of these subsets may increase our understanding of neuropathic pain and may aid in developing better pharmaceuticals that alleviate not only pain intensity but also the affective component of neuropathic pain.

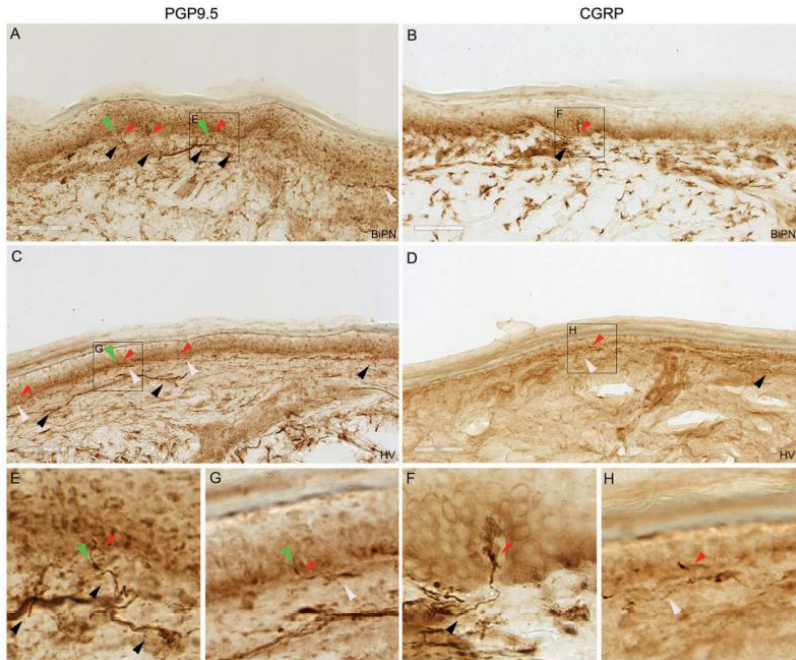
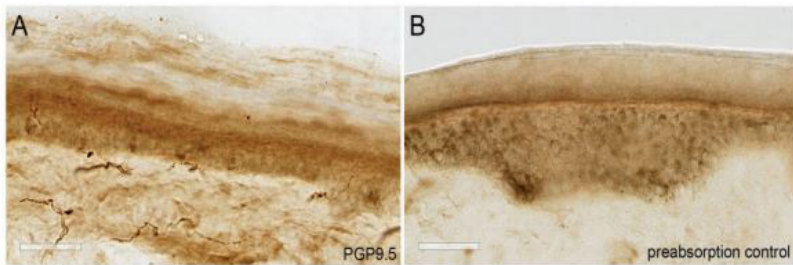


Figure 1. Immunohistochemical staining patterns of PGP9.5 (a and c) and CGRP (b and d) in BiPN patients (a and b) and healthy volunteers (c and d). (e) to (h) represent high-power insets, which enable to visualize the length of the intraepidermal fibers, branching pattern and intraepidermal axonal swellings. Red arrows represent intraepidermal nerve fibers, white arrows represent subepidermal nerve fibers, black arrows represent upper dermal nerve fibers, and green arrows represent axonal swellings. The white bars measure 50 μ m. CGRP: calcitonin gene-related peptide; PGP9.5: protein gene product 9.5.



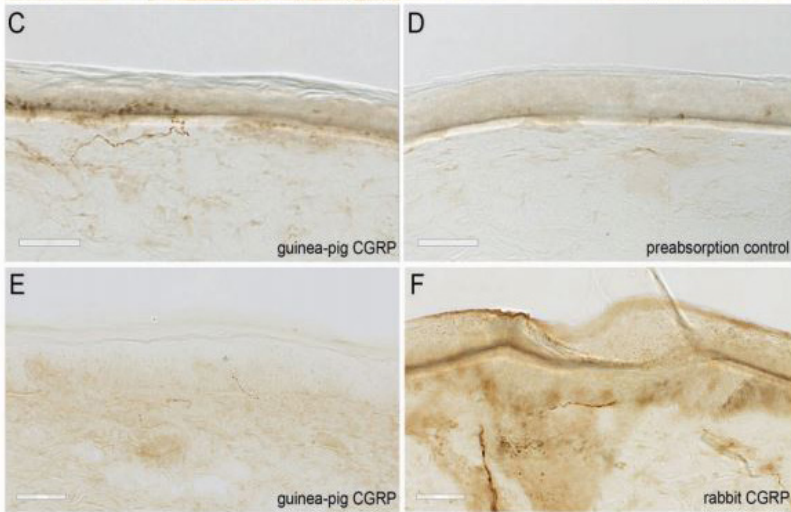


Figure 2. Immunohistochemical staining patterns of PGP9.5 (a) and CGRP (guinea-pig) (c) and using preabsorption controls (b and d), in normal skins. Immunohistochemical staining patterns in normal skins, comparing a guinea pig (e) and a rabbit anti-CCRP antibody (f). The white bar measures 50 μ m.

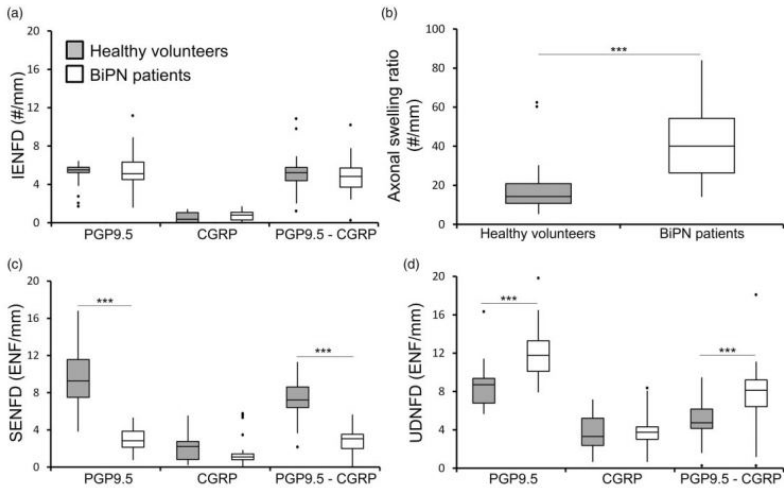


Figure 3. Skin innervation measurements in BiPN patients ($n = 22$) and healthy volunteers ($n = 17$). Box plots showing the median, interquartile range, range, and outliers of the number of intraepidermal (IENFD; a), subepidermal (SENFD; c), upper dermal (UDNFD; d) nerve fiber

density, and the axonal swelling ratios (b), using PGP9.5, CGRP, and (PGP9.5-CGRP) as markers to measure the total number of fibers and peptidergic and nonpeptidergic subclasses, ***p 0.001; Mann–Whitney tests, using Bonferroni correction with an adjusted significance level of 0.017.

Table 1. Demographic data and clinical characteristics.

	n (%) = 22	Mean ± SD Median [range]
Demographic data		
Age (years)		63 [39–79]
Sex (male)	19 (86%)	
Diagnosis (multiple myeloma)	18 (82%)	
Previous neurotoxic therapy	10 (45%)	
Previous neuropathy	1 (4.5%)	
Duration of BiPN (months)		2 [0.5–23]
Cumulative bortezomib dose (mg/m ²)		15 ± 7.9
Neurologic examination		
SSS (0–11)		6.8 ± 3.2
Orthostatic hypotension	8 (36%)	
NCI-CTCAE sensory neuropathy		2 [0–3]
NCI-CTCAE neuralgia/pain		2 [0–3]
Neuropathic pain		
Pain intensity (>4)	17 (77%)	7 [0–9]
McGill pain questionnaire		
PRI-Sensory (0–36 points)		11 [4–22]
PRI-Affective (0–15 points)		3 [0–8]
PRI-Evaluative (0–12 points)		6 [2–9]
PRI-Total (0–63 points)		20 [10–37]
NWC-Sensory (0–12 words)		7 [3–12]
NWC-Affective (0–5 words)		7 [0–5]
NWC-Evaluative (0–8 words)		3 [2–3]
NWC-Total (0–20 words)		13 [7–20]
Pain medication		
Adjuvant analgesics	12 (55%)	
Opioids/MED	6 (27%)	7 [7–60]

n = 22; SD: standard deviation; BiPN: bortezomib-induced peripheral neuropathy; SSS: sensory sum score; NCI-CTCAE: National Cancer Institute-Common Toxicity Criteria for Adverse Events; PRI: Pain Rating Index; NWC: number of words count; MED: morphine equivalent dose.

Table 2. Mean ± SD values of nerve conduction studies.

	SNAP (μV)	NCV (m/s)	CMAP (μV)
Sural nerve	1.5 ± 2.3 ^{***} (86%)	39.3 ± 5.9 ^a (50%)	–
Ulnar nerve	6.2 ± 7.4 (50%)	42.3 ± 6.9 ^a (60%)	–
Median nerve	9.9 ± 7.2 (43%)	43.5 ± 7.9 ^a (52%)	7.2 ± 1.6 (0%)
Peroneal nerve	–	39.3 ± 6.8 ^b (26%)	2.1 ± 2.3 (50%)

Note: Percentages between brackets indicate the fraction of patients with abnormal values compared to normative values; one sample t test; n = 22. CMAP: compound muscle action potential; SNAP: sensory nerve action potential; NCV: nerve conduction velocity; SD: standard deviation.

^{a,c}Sensory NCV; ^bMotor NCV.

^{***}p < 0.001.

Table 3. Correlations between immunohistochemical markers and MPQ, PRI, and NWC.

MPQ	IENFD			SENFd			UDNFd		
	PGP9.5	CGRP	PGP-CGRP	PGP9.5	CGRP	PGP-CGRP	PGP9.5	CGRP	PGP-CGRP
PRI-Sensory	0.637	0.106 0.079	–0.382 0.694 0.089 0.648	–0.103 0.139	–0.326	0.240 0.261 0.553	–0.134	0.050	–0.422 ^a 0.596 0.120
PRI-Affective	0.056	0.413 0.825	–0.050 0.075 0.388 0.466	0.164 0.903	–0.028	0.206 0.280 0.576	0.126	0.831	–0.048 0.533 0.140
PRI-Evaluative	0.271	0.245 0.276	0.243 0.388 0.193 0.192	0.289 0.618	0.113	0.943 0.016 0.037	0.447^a	0.427	0.179 0.231 0.266
NWC-Sensory	0.998	–0.001 0.064	–0.401 0.939 0.017 0.405	–0.187 0.050	–0.423 ^a	0.312 0.226 0.189	–0.291	0.071	–0.392 0.883 –0.033
NWC-Affective	0.457	0.167 0.421	–0.181 0.453 0.169 0.760	0.069 0.923	–0.022	0.216 0.275 0.926	–0.007	0.407	–0.186 0.674 0.095
NWC-Evaluative	0.621	0.111 0.088	0.373 0.805 0.056 0.935	–0.019 0.279	0.241	0.279 –0.241 0.047	0.427^a	0.870	–0.037 0.107 0.353

Note: Numerals in the left column refer to p values, and numerals in the right column refer to Spearman's correlation coefficients. Correlation coefficients with an uncorrected p ≤ 0.05 are printed in bold with an asterisk, correlation coefficients with a p ≤ 0.1 are printed in italics; n = 22. MPQ: McGill Pain Questionnaire; IENFD: intraepidermal nerve fiber density; SENFD: subepidermal nerve fiber density; UDNFD: upper dermis nerve fiber density; CGRP: calcitonin gene-related peptide; PGP: protein gene product.

CHAPTER VI

Pain-related changes in cutaneous innervation of patients suffering from bortezomib-induced, diabetic or chronic idiopathic axonal polyneuropathy⁵

Malik Bechakra, Mariska D. Nieuwenhoff, Joost van Rosmalen, Geert Jan Groeneveld, Frank J.P.M. Huygenc, Chris I. de Zeeuw, Pieter A. van Doorn and Joost LM Jongen

⁵This chapter has been published in Brain Research Volume 1730, 1 March 2020, 146621.

Abstract

Consistent associations between the severity of neuropathic pain and cutaneous innervation have not been described. We collected demographic and clinical data, McGill Pain Questionnaires (MPQ) and skin biopsies processed for PGP9.5 and CGRP immunohistochemistry from patients with bortezomib-induced peripheral neuropathy (BiPN; n = 22), painful diabetic neuropathy (PDN; n = 16), chronic idiopathic axonal polyneuropathy (CIAP; n = 16) and 17 age-matched healthy volunteers. Duration of neuropathic symptoms was significantly shorter in patients with BiPN in comparison with PDN and CIAP patients. BiPN was characterized by a significant increase in epidermal axonal swellings and upper dermis nerve fiber densities (UDNFD) and a decrease in subepidermal nerve fiber densities (SENF) of PGP9.5-positive fibers and of PGP9.5 containing structures that did not show CGRP labeling, presumably non-peptidergic fibers. In PDN and CIAP patients, intraepidermal nerve fiber densities (IENFD) and SENFD of PGP9.5-positive and of non-peptidergic fibers were decreased in comparison with healthy volunteers. Significant unadjusted associations between IENFD and SENFD of CGRP-positive, i.e. peptidergic, fibers and the MPQ sensory-discriminative, as well as between UDNFD of PGP9.5-positive fibers and the MPQ evaluative/affective component of neuropathic pain, were found in BiPN and CIAP patients. No significant associations were found in PDN patients. Cutaneous innervation changes in BiPN confirm characteristic features of early, whereas those in CIAP and PDN are in line with late forms of neuropathic pathology. Our results allude to a distinct role for non-peptidergic nociceptors in BiPN and CIAP patients. The lack of significant associations in PDN may be caused by mixed ischemic and purely neuropathic pain pathology.

Introduction

Neuropathic pain is a frequent complication of peripheral neuro-pathies, such as bortezomib-induced peripheral neuropathy (BiPN; occurring in 25–80% of patients (Jongen et al., 2015; Rampen et al., 2013), painful diabetic neuropathy (PDN; in 16–40% of patients (Javedet al., 2015; Jongen et al., 2018) and chronic idiopathic axonal poly-neuropathy (CIAP; in 42% of patient (Erdmann et al., 2010; Hanewinkel et al., 2016; Warendorf et al. 2017).

PDN and CIAP are both examples of chronic peripheral neuropathies, while an acute or subacute neuropathy often presents with BiPN, in contrast to other chemotherapy-induced peripheral neuropathies (Jongen et al., 2015; Rampen et al., 2013; Richardson et al., 2012). Specific alterations have been observed in (sub)acute as opposed to chronic neuropathies. Axonal swellings, containing accumulations of mitochondria, usually occur early in the course of distal symmetric peripheral neuropathies, while (epi)dermal nerve fiber loss and degenerative Schwann cell changes occur as late consequences (Bennett et al., 2014; Ebenezer et al., 2007; Lauria et al., 2003).

Apart from a recent study that showed a correlation between GAP43 intraepidermal nerve fiber density and the severity of burning pain in PDN patients (Galosi et al., 2018), no consistent associations between cutaneous innervation and the severity of neuropathic pain have been described (Kalliomaki et al., 2011; Lindenlaub and Sommer, 2002; Schley et al., 2012; Vlckova-Moravcova et al., 2008). This may be explained by mixed pathology, for example in painful diabetic neuropathy, or by the fact that selective degeneration of a subset of nociceptors, which may not be detected using the pan axonal marker PGP9.5, may drive hyperalgesia and eventually neuropathic pain. We have recently published two papers, one in a rat-model of nerve-injury induced pain (Bechakra et al., 2017) and one in patients with BiPN (Bechakra et al., 2018), suggesting that selective degeneration of nonpeptidergic nerve fibers may directly or indirectly (via parasympathetic sprouting) contribute to the affective and evaluative component of neuropathic pain. Non-peptidergic nerve fibers have already previously been considered to be more characteristically involved in neuropathic pain (Willcockson and Valtchanoff, 2008), since sensory qualities that are distinct in neuropathic pain, like paresthesias, burning pain and

tactile allodynia, are typically experienced in skin, which is predominantly innervated by non-peptidergic nerve fibers (Guedon et al., 2016). Peptidergic nerve fiber loss on the other hand may contribute to the sensory-discriminative component of neuropathic pain in BiPN patients (Bechakra et al., 2018). The McGill Pain questionnaire (Melzack and Torgerson, 1971; Melzack, 2005), a reliable and extensively validated test in many languages, was specifically designed to discern the sensory-discriminative, affective and evaluative components of neuropathic pain. More recently it has been suggested that separate anatomical pathways exist for these respective components (Braz et al., 2005; Craig, 2003).

The aim of the current study is to further explore the hypothesis that selective degeneration of nociceptors in neuropathic pain syndromes can be associated with distinctive pain qualities, by comparing the pathology and pain perception among BiPN, PDN and CIAP patients.

Results

In Table 1, demographic data and clinical characteristics of 17 healthy volunteers, 22 patients with BiPN (previously described in (Bechakra et al., 2018)), 16 patients with PDN (previously described in (Emanuel et al., 2017)) and 16 patients with CIAP are listed. Median ages and percentages of males were not significantly different among the four groups ($p = 0.453$ and $p = 0.139$, using Kruskal-Wallis and chi-square test respectively). Median and range of duration of neuropathy symptoms until the moment of study entry was significantly shorter in BiPN patients (2 [0.5–23] months) than in PDN (36 [8–60] months) and in CIAP patients (60 [12–132]), while the difference between PDN and CIAP patients was not significantly different ($p < 0.001$, $p < 0.001$ and $p = 0.831$ respectively; Kruskal-Wallis test with post-hoc comparisons using Dunn's test). Additionally, 16 out of 22 BiPN patients were considered to have (sub) acute neuropathies (i.e. duration of neuropathy symptoms ≤ 3 months), whilst none of the PDN or CIAP patients had. Median time between a diagnosis of diabetes and inclusion in the study of PDN patients was 144 [12–408] months.

In Fig. 1 representative PGP9.5 and CGRP immunohistochemical staining patterns in the epidermis, subepidermal layer and upper dermis are presented,

from healthy volunteers (Fig. 1A, B, I and J), patients with BiPN (Fig. 1C, D, K and L), patients with PDN (Fig. 1E, F, M and N) as well as patients with CIAP (Fig. 1G, H, O and P). Characteristic staining patterns of these fibers, including orientation, morphology and branching of PGP9.5 and CGRP positive fibers as well as immunohistochemical control experiments have been previously described by our group (Bechakra et al., 2018). The density of PGP9.5 positive intraepidermal nerve fibers appeared lower in PDN and in CIAP patients, while the density of upper dermal fibers appeared higher in BiPN patients. Looking in close detail (see insets in Fig. 1), PGP9.5- positive intraepidermal nerve fibers also showed axonal swellings, both small (2–3× the nerve diameter) and large (> 5× the nerve diameter). These nerve swellings appeared more abundant in BiPN patients compared to the other groups.

In Fig. 2 the results of IENFD (Fig. 2A), SENFD (Fig. 2C) and UDNFD (Fig. 2D) of PGP9.5, CGRP and (PGP9.5-CGRP) are summarized. Swelling ratios of intraepidermal PGP9.5 fibers are presented in Fig. 2B. In CIAP patients, IENFD of PGP9.5 and of (PGP9.5-CGRP), i.e. presumed non-peptidergic fibers, were significantly decreased in comparison with healthy volunteers ($p = 0.007$ and $p = 0.015$ respectively), while in PDN patients IENFD of (PGP9.5-CGRP) was significantly decreased ($p = 0.030$) and the decrease in IENFD of PGP9.5 almost reached statistical significance ($p = 0.054$; Kruskal-Wallis test with post-hoc comparisons using Dunn's test). Similarly, significant decreases were found for SENFD of PGP9.5 ($p = 0.006$) and of (PGP9.5-CGRP) ($p = 0.006$) in CIAP and in PDN patients ($p = 0.006$ and $p = 0.006$ respectively). BiPN patients were characterized by a significant increase in epidermal axonal swellings ($p < 0.001$) and upper dermis nerve fiber densities (UDNFD) of PGP9.5 ($p = 0.015$) and of (PGP9.5-CGRP) ($p = 0.015$), whilst a significant decrease was found in SENFD of PGP9.5 ($p < 0.001$) and of presumed non-peptidergic fibers ($p < 0.001$; Kruskal-Wallis test with post-hoc comparisons using Dunn's test), as previously described (Bechakra et al., 2018). IENFD, SENFD and UDNFD of CGRP fibers in BiPN, PDN and CIAP patients were not significantly different from healthy volunteers.

In Table 2 correlations between the nerve fiber densities for each immunohistochemical marker and the sensory-discriminative, affective and evaluative PRIs and NWCs with corresponding p-values and Spearman's rank correlation

coefficients are presented. In BiPN patients, the correlations between UDNFD of PGP9.5 and the evaluative MPQ PRI and NWC were $\rho = 0.447$; $p = 0.037$ and $\rho = 0.427$; $p = 0.047$ respectively (not significant following Bonferroni correction with an adjusted significance level of 0.017) and there was an unadjusted significant negative correlation between SENFD of CGRP and the sensory-discriminative MPQ NWC with $\rho = -0.423$; $p = 0.050$, as previously described (Bechakra et al., 2018). In CIAP patients, the correlation between UDNFD of PGP9.5 and the affective MPQ PRI was $\rho = 0.542$ ($p = 0.030$; not significant following Bonferroni correction with an adjusted significance of 0.017), and there were unadjusted significant correlations between IENFD of CGRP and the sensory-discriminative MPQ PRI was $\rho = 0.574$ ($p = 0.020$) and NWC ($\rho = 0.517$; $p = 0.040$). The evaluative MPQ NWC was 3 in all CIAP patients and therefore no correlation coefficients could be calculated. Finally, correlation coefficients in PDN patients were not statistically significant.

Discussion

This study describes changes in (epi)dermal innervation and associations with pain qualities in cohorts of BiPN, PDN and CIAP patients with neuropathic pain. Cutaneous innervation changes in BiPN patients, which mostly presented as (sub)acute neuropathies, were characterized by a decrease in SENFD, as opposed to an increase in UDNFD of PGP9.5 and of presumed non-peptidergic nerve fibers as well as by an increase in epidermal axonal swellings. PDN and CIAP on the other hand, which invariably presented as chronic neuropathies, were characterized by a decrease in IENFD and SENFD of PGP9.5 and of presumed non-peptidergic fibers. Significant unadjusted associations between IENFD and SENFD of peptidergic fibers and the sensorydiscriminative component, and between UDNFD of PGP9.5 and the evaluative/affective component of neuropathic pain, were found in BiPN and CIAP patients. No significant associations were found in PDN patients.

Concerning the immunohistochemical quantification of cutaneous innervation, one should be aware that PGP9.5 may be expressed not only in nerve terminals, but also in Langerhans cells in denervated skin (Hsieh et al., 1996) and under certain conditions in fibroblasts (Olerud et al., 1998). Thus, it

could have been of additional value to incorporate additional specific markers of cutaneous innervation, especially to label the non-peptidergic nerve fiber population and possibly also functional markers of excitability such as sodium channel subtypes (Kalliomaki et al., 2011; Schley et al., 2012). However, as we are aware thus far there have been no reports of reproducible immunohistochemical staining patterns allowing for quantification of non-peptidergic fibers and of sodium channels in humans. Furthermore, we do believe that based upon morphology and predefined quantification criteria nerve fiber (terminals) can be selectively separated from non-nerve cells.

Since no consistent associations between cutaneous innervation and neuropathic pain intensities have been described so far, mainly in patient cohorts containing different types of nerve-injury induced pain (Kalliomaki et al., 2011; Schley et al., 2012), we analyzed three cohorts representing distinctive types of painful peripheral neuropathy separately, i.e. (sub)acute (BiPN), chronic (CIAP) and chronic mixed pathology (PDN) neuropathic pain. The specific epidermal innervation changes that we found in BiPN (increased axonal swellings) as opposed to the changes in PDN and CIAP (decreased IENFD of PGP9.5 and of (PGP9.5-CGRP) fibers) are consistent with previously described differential neuropathic changes in (sub)acute versus chronic neuropathies (Bennett et al., 2014; Ebenezer et al., 2007; Lauria et al., 2003). This match with prior results enhances the notion that any further results should be valid. The decrease in IENFD of PGP9.5 in PDN patients as compared to healthy volunteers just failed to reach statistical significance ($p = 0.054$), but this may be due to the sample size. The increased density of upper dermis PGP9.5 fibers that we observed in BiPN patients has been described in an animal model of subacute neuropathy, see also below (Grelik et al., 2005; Ramien et al., 2004; Taylor and Ribeiro-da-Silva, 2011; Taylor et al., 2012).

Mixed pathology is common in PDN, especially in patients with long standing diabetes as was the case in our cohort of PDN patients. In long standing diabetes, pain in the feet may be explained by other factors than nociceptor degeneration, like myelinated nerve fiber degeneration (Vlckova-Moravcova et al., 2008), autonomic nerve dysfunction (Vlckova-Moravcova et al., 2008), ischemia and inflammation (Schmidt and Holmes, 2018). This may explain why no significant associations of cutaneous innervation parameters (mainly representing nociceptors)

and neuropathic pain descriptors were found in our cohort of PDN patients, which is in line with previous findings (Shun et al., 2004).

In a previous publication (Bechakra et al., 2017) we have demonstrated changes in cutaneous innervation following nerve injury in rats, of peptidergic nerve fibers that were labeled by CGRP-ir and of nonpeptidergic nerve fibers that were labeled by P2X3-ir. It is generally known that these two classes of nociceptors target specific neurons in the spinal dorsal horn (Jongen et al., 2005), are modality-specific (Zhang et al., 2013) and supposedly may each convey specific information about pain along labeled lines to the spinal cord and brain (Bechakra et al., 2017, 2018; Braz et al., 2005; Craig, 2003). Peptidergic nerve fibers can be labeled by CGRP-ir, substance P-ir, but also contain the TrkA receptor for Nerve Growth Factor and the TRPV1 receptor for capsaicin. Non-peptidergic nerve fibers can be labeled with P2X3-ir, Isolectin B4, Mrgprd-ir and contain the RET receptor for glial cell line-derived neurotrophic factor (GDNF) (Jongen et al., 2007). While these two classes of neurons are for the greatest part mutually exclusive, there is some overlap depending on the markers used to label them (Bechakra et al., 2017; Price and Flores, 2007). Thus, peptidergic and non-peptidergic nerve fibers may be considered complementary, because they serve different functions and are more or less mutually exclusive. Since we and others were unable to immunohistochemically label cutaneous non-peptidergic nerve fibers for quantification in the human skin, we decided to use IENFD, SENFD and UDNFD of the difference between PGP9.5 and CGRP labeled fibers as surrogate markers for the number of nonpeptidergic fibers in order to get a complete picture of cutaneous innervation in our cohorts of BiPN, PDN and CIAP patients. Our findings in BiPN and CIAP patients on associations of peptidergic nerve fiber innervation with the sensory-discriminative component of neuropathic pain on the one hand and that of upperdermis nerve fiber sprouting resulting from non-peptidergic nerve fiber degeneration (see below) with the affective/evaluative component on the other hand are both in line with the labeled lines hypothesis mentioned above (see also Grelik et al., 2005; Ramien et al., 2004; Taylor and Ribeiro-da-Silva, 2011; Taylor et al., 2012).

As far as the upper dermis is concerned, a rapid decrease followed by a slow return (at 10 weeks after ligation) to normal values of UDNFD of

NF-200-labeled myelinated nerves has been described in rats with partial nerve ligation (Duraku et al., 2013). However, although myelinated nerves are affected in BiPN as well as in CIAP patients given EMG abnormalities (Bechakra et al., 2018; Hanewinckel et al., 2016), (neuropathic) pain is a cardinal symptom alluding to significant small nerve fiber involvement. It has been shown repeatedly in experimental animals (Grelík et al., 2005; Ramien et al., 2004; Taylor et al., 2012) that peptidergic nerve-fiber degeneration causes sympathetic nerve fibers to sprout in the upper dermis, while non-peptidergic nerve fiber degeneration, which was demonstrated in our BiPN patients in the sub-epidermal layer and in CIAP patients in the epidermis as well as in the subepidermal layer, induces parasympathetic fibers to sprout. Thus, the increased UDNFD of PGP9.5 in BiPN patients likely represents parasympathetic sprouting as a consequence of non-peptidergic nerve fiber degeneration. This upregulation is temporary (Grelík et al., 2005) and may therefore explain why an absolute increase in UDNFD of PGP9.5 was not observed in chronic neuropathies like PDN and CIAP. Although the correlations between UDNFD of PGP9.5 and the evaluative/affective pain components in BiPN and CIAP patients just failed to reach statistical significance after correction for multiple testing ($p \leq 0.05$, but $p > 0.017$), we still conclude that our results allude to a distinct role for non-peptidergic nociceptors in BiPN and CIAP patients, in light of consistent findings across the BiPN and CIAP groups, our previous data in rats, clinical observations and the literature regarding labeled lines.

The inverse association of subepidermal peptidergic nerve fibers with the sensory-discriminative component of neuropathic pain in BiPN patients may imply that in (sub)acute neuropathies this pain component is driven by increased degeneration or impaired regeneration of CGRP fibers in the subepidermal layer, while the positive associations in the epidermis of CIAP patients may imply that in chronic neuropathies this component is driven by decreased degeneration or increased regeneration of CGRP fibers in the epidermis. However, the significant associations between IENFD of CGRP and the sensory-discriminative pain component in CIAP patients should be interpreted with caution due to the scarcity of intraepidermal CGRP fibers.

Finally, although the evaluative component is classified as a separate entity within the MPQ, we analyzed it here in conjunction with the affective pain

component, because many of its descriptors have an emotional-affective connotation (Melzack and Torgerson, 1971; van der Kloot et al., 1995).

Conclusion

Changes in cutaneous innervation in BiPN represent early, whereas those in PDN and CIAP represent late neuropathic pathology. Furthermore, our results allude to a distinct role for non-peptidergic nociceptors in BiPN and CIAP patients. The significant associations between IENFD of CGRP and the sensory-discriminative pain component in CIAP patients should be interpreted with caution due to the scarcity of intraepidermal CGRP fibers. The lack of significant associations in PDN may be caused by mixed ischemic and purely neuropathic pain pathology. Although the MPQ may be impractical for use in routine clinical practice, we suggest to rate pain intensity as well as pain unpleasantness separately in neuropathic pain patients using a numerical rating scale, to consider both sensory-discriminative and affective components.

Methods and materials

Patients, clinical data and skin biopsies

The study was approved by the medical ethical committees of Leiden University Medical Centre, Leiden (NL46921.058.13) and of Erasmus MC, Rotterdam (NL24284.078.08) in the Netherlands and was performed in accordance with the Declaration of Helsinki of 2013 (World Medical, 2013). All participants had given written informed consent. Parts of the study results have been published previously (Bechakra et al., 2018; Emanuel et al., 2017), which is indicated in the results section.

A total of 71 subjects were included: 17 healthy volunteers (HV), 22 patients with BiPN, 16 patients with PDN, and 16 patients with CIAP. The diagnosis of BiPN was established on clinical grounds by a neurologist as a new-onset peripheral neuropathy or a (sub)acute clear deterioration of previously minimally symptomatic peripheral neuropathy following start of bortezomib, fulfilling the ACTION-APS Pain Taxonomy (AAPT) diagnostic

criteria for a diagnosis of CiPN (Paice et al., 2017). Patients were treated with either intravenous bortezomib monotherapy or intravenous bortezomib in combination with nonneurotoxic chemo/immunotherapy, that is, hydroxydaunorubicin (n = 8) (Sonneveld et al., 2012), lenalidomide (n = 2) (Broijl et al., 2016), or rituximab (n = 2). The diagnosis of PDN was established by a neurologist based on the medical history, signs and symptoms upon clinical examination in patients with diabetes mellitus type 2 (Emanuel et al., 2017). The diagnosis of CIAP was established by a neurologist who interpreted the combination of clinical manifestation, nerve conduction parameters as well as relevant laboratory tests as an axonal peripheral neuropathy in the absence of identifiable underlying etiology (Hanewinkel et al., 2016).

The study consisted of the collection of demographic data and clinical data, including pain intensity on a numerical rating scale (NRS) and McGill Pain Questionnaires (Dutch (n = 70) or English (n = 1) language versions) (Melzack and Torgerson, 1971; van der Kloot et al., 1995). For the McGill Pain Questionnaire, the sum of the sensory-discriminative, affective and evaluative Pain Rating Indices (PRI) and the overall sum of PRIs were calculated. In addition, the Number of Words Chosen (NWC) for these items were used.

Obtaining, processing and analysis of skin biopsies

Three-mm skin biopsies were taken 10 cm proximal to the lateral ankle under local anesthesia and stored, according to international guidelines (Lauria et al., 2010). From these biopsies, 50 μ m sections were cut on a freezing microtome and processed for free-floating immunohistochemistry using rabbit anti-PGP9.5 (Catalog# ADI-905-520; Enzo Life Sciences, Farmingdale, NY), representing all cutaneous nerve fibers, and guinea-pig anti-CGRP (Catalog # 16013; Progen Biotechnik, Heidelberg, DE), representing peptidergic nerve fibers, as previously described (Bechakra et al., 2018). After the sections had been mounted to glass slides they were scanned, digitized using a Hamamatsu NanoZoomer 2.0-HT slide scanner (Hamamatsu Photonics, Hamamatsu City, JP), analyzed and quantified using Leica Aperio ImageScope freeware, as previously described (Bechakra et al., 2018) (see also Supplemental Methods file).

Cutaneous innervation was expressed as intra-epidermal nerve fiber density (IENFD), subepidermal nerve fiber density (SENFDF), upper dermis nerve fiber density (UDNFD) of PGP9.5- and CGRP-fibers and as the axonal swelling ratio of PGP9.5-fibers. Definitions of IENFD, SENFD, UDNFD and axonal swelling ratio were previously published (Lauria et al., 2010; Schley et al., 2012) and extensively described and validated in our recent publications (Bechakra et al., 2017, 2018). As a surrogate for non-peptidergic innervation, we also calculated IENFD, SENFD and UDNFD of the difference between the number of PGP9.5 fibers (i.e. the total number of nerve fibers) and the number of CGRP fibers (i.e. peptidergic nerve fibers) and called this (PGP9.5-CGRP). As we are aware, thus far there are no reports of reproducible immunohistochemical staining patterns allowing for quantification of these fibers in humans (Bechakra et al., 2018). Besides, the population of peptidergic and non-peptidergic nerve fibers are mostly complementary (Bechakra et al., 2017).

Statistical analysis

Given that most variables had a non-normal distribution, as assessed with Kolmogorov-Smirnov test, data were summarized using medians and ranges. The Kruskal-Wallis test with post-hoc comparisons using Dunn's test and the chi-square test were used to compare age, duration of neuropathy symptoms and sex of healthy volunteers, BiPN, PDN and CIAP patients. The Kruskal-Wallis test with post-hoc comparisons using Dunn's test were used to compare IENFD, SENFD and UDNFD of PGP9.5, CGRP and (PGP9.5-CGRP) and to compare axonal swelling ratios of healthy volunteers with those of BiPN, PDN and CIAP patients. The Dunn's tests were performed for each comparison between healthy volunteers and a patient group, with Bonferroni-adjusted p-values to correct for multiple testing due to these three comparisons. Spearman's rank correlation coefficients between immunohistochemical markers and neuropathic pain descriptors were determined. Correction for multiple testing was not applied to the correlation analysis, apart from Bonferroni correction with an adjusted significance level of 0.017 for comparisons of UDNFD of PGP9.5 with sensory-discriminative, affective and evaluative components of the MPQ, since this part of the analysis was hypothesis driven. All remaining statistical tests were

twosided with a significance level of 0.05. The statistical analysis was performed using IBM SPSS Statistics v.24.0.0.0 software (IBM Corp., Armonk, NY).

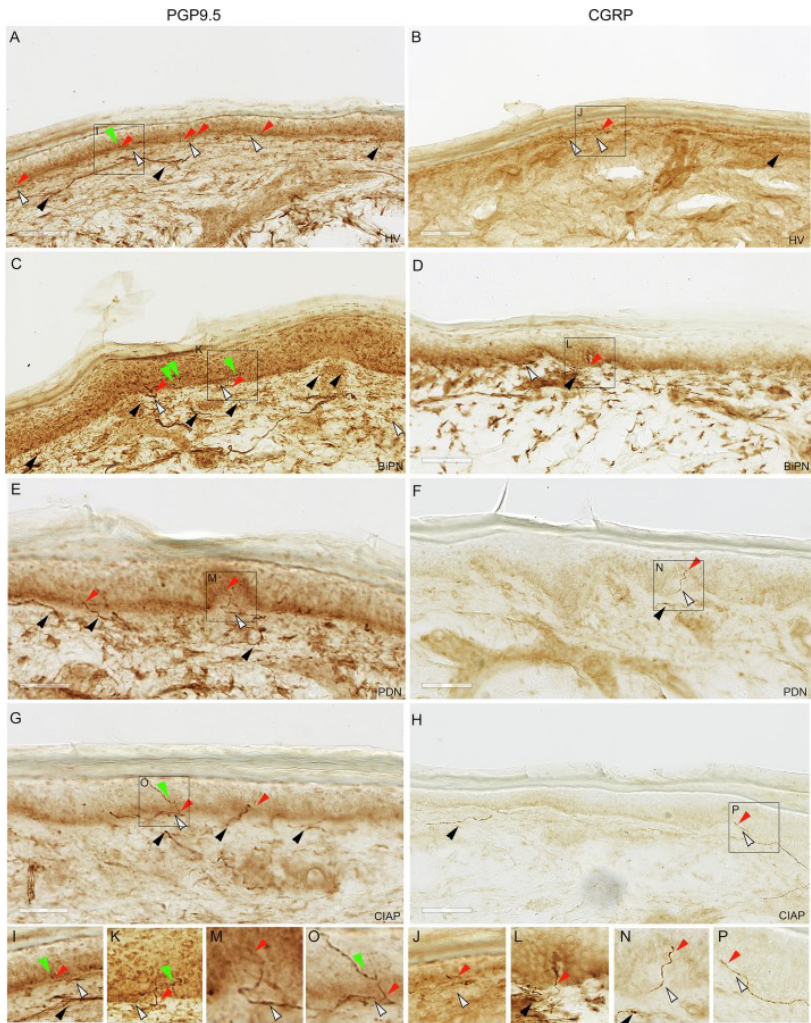


Fig. 1. Immunohistochemical staining patterns of PGP9.5 (A, C, E, G) and CGRP (B, D, F, H), in healthy volunteers (A, B), in BiPN patients (C, D), in PDN patients (E, F) and in CIAP patients (E, F). I, K, M, O, J, L, N and P represent high-power insets, which enable to visualize the length of the intra-epidermal fibers, branching

pattern and intra-epidermal axonal swellings. Red arrowheads represent intra-epidermal nerve fibers, green arrowheads axonal swellings, white arrowheads subepidermal nerve fibers and black arrowheads upper-dermal nerve fibers. The white bars measure 50 μm .

Patients	Median (range) or n (%)			
	HV	BiPN	PDN	CIAP
	n = 17	n = 22	n = 16	n = 16
Demographic data				
Age (years)	63 (27-75)	63 (39-79)	66 (30-76)	67 (49-76)
Sex (male)	10 (59%)	19 (86%)	9 (56%)	12 (75%)
Duration of neuropathy (months)		2 (0.5-23)	144 (12-408)	60 (12-132)
Neuropathic pain				
McGill pain questionnaire				
PRI-Sensory (0-36 points)		11 (4-22)	10 (4-22)	11 (3-23)
PRI-Affective (0-15 points)		3 (0-8)	2 (0-11)	4 (0-11)
PRI-Evaluative (0-12 points)		6 (2-9)	5 (3-7)	5 (3-9)
PRI-Total (0-63 points)		20 (10-37)	18 (9-38)	22 (6-54)
NWC-Sensory (0-12 words)		7 (3-12)	7 (4-12)	7 (3-12)
NWC-Affective (0-5 words)		7 (0-5)	2 (0-4)	3 (0-5)
NWC-Evaluative (0-8 words)		3 (2-3)	3 (3-3)	3 (3-3)
NWC-Total (0-25 points)		13 (7-20)	13 (7-20)	14 (6-20)
Pain Medication				
Adjuvant medication		12 (55%)	6 (38%)	4 (25%)

Table 1. Demographic data and clinical characteristics of healthy volunteers (HV), bortezomib-induced peripheral neuropathy (BiPN), painful diabetic neuropathy (PDN) and chronic idiopathic axonal polyneuropathy (CIAP) patients. PRI = Pain Rating Index, NWC = Number of Words Count. Adjuvant medication included anti-epileptics and anti-depressants. *** $p < 0.001$, Kruskal-Wallis test with post-hoc comparisons using Dunn's test.

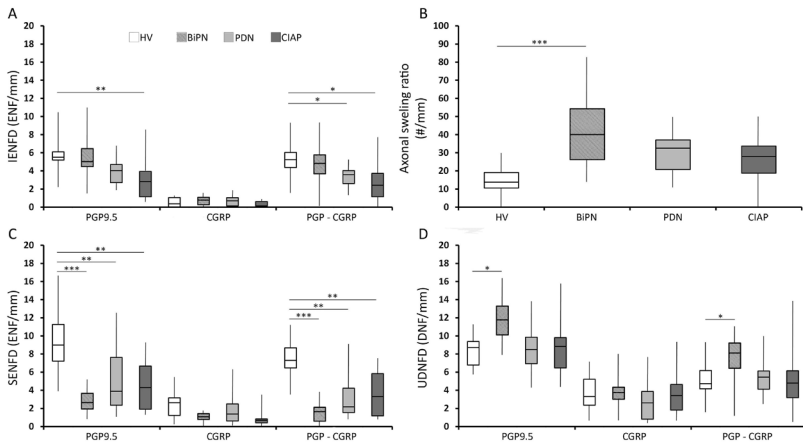


Fig. 2. Skin innervation measurements in healthy volunteers (n = 17), BiPN patients (n = 22), PDN patients (n = 16) and CIAP patients (n = 16). Box-plots showing the median, interquartile range and total range of the number of intra-epidermal (IENFD; A), sub-epidermal (SENFDF; C), upper-dermal (UDNFD; D) nerve fiber densities and the axonal swelling ratios (B), using PGP9.5, CGRP and (PGP9.5-CGRP) as markers to measure the total number of fibers and peptidergic and nonpeptidergic subclasses, *p ≤ 0.05, **p ≤ 0.01 ***p ≤ 0.001; Kruskal-Wallis test with post-hoc comparisons using Dunn's test

Patients	MPQ Pain Glossary	IENFD			SENFDF			UDNFD		
		PGP9.5	CGRP	PGP-CGRP	PGP9.5	CGRP	PGP-CGRP	PGP9.5	CGRP	PGP-CGRP
BiPN	PRI-Sensory	0.637	0.079	0.694	0.648	0.139	0.240	0.553	0.050	0.596
		0.106	-0.382	0.089	-0.103	-0.326	0.261	-0.134	-0.422	0.120
	PRI-Affective	0.056	0.825	0.075	0.466	0.903	0.206	0.576	0.831	0.533
		0.413	-0.050	0.388	0.164	-0.028	0.280	0.126	-0.048	0.140
	PRI-Evaluative	0.271	0.276	0.388	0.192	0.618	0.943	0.037	0.427	0.231
		0.245	0.243	0.193	0.289	0.113	0.016	0.447*	0.179	0.266
	NWC-Sensory	0.938	0.064	0.939	0.465	0.050	0.312	0.189	0.071	0.383
		-0.001	-0.401	0.017	-0.187	-0.423*	0.226	-0.291	-0.392	-0.033
	NWC-Affective	0.457	0.421	0.453	0.760	0.923	0.216	0.926	0.407	0.674
		0.167	-0.181	0.169	0.069	-0.022	0.275	-0.007	-0.186	0.095
PDN	NWC-Evaluative	0.621	0.088	0.805	0.935	0.279	0.279	0.047	0.870	0.107
		0.111	0.373	0.056	-0.019	0.241	-0.241	0.427*	-0.037	0.353
	PRI-Sensory	0.127	0.307	0.311	0.598	0.835	0.806	0.780	0.356	0.427
		0.398	0.273	0.270	0.143	0.129	0.067	0.076	0.247	-0.214
	PRI-Affective	0.329	0.510	0.371	0.240	0.119	0.350	0.877	0.351	0.217
		0.261	0.178	0.240	0.612	0.240	0.250	-0.042	0.250	-0.327
	PRI-Evaluative	0.851	0.349	0.609	0.400	0.320	0.859	0.467	0.329	0.400
		0.051	0.251	-0.139	0.226	0.266	0.048	-0.196	0.261	-0.226
	NWC-Sensory	0.142	0.299	0.331	0.531	0.643	0.610	0.743	0.359	0.411
		0.384	0.277	0.260	0.169	0.126	0.138	0.089	0.246	-0.321
CIAP	NWC-Affective	0.288	0.450	0.342	0.158	0.078	0.252	0.864	0.352	0.204
		0.283	0.203	0.254	0.370	0.453	0.304	-0.047	0.249	-0.336
	NWC-Evaluative	0.918	0.754	0.918	0.346	0.757	0.166	0.346	0.105	0.105
		-0.028	-0.085	-0.028	0.252	0.084	0.364	-0.252	0.420	-0.420
	PRI-Sensory	0.970	0.020	0.892	0.542	0.446	0.710	0.595	0.404	0.718
		0.010	0.574*	-0.037	-0.165	0.205	-0.101	0.144	0.224	0.098
	PRI-Affective	0.465	0.249	0.386	0.468	0.052	0.497	0.030	0.278	0.327
		0.197	0.306	0.233	0.196	0.494	0.183	0.542*	0.289	0.262
	PRI-Evaluative	0.830	0.784	0.736	0.687	0.793	0.996	0.139	0.741	0.195
		0.058	0.075	0.091	-0.109	0.071	0.001	0.387	-0.090	0.342
CIAP	NWC-Sensory	0.375	0.040	0.432	0.904	0.247	0.926	0.637	0.456	0.669
		0.238	0.517*	0.211	0.033	0.307	0.025	0.128	0.201	0.116
	NWC-Affective	0.649	0.224	0.601	0.881	0.215	0.643	0.191	0.613	0.302
		0.123	0.322	0.141	0.041	0.328	0.126	0.344	0.137	0.275
	NWC-Evaluative	-	-	-	-	-	-	-	-	-
		-	-	-	-	-	-	-	-	-
		-	-	-	-	-	-	-	-	-
		-	-	-	-	-	-	-	-	-
		-	-	-	-	-	-	-	-	-
		-	-	-	-	-	-	-	-	-

Table 2. Correlations between immunohistochemical markers and McGill Pain Questionnaire (MPQ) Pain Rating Index (PRI) and Number of Words Count (NWC), in bortezomib-induced peripheral neuropathy (BiPN) (n = 22), painful diabetic neuropathy (PDN) (n = 16) and chronic idiopathic axonal polyneuropathy (CIAP) patients (n = 16). Numerals in the upper left part of the cells refer to p values, numerals in the lower right part of all the cells refer to Spearman's correlation coefficients. Correlation coefficients with an uncorrected p ≤ 0.05 are printed in bold with an asterisk. IENFD = IntraEpidermal Nerve Fiber Density, SENFDF = SubEpidermal Nerve Fiber Density, UDNFD = Upper Dermis Nerve Fiber Density.

CHAPTER VII

Opioid responsiveness of nociceptive versus mixed pain in clinical cancer patients⁶

Malik Bechakra, Floor Moerdijk, Joost van Rosmalen, Birgit C.P. Koch,
Carin C.D. van der Rijt, Peter A.E. Sillevius Smitt, Joost L.M. Jongen

⁶This chapter has been published in Eur J Cancer. 2018 Dec;105:79-87.

Abstract

Objective: To investigate whether clinical cancer patients with mixed nociceptive neuropathic pain are less responsive to opioids than patients with nociceptive pain.

Background: Pain is common in advanced cancer patients. Pain driven by neuropathic mechanisms is considered to be resistant to opioids. This hypothesis is mainly based on animal studies and single-dose opioid studies in humans but has not been confirmed in clinical practice.

Methods: Data were prospectively collected from 240 clinical cancer pain patients using opioids. Multiple linear regression was used for assessing the associations between the logarithm of the morphine equivalent dose (MED) at three days after admission (T = 3d) relative to admission (T = 0d) (logRMED) and type of pain (nociceptive versus mixed pain), corrected for gender, age, primary cancer site and use of non-opioid and adjuvant analgesics. As secondary outcome measures, associations between logMED and logPFent (fentanyl plasma level) at T = 3d and type of pain were assessed.

Results: Pain intensity between T = 0d and T = 3d was significantly and evenly reduced in patients with nociceptive pain (n = 173) and mixed pain (n = 67). Median (interquartile range) MED was 20 (10-52) and 20 (20-80) mg (T = 0d), 40 (10-67) and 40 (20-100) mg (T = 3d), median PFent (T = 3d) was 1.59 (0.58-3.19) and 1.38 (0.54-4.39) ng/ml, none of them significantly different, in patients with nociceptive and mixed pain, respectively. Neither logRMED, logMED (T = 3d), or logPFent (T = 3d) was significantly associated with type of pain, after correction for confounding factors.

Conclusions: We conclude that, at least in clinical cancer patients, mixed pain is as responsive to opioids as nociceptive pain.

Introduction

Pain is the first symptom of cancer in 20-50% of all cancer patients and 70-90% of advanced or terminal cancer patients must cope with chronic pain syndromes related to tumour progression and/or failed treatment (vd Beuken-v Everdingen, 2007). An estimated 20-40% of cancer pain patients have either purely neuropathic pain, mostly caused by cancer treatment, or mixed nociceptive-neuropathic pain, caused by the cancer itself (Garcia, 2011 ; Bennett, 2012 ; Jongen, 2013). It is believed that one of the reasons for inadequate pain control in cancer patients is a failure to identify underlying neuropathic pain mechanisms (Garcia, 2011 ; Bennett, 2012 ; Oldenmenger, 2009 ; Bennett, 2006).

Several animal studies (Puke, 1993 ; Luger, 2002) and single-dose or dose-titrating opioid studies in humans (Arner, 1988 ; Cherny, 1994 ; Portenoy, 1990 ; DelleMijn, 1900) have suggested that cancer pain driven by neuropathic mechanisms (i.e. purely neuropathic pain or mixed pain) is resistant or at least less responsive to opioids than purely nociceptive pain. However, this hypothesis has not been confirmed in routine clinical practice. In a more recent clinical study in mixed cancer pain patients who were labelled as having a definite, possible and unlikely neuropathic pain, patients with definite neuropathic pain required “more intensive opioid treatment” (Mercadante, 2009). The objective of the present study was to investigate whether clinical cancer patients with nociceptive cancer pain differ in opioid responsiveness from patients with mixed nociceptive-neuropathic cancer pain.

Methods

Patients, demographical and clinical data

The study was approved by the institutional review board of Erasmus MC (MEC2008-166) and registered at www.clinicaltrials.gov (NCT00956878). All patients have given written informed consent.

Between October 2008 and December 2012, 243 hospitalized patients with advanced cancer, for whom the multidisciplinary palliative care team (PCT) of Erasmus MC (Jongen, 2011) was consulted to treat pain, were included in the

present study. Clinical data were prospectively collected from a structured data collection sheet (demographical data, primary cancer site, metastases, therapy, pain intensities and medication) and from the electronic health record (type of pain). Pain always presented as an acute or subacute episode at admission or during hospitalization. Thus, purely neuropathic pain solely resulting from adaptive changes to nerve injury did not occur, because these changes take time to develop and almost invariably present in an outpatient setting. The type of pain (nociceptive versus mixed nociceptive-neuropathic pain) was established in all patients by a clinical neurologist (JJ), using the definition of neuropathic pain of the International Association for the Study of Pain and the algorithm described by Treede et al. [15], which is in accordance with previous literature on the clinical distinction between nociceptive and mixed pain (Cherny, 1994). A diagnosis of mixed pain was established by compression or (malignant) infiltration of a nervous structure, based upon history, neurological examination and ancillary investigations, mostly magnetic resonance imaging. By closely adhering to the International Association for the Study of Pain definition of neuropathic pain as opposed to solely relying on pain descriptors (e.g. paraesthesias, allodynia or irradiation), mixed pain could be reliably distinguished from referred pain, which is in fact a consequence of nociceptive pain that commonly occurs in cancer patients. Because the definition of mixed nociceptive-neuropathic pain relies on neurological examination and usually interpretation of MR imaging, the verdict of a clinical neurologist was considered the gold standard. However, the pain diagnosis was always critically evaluated in the multidisciplinary PCT meetings, which were routinely attended by medical oncologist- and anaesthesiologist-pain specialists.

Present pain intensity (on a Numerical Rating Scale, NRS) and opioid requirement (morphine equivalent dose, MED) were assessed at the time of first consultancy (T Z 0 days, T Z 0d) and after the dose was changed or after the patient was switched to another analgesic (T Z 3 days, T Z 3d).

MED of oral morphine, oral oxycodone and transdermal/intravenous/subcutaneous fentanyl was expressed as 10 mg parenteral morphine/24 hh. Conversion factors from the Dutch consensus guideline “Cancer Pain” (Landelijke, 2008) were used. For intravenous/subcutaneous hydromorphone (Pereira, 2001), transdermal buprenorphine (Sittl, 2006), oral tramadol and

oral codeine conversion factors of 6.67, 100, 0.07 and 0.05, respectively, were used. Sustained release and continuous intravenous/ subcutaneous medication was used for calculating MED. Although the number of rescues for individual patients was not collected, the maximum daily dose of oral and intravenous/subcutaneous rescue medication as a rule consisted of 100% of the sustained release or continuous intravenous/subcutaneous opioid dose. When patients were using more than 50% of the rescue doses, the sustained release or continuous intravenous/ subcutaneous opioid dose was increased. Thus, the MED that we calculated represents 67e100% of the actual MED.

Fentanyl plasma levels

Because the majority of our patients (176/240) used transdermal or intravenous/ subcutaneous fentanyl as continuous opioid medication and plasma at T Z 3d was available in 165 of these patients, liquid chromatography tandem mass spectrometry was used to determine plasma levels of fentanyl (PFent). The method was US Food and Drug Administration validated and described earlier (de Bruijn, 2018). The collection of plasma was part of a larger project (NCT00956878) in which also DNA was isolated from peripheral blood samples (Matic, 2017).

Outcome measures and statistical analysis

The logarithm of the MED at T Z 3d relative to T Z 0d (logRMED) was the primary outcome measure for this study, because by adjusting the dose at T Z 3d for the dose received at baseline, the large variability between patients was reduced. The logMED (T Z 3d) and logPFent (T Z 3d) were secondary outcome measures.

Median and interquartile range [IQR] of no normally distributed continuous variables were calculated. Mann-Whitney tests were used to compare age; to compare pain intensities at T Z 0d and T Z 3d; and to compare MED (T Z 0d), MED (T Z 3d), RMED and PFent (T Z 3d) between patients with nociceptive and mixed pain. Wilcoxon signed-rank tests were used to compare pain intensities between T Z 0d and T Z 3d within the two groups of patients. Chi-square tests were used to compare gender, primary cancer site,

metastases, type of therapy, type of opioid, type of non-opioid and adjuvant analgesic and to compare proportions of patients with mild (NRS, 0e4), moderate (NRS, 5e7) and severe (NRS, 8e10) nociceptive pain and mixed pain at T Z 0d and T Z 3d between patients with nociceptive and mixed pain. Bowker's test was used to compare proportions of patients with mild (NRS, 0e4), moderate (NRS, 5e7) and severe (NRS, 8e10) nociceptive pain and mixed pain between T Z 0d and T Z 3d within the two groups of patients.

Finally, multiple linear regression analyses were conducted to study associations between the dependent variables logRMED, logMED (T Z 3d) and logPFent (T Z 3d) and the independent variables type of pain (nociceptive versus mixed), pain intensity (T Z 0d) (only for MED [T Z 3d] and PFent [T Z 3d]), gender, age, primary cancer site and use of non-opioid and adjuvant analgesics. Multicollinearity between the independent factors was excluded because none of the independent variables had a variation inflation factor >3.

The statistical analysis was performed using IBM SPSS Statistics v.24.0.0.0 software (IBM Corp., Armonk, NY). All statistical tests were two-sided with a significance level of 0.05. An adjusted significance level using Bonferroni correction for multiple testing was used for the chi-square tests of primary cancer site, type of treatment, type of opioid, type of non-opioid and adjuvant analgesic, ManneWhitney tests of RMED, MED (T Z 3d) and PFent (T Z 3d) and the multiple linear regression analyses.

Results

Two-hundred and forty-three cancer patients were included in this prospective, observational study. Three patients were not using opioids at baseline and after consultation of the PCT. These patients were consequently excluded from further analysis. Demographic and clinical characteristics of the 240 patients are reported in Table 1. The cohort included 173 cancer patients with nociceptive pain (median [IQR] age, 61.5 [54e68] years; 100 or 57.8% male) and 67 cancer patients with mixed pain (median [IQR] age, 64.0 [59e70] years; 38 or 56.7% male), mixed pain patients being slightly but significantly older ($p < 0.006$; ManneWhitney test). Gastrointestinal, urologi-

cal and lung were the most prevalent primary cancer sites. Nociceptive pain was significantly more common in gastrointestinal cancer patients and mixed pain was significantly more common in lung cancer patients ($p < 0.001$ and $p < 0.001$, respectively; chi square tests, using Bonferroni correction with an adjusted significance level of 0.006). Almost 80% had metastasized cancer and almost 45% of the entire cohort only received supportive care. Patients with mixed pain received radiation therapy significantly more often than patients with nociceptive pain (48% versus 18%; $p < 0.001$; chi square test, using Bonferroni correction with an adjusted significance level of 0.007).

Fig. 1 depicts the course of the median pain intensity and the percentages of patients with mild, moderate and severe pain, in patients with nociceptive and mixed pain. The decrease in median (IQR) nociceptive (6 [4e8] at T Z 0d to 4 [2e5] at T Z 3d) and mixed (6.5 [4e8] at T Z 0d to 3 [2e5] at T Z 3d) pain intensities and the change in proportions with mild, moderate and severe nociceptive and mixed pain were both significant ($p < 0.001$ and $p < 0.001$; Wilcoxon signed-rank tests and $p < 0.001$ and $p < 0.001$; Bowker's tests), although the differences between nociceptive and mixed pain patients, both at T Z 0d and T Z 3d, were not significant ($p \geq 0.67$ and $p \geq 0.30$, respectively; ManneWhitney tests and $p \geq 0.85$ and $p \geq 0.14$, respectively; chisquare tests). In a minority of patients ($n \geq 72$ with nociceptive pain and 25 with mixed pain), also NRS at discharge from the hospital was available. Median NRS at discharge was 3 (0-7) and 3 (0-5), respectively, suggesting durable pain reductions in both groups.

Table 2 reports type of opioid, non-opioid and adjuvant analgesic use as well as RMED, MED (T Z 0d), MED (T Z 3d) and PFent (T Z 3d) for patients with nociceptive and mixed pain. Fentanyl use was significantly more prevalent among patients with nociceptive pain, while hydromorphone was more prevalent among patients with mixed pain ($p \geq 0.003$ and $p \geq 0.007$, respectively; ManneWhitney tests, using Bonferroni correction with an adjusted significance level of 0.01). Median (IQR) RMED, MED (T Z 0d), MED (T Z 3d) and PFent (T Z 3d) were not significantly different in patients with nociceptive and mixed pain ($p \geq 0.963$, $p \geq 0.987$, $p \geq 0.587$ and $p \geq 0.465$, respectively; ManneWhitney test, using Bonferroni correction with an adjusted significance level of 0.013). Anticonvulsant and ketamine use was more prevalent among patients with mixed pain compared to patients

with nociceptive pain ($p < 0.001$ and $p Z 0.009$, respectively; chi square test, using Bonferroni correction with an adjusted significance level of 0.01).

Table 3 summarizes the results of the multiple linear regression analysis. Neither logRMED, logMED (T Z 3d) or logPFent (T Z 3d) was significantly associated with type of pain, after correction for the independent variables pain intensity (T Z 0d) (only used for MED [T Z 3d] and PFent [T Z 3d]), gender, age, primary cancer site and use of non-opioid and adjuvant analgesics ($p Z 0.724$, $p Z 0.084$ and $p Z 0.547$, respectively). Ketamine use was significantly associated with logMED (T Z 3d) and logPFent (T Z 3d) ($p < 0.001$; t-test using Bonferroni correction with an adjusted significance level of 0.006), but not with logRMED.

Discussion

This study describes opioid responsiveness in a prospective cohort of 240 cancer patients with purely nociceptive versus mixed nociceptive/neuropathic pain. The results indicate similar pain intensities in both groups at baseline and after consultation of the PCT. RMED, MED (T Z 3d) and PFent (T Z 3d) were not significantly different between nociceptive and mixed cancer pain patients, although anticonvulsant and ketamine use were more prevalent in the mixed cancer pain group in the univariate analyses. In the multiple linear regression analyses however, neither logRMED (the primary outcome measure), logMED (T Z 3d) nor logPFent (T Z 3d) was significantly associated with type of pain, after correction for confounding factors. LogMed (T Z 3d) and logPFent (T Z 3d) were significantly associated with ketamine use in the multiple linear regression analyses.

The fact that mixed pain was significantly more common in lung cancer patients and nociceptive pain was significantly more common in gastrointestinal cancer patients reflects a high prevalence of spinal epidural metastases, the most prevalent cause of mixed cancer pain, in lung cancer and a much lower prevalence in gastrointestinal cancer patients (Loblaw, 2003 ; Patchell, 2005). Similarly, patients with mixed pain received radiation therapy significantly more often than patients with nociceptive pain. In theory, given the hypothesis that pain driven by neuropathic mechanisms is considered to be resistant

to opioids, the increased rate of radiation therapy in the mixed cancer pain group might have caused the similar decrease in pain intensities and the similar opioid requirements in mixed pain as compared to nociceptive pain patients that we have found. However, this is highly unlikely because radiation therapy was initiated after admission and will not lead to decreased pain intensities and/or decreased opioid requirements within a 3-day time span. In contrast, initiation of radiation therapy may lead to a temporary pain flare in the short term (Gomez-Iturriaga, 2015), giving rise to an opposite effect.

Fentanyl use was more common in the nociceptive cancer pain group. This probably reflects a higher prevalence of constipation in this group, in which the gastrointestinal tract was by far the most common primary cancer site. Transdermal fentanyl is generally preferred over other opioids in patients with constipation, due to its more favourable site-effects profile in this regard (Hadley, 2013). The significantly more common use of hydromorphone in the mixed cancer pain patients only occurred in a small minority of patients (4 and 7, respectively). A recent clinical trial in head-and-neck cancer patients with a mean pain score of 6 and a presumed neuropathic pain component compared methadone, an opioid with an additional effect on the Nmethyl-D-aspartate receptor, with fentanyl, a pure muopioid receptor agonist. In this study with presumed neuropathic pain patients, methadone appeared superior to fentanyl (Haumann, 2016). However, another study using methadone in both neuropathic and non-neuropathic pain patients could not demonstrate superior efficacy of methadone over morphine in any of the groups (Bruera, 2004). Because at T Z 3d all of our patients used pure muopioid receptor agonists and because no convincing evidence exists for a superior efficacy of some opioids over other specifically in neuropathic pain, we conclude that it is highly unlikely that differences in type of opioids among the two groups may affect our conclusion.

In addition to equivalent doses of prescribed sustained release and continuous intravenous/subcutaneous opioids, plasma fentanyl levels were obtained in almost 70% of patients to control for a potential bias that might have been introduced by differences in pharmacokinetic factors between nociceptive and mixed cancer pain patients. Although plasma samples were collected randomly during the day, this occurred in both groups. PFent (T Z 3d) was

not significantly different between nociceptive and mixed cancer pain patients, arguing against a potential bias caused by differences in pharmacokinetic factors.

It is a widely held belief that cancer pain driven by neuropathic mechanisms is opioid resistant or at least less responsive to opioids than purely nociceptive pain. This assumption is mainly based on preclinical data and single-dose or dose-titrating opioid studies in humans (reviewed by DelleMijn). In 2009, a study with 213 cancer pain patients with a clinical diagnosis of definite, possible or unlikely neuropathic pain showed significant differences in opioid response (Mercadante, 2009) and seemed to confirm the assumption. However, it was unclear whether the group with “unlikely neuropathic pain” actually represented patients with purely nociceptive pain. Secondly, opioid response was a subjective and compound outcome measure, not only based on a decrease in pain intensities or (equivalent) opioid dose but also based on side-effects. In the present study, a distinction between purely nociceptive pain and mixed nociceptive/neuropathic cancer pain was based on clinical grounds, according to firmly established criteria (Treede, 2008) by a single, experienced clinical neurologist. Secondly, we used quantifiable and robust outcome measures for analgesic efficacy. We believe that this study design is best suited to compare opioid responsiveness in nociceptive and mixed cancer pain patients.

Although anticonvulsant use was significantly more common in the mixed cancer pain group in the univariate analysis, it was not a significant predictor of any of the outcome measures in the multiple linear regression analyses. Ketamine use was significantly more common in the mixed pain group in the univariate analysis and significantly associated with logPFent (T Z 3d). However, ketamine was used in only a small minority of patients and, more importantly, was not significantly associated with the primary outcome measure logRMED. In addition, there is insufficient evidence for a beneficial effect of ketamine as an adjuvant to opioids for the relief of cancer pain (Bell, 2012). We therefore conclude that similar pain reductions and similar opioid requirements in both nociceptive and mixed cancer pain patients may be explained by similar opioid responsiveness in both groups and not by an increased prevalence of anticonvulsant or ketamine use in the mixed cancer pain group.

Conclusion

We suggest that mixed cancer pain may be considered a type of nociceptive pain that should be treated primarily with opioids and that adjuvant analgesics or ketamine may only be added in case of insufficient analgesia or unacceptable side-effects from opioids.

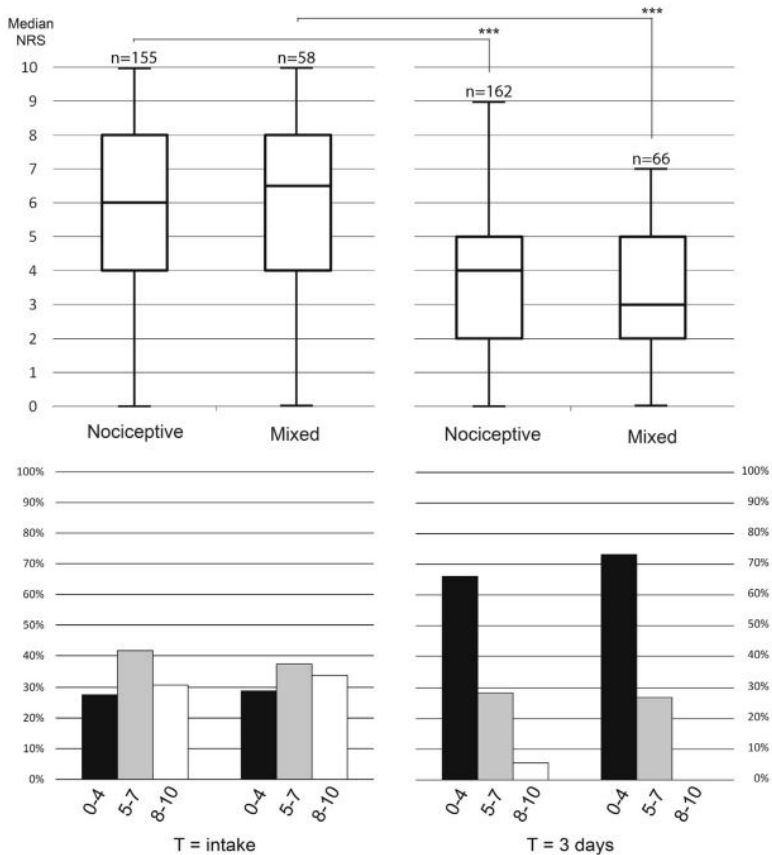


Fig. 1. Changes in pain severity in patients with nociceptive and mixed cancer pain. The upper panels represent median numerical rating scale (NRS) pain intensities, interquartile ranges and total range, at intake and at 3 days. The lower panels represent proportions of mild (NRS, 0e4), moderate (NRS, 5e7) and severe pain (NRS, 8e10), at intake and at 3 days. The decrease in pain intensities and the change in proportions of mild, moderate and severe pain were statistically

significant, in both groups, while differences between nociceptive and mixed pain groups were not significant, at intake and at T Z 3d. *** $p < 0.001$; Wilcoxon signed-rank tests, ManneWhitney tests, Bowker's tests and chi-square tests. Numbers above the boxes indicate numbers of patients.

	Median (IQR) or n (%)			<i>p</i> -value
	Nociceptive and mixed pain	Nociceptive pain	Mixed pain	
Number of patients (%)	240	173 (72.1)	67 (27.9)	
Age (years)	61.5 (54–68)	61.0 (52–67)	64.0 (59–70)	<i>0.006</i>
Gender (male)	138 (57.5)	100 (57.8)	38 (56.7)	0.841
Primary cancer site				
Gastrointestinal	90 (37.5)	81 (46.8)	9 (13.4)	<i>0.000</i>
Urological	36 (15.0)	22 (12.7)	14 (21.9)	0.110
Lung	34 (14.2)	16 (9.2)	18 (26.9)	<i>0.000</i>
Gynaecological	22 (9.2)	17 (9.8)	5 (7.6)	0.548
ENT	13 (5.4)	11 (6.4)	2 (3.0)	0.317
Breast	9 (3.8)	5 (2.9)	4 (6.0)	0.271
Haematological	8 (3.3)	4 (2.3)	4 (6.0)	0.162
Unknown	14 (5.8)	9 (5.2)	5 (7.5)	0.193
Other	14 (5.8)	8 (4.6)	6 (9.0)	0.194
Metastases (present)	189 (78.8)	135 (78.0)	54 (80.6)	0.689
Type of therapy				
None or supportive	108 (45.0)	87 (50.3)	21 (30.3)	0.009
Radiation therapy	63 (26.3)	31 (17.9)	32 (47.8)	<i>0.000</i>
Chemotherapy	34 (14.2)	27 (15.6)	7 (10.4)	0.317
Surgery	18 (7.5)	17 (9.8)	1 (1.5)	0.028
Radiation therapy and chemotherapy	11 (4.6)	7 (4.0)	4 (6.0)	0.549
Surgery and radiation therapy	5 (2.1)	4 (2.3)	1 (1.5)	0.689
Surgery and chemotherapy	1 (0.4)	0 (0.0)	1 (1.5)	0.110

Table 1 Demographic data and clinical characteristics. IQR Z interquartile range; ENT, ear, nose and throat. Significant *p*-values are printed in italic; Mann-Whitney test and chi-square tests, the Bonferroni-adjusted significance levels were 0.006 and 0.007, respectively.

	Median (IQR) or n (%)			<i>p</i> -value
	Nociceptive and mixed pain	Nociceptive pain	Mixed pain	
Number of patients	240	173 (72.1)	67 (27.9)	
Type of opioid (T = 3d)				
Fentanyl	176 (73.3)	136 (78.6)	40 (59.7)	<i>0.003</i>
Oxycodone	43 (17.9)	26 (15.0)	17 (25.4)	0.057
Hydromorphone	11 (4.6)	4 (2.3)	7 (10.4)	<i>0.007</i>
Morphine	5 (2.1)	4 (2.3)	1 (1.5)	0.689
Buprenorphine	5 (2.1)	3 (1.7)	2 (3.0)	0.549
RMED	1.50 (1–2.85)	1.50 (1–2.38)	1.50 (0.74–3.00)	0.963
MED (T = 0d)	20 (10–53)	20 (10–52)	20 (20–80)	0.987
MED (T = 3d)	40 (20–80)	40 (10–67)	40 (20–100)	0.587
PFent (T = 3d)	1.56 (0.58–3.22) (<i>n</i> = 165)	1.59 (0.59–3.07) (<i>n</i> = 131)	1.38 (0.57–4.04) (<i>n</i> = 34)	0.465
Adjuvant analgesic medication (T = 3d)				
Paracetamol	227 (94.6)	164 (94.8)	63 (94.0)	0.842
NSAIDs/coxibs	142 (59.2)	104 (60.1)	38 (56.7)	0.617
Anticonvulsants	73 (30.4)	36 (20.8)	37 (55.2)	<i>0.000</i>
Antidepressants	30 (12.5)	17 (9.8)	13 (19.4)	0.046
Ketamine	21 (8.8)	10 (5.8)	11 (16.4)	<i>0.009</i>

Table 2 Proportions of type of opioid, median and interquartile range (IQR) of morphine equianalgesic dose at T Z 3d relative to T Z 0d (RMED), MED at T Z 0d, MED at T Z 3d, plasma fentanyl levels (PFent) at T Z 3d and proportions of non-opioid and adjuvant analgesic medication. NSAIDs Z non-steroidal anti-inflammatory drugs. Significant *p*-values are printed in italic; chi-square tests and Mann-Whitney tests, the Bonferroni-adjusted significance levels were 0.01, 0.013 and 0.01, respectively.

			B	95% CI	p
Log RMFD	Type of pain	Noiceptive	0.038	-0.176 to 0.252	0.724
		Mixed	Reference		
	Gender	Male	-0.016	-0.210 to 0.178	0.870
		Female	Reference		
	Age (years)		-0.005	-0.014 to 0.004	0.258
	Type of cancer	Lung	-0.203	-0.623 to 0.217	0.342
		Gynaecological	-0.123	-0.834 to 0.136	0.157
		Urological	0.160	-0.540 to 0.294	0.562
		ENT	-0.226	-0.389 to 0.680	0.543
		Gastrointestinal	-0.333	-0.616 to 0.164	0.254
		Breast	-0.207	-0.811 to 0.396	0.499
		Haematological	0.149	-0.451 to 0.749	0.624
		Unknown primary	-0.042	-0.545 to 0.460	0.868
		Other	Reference		
		Paracetamol	No	0.265	-0.135 to 0.666
	NSAID/coxib	Yes	Reference		
		No	0.165	-0.014 to 0.344	0.070
	Anticonvulsants	Yes	Reference		
		No	0.088	0.112 to 0.287	0.389
	Antidepressants	Yes	Reference		
No		0.213	-0.047 to -0.474	0.108	
Ketamine	Yes	Reference			
	No	-0.372	-0.670 to -0.074	0.015	
Log MED (T = 3d)	Type of pain	Noiceptive	0.066	-0.232 to 0.364	0.663
		Mixed	Reference		
	Pain intensity T = 0d		0.044	-0.006 to 0.094	0.084
		Gender	Male	0.180	-0.083 to 0.444
	Female		Reference		
	Age (years)		-0.013	-0.025 to 0.002	0.023
	Type of cancer	Lung	0.154	-0.411 to 0.718	0.592
		Gynaecological	-0.404	-1.031 to 0.223	0.206
		Urological	0.058	-0.499 to 0.614	0.838
		ENT	-0.368	-1.053 to 0.318	0.292
		Gastrointestinal	-0.233	0.755 to 0.290	0.381
		Breast	0.218	0.598 to 1.034	0.599
		Haematological	-0.209	-1.017 to 0.600	0.611
		Unknown primary	0.411	-0.323 to 1.144	0.271
		Other	Reference		
		Paracetamol	No	-0.371	-0.934 to 0.191
	NSAID/coxib	Yes	Reference		
		No	0.016	-0.228 to 0.260	0.895
	Anticonvulsants	Yes	Reference		
		No	-0.092	-0.373 to 0.190	0.520
Antidepressants	Yes	Reference			
	No	-0.223	-0.579 to 0.132	0.217	
Ketamine	Yes	Reference			
	No	-0.968	-1.383 to -0.553	0.000	
Log PFent (T = 3d)	Type of pain	Noiceptive	0.161	0.367 to 0.689	0.547
		Mixed	Reference		
	Pain intensity T = 0d		0.066	0.018 to 0.150	0.123
		Gender	Male	0.043	0.383 to 0.468
	Female		Reference		
	Age (years)		-0.012	0.032 to 0.007	0.209
	Type of cancer	Lung	0.166	0.808 to 1.140	0.737
		Gynaecological	-0.362	-1.385 to 0.661	0.485
		Urological	0.495	1.447 to 0.457	0.305
		ENT	-0.803	-1.847 to 0.242	0.131
		Gastrointestinal	-0.333	-1.189 to 0.523	0.443
		Breast	-0.135	-1.761 to 1.491	0.870
		Haematological	-0.379	-1.837 to 1.079	0.608

Table 3 Results of the multiple linear regression analysis. B represents unstandardized B coefficients, with their respective 95% confidence intervals. ENT Z ear, nose and throat; NSAIDs Z non-steroidal anti-inflammatory drugs. Significant p-values are printed in italic; t-tests, the Bonferroniadjusted significance levels were 0.007 (log RMED) and 0.006 (log MED [T Z 3d] and log PFent [T Z 3d]), respectively.

Table 3 (continued)

Dependent variables	Independent variables	Values	B	95% Confidence interval of B	<i>p</i> -value
		Unknown primary	0.106	-1.083 to 1.296	0.860
		Other	Reference		
	Paracetamol	No	-0.730	-1.730 to 0.270	0.151
		Yes	Reference		
	NSAID/coxib	No	0.233	0.171 to 0.638	0.256
		Yes	Reference		
	Anticonvulsants	No	0.193	0.290 to 0.676	0.432
		Yes	Reference		
	Antidepressants	No	-0.051	-0.638 to 0.535	0.863
		Yes	Reference		
	Ketamine	No	-1.072	-1.693 to -0.451	0.001
		Yes	Reference		

CHAPTER VIII

Summary, discussion and future perspectives

Summary and discussion

This thesis is about the pathophysiology of neuropathic pain and cancer pain. It is a clinical observation that, unlike nociceptive pain patients who may experience high pain intensities but generally describe the quality of their pain as “normal”, patients with neuropathic pain do not necessarily experience high pain intensities, but usually use a lot of adjectives to describe their pain, e.g. burning, deep, tingling, drilling, annoying, tiring etc., i.e. the quality of their pain is “abnormal”. Some of these adjectives may have a sensory-discriminative connotation (like burning, deep, tingling, drilling), while others have an affective-evaluative connotation (like annoying, tiring). Furthermore, it is a widely held belief, that cancer pain patients with mixed nociceptive-neuropathic pain are less responsive to opioids than patients with purely nociceptive pain. This observation and this belief spurred the experiments and research in this thesis.

In **Chapter 2**, changes in neuronal metabolic activity in the superficial dorsal horn following nerve injury and a reduction of activity to epidural spinal cord stimulation (SCS) are described. Nerve injury-induced pain is a complex disorder, which is driven by a multitude of plastic changes, like sensitization of (peripheral) nociceptors, increased excitability of spinal cord projection neurons, decreased propriospinal and descending spinal inhibition, spinal glia activation and changes in the transmission of nociceptive signals in the brainstem and cortex. Autofluorescent flavoprotein imaging (AFI) is a technique by which the excitability of superficial dorsal horn neurons, which include nociceptive projection neurons to the thalamus and other brainstem relay centers, can be quantified through the AFI response, which is a direct measure of neuronal metabolic activity. In this study, we demonstrate that, although the AFI response to a (supramaximal) nociceptive stimulus is comparable in animals with nerve injury and controls, innocuous palpation only induced an AFI response in animals with nerve injury (71). Thus, AFI enabled us to directly visualize the spinal component of central sensitization. Furthermore, our experiment revealed that SCS acts through rapid modulation of nociceptive processing at the spinal level. AFI turned out to be an elegant method to directly visualize central sensitization in superficial dorsal horn neurons. AFI, however, suffers from a low signal to noise ratio, as a result of which it is extremely sensitive to motion artifacts. The very high variability in our experiments

may be a direct consequence of this and may have influenced (the lack of a significant difference in) the AFI response following nociceptive stimulation in neuropathic versus control rats. Furthermore, AFI may not be feasible as an instrument for diagnostic imaging of spinal cord activity in patients (72, 73).

In **Chapter 3**, a case study is presented of a patient with anti-dipeptidyl peptidase-like protein 6 (DPPX) encephalitis in which severe pruritus was the preeminent symptom. The patient had scratching marks on the skin of his trunk and could not tolerate the contact of clothing on his skin, which was interpreted as tactile allodynia. Nonetheless, the intraepidermal nerve fiber density in a skin biopsy from the leg was not significantly decreased from healthy volunteers and the intraepidermal nerve fiber density on the trunk did not seem to differ from a small series of patients with bortezomib-induced (i.e length-dependent) peripheral neuropathy. Thus, the normal intraepidermal nerve fiber densities and the absence of an effect from local dermatological treatments suggested that the pruritus in this patient was of central origin, localized in the dorsal horn and induced by centrally acting anti-DPPX antibodies. Chapter 2 and chapter 3 thus highlight spinal mechanisms of central sensitization of neuropathic pain and itch, in both experimental animals and humans. It is suggested that spinal sensitization plays an important role in both neuropathic pain and neuropathic itch and that at least neuropathic pain may be reduced by a propriospinal inhibitory effect of spinal cord stimulation (31).

In **Chapter 4**, changes in epidermal innervation, and the relation between epidermal innervation and pain behavior were studied in a rat model of nerve injury-induced pain. Nerveinjury was induced by partial ligation of the proximal sciatic nerve, which resulted in varying degrees of nerve fiber terminal loss in the epidermis of the animal footpad. Firstly, we demonstrated that non-peptidergic nerve fibers were more prevalent than peptidergic fibers in the epidermis. Furthermore, we demonstrated a selective reduction of non-peptidergic fibers, but not peptidergic nerve fibers, following nerve-injury. Finally, we demonstrated that this reduction of non-peptidergic nerve fibers correlated with behavioral hyperalgesia in an animal model of nerve injury-induced pain, i.e. neuropathic pain. Our findings are in line with a predominant role of nonpeptidergic nociceptors in neuropathic pain (74, 75). Of note, the central terminals of peptidergic and non-peptidergic nociceptors project to dif-

ferent areas in the spinal cord: peptidergic nerve fibers to the most superficial laminae of the dorsal horn (lamina I and II-outer) and non-peptidergic nerve fibers to lamina II-inner. This differential projection highlights the possibility that in fact the peptidergic and non-peptidergic subclass of peripheral nociceptors are functionally different, i.e. may serve different pain qualities (4).

In **Chapter 5** changes in cutaneous innervation and associations with pain qualities were studied in a cohort of 22 patients with bortezomib-induced peripheral neuropathy and 17 healthy volunteers which served as controls. Firstly, we demonstrated that BiPN is a sensory neuropathy, in which neuropathic pain is the most striking clinical finding. Secondly, although intraepidermal nerve fiber density was not reduced, we demonstrated a significant increase in both epidermal axonal swellings as well as an increased upper dermis nerve fiber density. While the former may be considered a sign of early neuropathic changes (the majority of BiPN patients presented with (sub)acute neuropathy), the latter reflects sprouting of parasympathetic nerve fibers as a consequence of non-peptidergic nerve fiber degeneration, which unfortunately could not be directly visualized due to the impossibility to immunohistochemically stain non-peptidergic nerve fibers in humans. Finally, a correlation between impaired regeneration of peptidergic nerve fibers and the sensory-discriminative component of neuropathic pain and a correlation between sprouting of parasympathetic fibers/non-peptidergic nerve fiber degeneration and the affective/evaluative component of neuropathic pain were found. These findings in neuropathic pain patients further strengthened our hypothesis of labeled lines for distinct neuropathic pain qualities. It is now widely accepted that pain is a multidimensional experience and has sensory-discriminative, affective, motivational and evaluative components (76). These are likely to be processed within a neural matrix (77). Based on post mortem reports and neurosurgical observations, a division of function between the lateral and medial components of the human pain processing system of the brain was proposed already several decades ago (78).

In **Chapter 6**, in addition to patients with (sub)acute neuropathy (i.e. BiPN), changes in cutaneous innervation and their associations with pain qualities were studied in two cohorts of

patients with chronic neuropathy, i.e. chronic idiopathic axonal neuropathy (CIAP) and painful diabetic neuropathy (PDN). Although the changes in cutaneous innervation in (sub)acute (BiPN) versus chronic (CIAP, PDN) neuropathy were distinct, also in patients with CIAP we found significant associations of peptidergic innervation changes with the sensory-discriminative component and of non-peptidergic innervation changes with the affective/evaluative component.

The lack of any associations in PDN patients may be explained by mixed ischemic and purely neuropathic pain pathology in this cohort, although relatively low numbers of subjects may also play a role. Based on the results in Chapter 4, 5 and 6, which allude to the existence of separate anatomical pathways for sensory-discriminative and affective/evaluative pain qualities in patients suffering from BiPN and CIAP, we suggest to rate pain intensity as well as pain unpleasantness separately in neuropathic pain patients. We conclude that, similar to a predominant role for nonpeptidergic nociceptors in neuropathic pain behavior in rats, suffering in neuropathic pain patients is predominantly determined by changes in the “non-peptidergic pain line”. One should realize however, that our conclusions were “merely” based on associations and that no direct evidence was provided. Also, the numbers of experimental animals and patients were relatively small, which prevented correction for multiple testing in the association analyses and we were not able to directly label non-peptidergic nerve fibers in humans. On the other hand, the fact that similar findings were obtained across species and across various neuropathic pain conditions strengthens our observation.

Finally, in **Chapter 7**, opioid responsiveness in a prospective cohort of cancer patients with purely nociceptive versus mixed nociceptive-neuropathic pain was described. Opioid requirement in cancer patients is determined by the severity of pain, genetic susceptibility factors (79, 80) and possibly also by type of pain, since it has been previously postulated that (cancer) pain driven by neuropathic mechanisms is resistant to opioids. In our cohort of 240 clinical cancer pain patients, roughly two thirds had purely nociceptive pain, while one third suffered from mixed nociceptiveneuropathic pain. The two groups of patients, i.e. purely nociceptive and mixed nociceptiveneuropathic pain, were not stratified for disease severity and genetic background, which may have influenced our results. Furthermore, patients with mixed

nociceptive-neuropathic pain used ketamine and co-analgesics more often. On the other hand, our main outcome measure relative morphine equianalgesic dose was not significantly associated with type of pain in the multivariate analysis, after correction for confounding factors. Additionally, since our cohort represents real world data and a considerable number of patients, we conclude that the previous claim of opioid resistance in cancer patients with mixed nociceptive-neuropathic pain does not hold true in clinical practice.

Future Perspectives

As mentioned above, autofluorescent flavoprotein imaging is an elegant way to directly visualize mechanisms of spinal sensitization in various chronic pain syndromes. A major drawback, however, is a quite dramatic liability to motion artifacts, which renders this technique unsuitable for clinical applications. Conventional functional imaging techniques on the other hand (like fMRI), lack the spatial and temporal resolution of AFI and for that reason do not provide a realistic alternative to quantify spinal nociceptive transmission and sensitization. Currently, a new technique named functional ultrasound (fUS) is being developed and offers hope that the practical limitations of AFI can be overcome, while at the same time provide high spatial and temporal resolution functional imaging of the spinal cord dorsal horn (81).

Concerning the non-peptidergic subpopulation of nociceptors, new methods should be developed to directly visualize these fibers in human skin, either by means of an improved immunohistochemical/immunofluorescence protocol for P2X3-immunohistochemistry or by new antibodies that specifically label non-peptidergic nociceptors. The number of patients with neuropathic pain involved in these studies however should also be considerably increased, to allow for correction for multiple testing in the association studies. For example, to detect a difference of 30% in IENFD with a standard deviation of 0.5, an alpha of 5% and a power of 80%, the cohort would contain 45 patients per group.

Functional brain imaging, e.g. using resting state fMRI (82) or even resting state fUS (83), if possible should be added to clinical outcome measures like the McGill Pain Questionnaire, since correlations of cutaneous innervation changes in

non-peptidergic nociceptors with activation of areas of the “medial pain system” (84) would greatly strengthen our conclusions regarding the labeled line hypothesis mentioned in paragraph 1 of the introduction. The recognition of a separate sensory discriminative and affective-evaluative component of neuropathic pain opens research opportunities for studying nonpharmacological strategies like supportive psychotherapy and cognitive-behavioral therapy (CBT) (85).

Finally, concerning pain in cancer patients, we have (indirectly) demonstrated that coanalgesics including ketamine did not significantly contribute to pain control in cancer patients with mixed nociceptive-neuropathic pain. Therefore, this population may also benefit from psychological interventions mentioned above, either having a direct effect on pain intensity/painunpleasantness or by helping the patient in managing the stress associated with cancer pain (86, 87). In addition, to gain a better understanding of cancer pain and its response to analgesic treatment, we suggest that the relative contributions of cancer pain severity, genetic susceptibility to pain and opioids, and the type of pain should be analyzed in a systematic way, ultimately to improve the quality of life of this devastating condition.

In summary, in this thesis mechanisms of nerve-injury induced pain and itch, and a working mechanism of spinal cord stimulation in neuropathic pain were exposed. Furthermore, the relation between cutaneous innervation changes versus hyperalgesia and the perception of pain in animals with nerve-injury induced pain and neuropathic pain patients were investigated. Finally, opioid sensitivity in nociceptive versus mixed cancer pain patients was studied. This thesis may form a foundation for further development of SCS in neuropathic pain conditions, for future analgesic treatments specifically aimed at the affective/evaluative component of neuropathic pain and finally for an optimal treatment strategy for mixed cancer pain patients.

Summary

This thesis is about the pathophysiology of neuropathic pain and cancer pain. It is a clinical observation that, unlike nociceptive pain patients who may experience high pain intensities but generally describe the quality of their pain as “normal”, patients with neuropathic pain do not necessarily experience high pain intensities but usually use a lot of adjectives to describe their pain, e.g. burning, deep, tingling, drilling, annoying, tiring etc., i.e. the quality of their pain is “abnormal”. Some of these adjectives may have a sensory-discriminative connotation (like burning, deep, tingling, drilling), while others have an affective-evaluative connotation (like annoying, tiring). Furthermore, it is a widely held belief, that cancer pain patients with mixed nociceptive-neuropathic pain are less responsive to opioids than patients with purely nociceptive pain. This observation and this belief spurred the experiments in this thesis.

Firstly, central mechanisms of neuropathic pain and the effect of epidural spinal cord stimulation (SCS) were studied. In the second section support for the existence of two separate pain systems is presented, one for the sensory-discriminating pain component and one for the affective/evaluative pain component, based upon correlations between skin innervation and pain (behavior) in experimental animals and patients with neuropathy.

Finally, it was shown that there is no clinical evidence for reduced sensitivity to opioids in mixed cancer pain patients. The experiments in thesis may form a foundation for the further development of SCS in neuropathic pain conditions, for future analgesic treatments specifically aimed at the affective/evaluative component of neuropathic pain and finally for an optimal treatment strategy for mixed cancer pain patients.

Samenvatting

Dit proefschrift gaat over de pathofysiologie van neuropathische pijn en kankerpijn. Het is een klinische observatie dat, in tegenstelling tot patiënten met nociceptieve pijn die hoge pijnintensiteiten kunnen ervaren maar over het algemeen de kwaliteit van hun pijn als “normaal” beschrijven, patiënten met neuropathische pijn niet noodzakelijkerwijs hoge pijnintensiteiten ervaren maar over het algemeen wel veel bijvoeglijke naamwoorden gebruiken om hun pijn te beschrijven, zoals bijvoorbeeld brandend, diep, tintelend, borend, irritant, vermoeiend etc. Met andere woorden, de kwaliteit van hun pijn is “abnormaal”. Sommige van deze bijvoeglijke naamwoorden kunnen een sensorisch-discriminerende connotatie hebben (zoals brandend, diep, tintelend, borend), terwijl andere een affectieve/evaluatieve connotatie hebben (zoals irritant, vermoeiend). Daarnaast wordt algemeen aangenomen dat kankerpatiënten met gemengde nociceptieve en neuropathische pijn minder goed reageren op opioïden dan patiënten met puur nociceptieve pijn.

Allereerst werden centrale mechanismen van neuropathische pijn en het effect van epidurale ruggenmergstimulatie bestudeerd. In de tweede sectie is de hypothese van twee aparte pijnsystemen, te weten eentje voor de sensorisch-discriminerende pijncomponent en eentje voor de affectieve/evaluatieve pijncomponent aannemelijk gemaakt aan de hand van correlaties tussen huid-innervatie en pijn(gedrag) in proefdieren en patiënten met neuropathie. Tenslotte werd aangetoond dat er in de klinische praktijk geen aanwijzingen zijn voor verminderde gevoeligheid voor opioïden bij gemengde kankerpijn.

De bevindingen in dit proefschrift vormen een basis voor de verdere ontwikkeling van ruggenmergstimulatie bij neuropathische pijn, voor de ontwikkeling van toekomstige analgetische behandelingen specifiek gericht op de affectieve/evaluatieve component van neuropathische pijn en ten slotte voor een optimale behandelingsstrategie voor patiënten met gemengde kankerpijn.

Reference List

1. Jongen JL, Haasdijk ED, Sabel-Goedknecht H, van der Burg J, Vecht Ch J, Holstege JC. Intrathecal injection of GDNF and BDNF induces immediate early gene expression in rat spinal dorsal horn. *Experimental neurology*. 2005;194(1):255-66.
2. Zhang J, Cavanaugh DJ, Nemenov MI, Basbaum AI. The modality specific contribution of peptidergic and non-peptidergic nociceptors is manifest at the level of dorsal horn nociceptive neurons. *The Journal of physiology*. 2013;591(4):1097-110.
3. Craig AD. Pain mechanisms: labeled lines versus convergence in central processing. *Annu Rev Neurosci*. 2003;26:1-30.
4. Braz JM, Nassar MA, Wood JN, Basbaum AI. Parallel “pain” pathways arise from subpopulations of primary afferent nociceptor. *Neuron*. 2005;47(6):787-93.
5. Bechakra M, Schuttenhelm BN, Pederzani T, van Doorn PA, de Zeeuw CI, Jongen JLM. The reduction of intraepidermal P2X3 nerve fiber density correlates with behavioral hyperalgesia in a rat model of nerve injury-induced pain. *The Journal of comparative neurology*. 2017.
6. Bechakra M, Nieuwenhoff MD, van Rosmalen J, Groeneveld GJ, Scheltens-de Boer M, Sonneveld P, et al. Clinical, electrophysiological, and cutaneous innervation changes in patients with bortezomib-induced peripheral neuropathy reveal insight into mechanisms of neuropathic pain. *Molecular pain*. 2018;14:1744806918797042.
7. Jongen JL, Jaarsma D, Hossaini M, Natarajan D, Haasdijk ED, Holstege JC. Distribution of RET immunoreactivity in the rodent spinal cord and changes after nerve injury. *The Journal of comparative neurology*. 2007;500(6):1136-53.
8. Price TJ, Flores CM. Critical evaluation of the colocalization between calcitonin gene-related peptide, substance P, transient receptor potential vanilloid subfamily type 1 immunoreactivities, and isolectin B4 binding in

primary afferent neurons of the rat and mouse. The journal of pain : official journal of the American Pain Society. 2007;8(3):263-72.

9. Melzack R, Wall PD. Pain mechanisms: a new theory. Science. 1965;150(3699):971-9.

10. Melzack R, Rose G, Mc GD. Skin sensitivity to thermal stimuli. Exp Neurol. 1962;6:300-14.

11. Woolf CJ, Salter MW. Neuronal plasticity: increasing the gain in pain. Science. 2000;288(5472):1765-9.

12. Treede RD, Jensen TS, Campbell JN, Cruccu G, Dostrovsky JO, Griffin JW, et al. Neuropathic pain: redefinition and a grading system for clinical and research purposes. Neurology. 2008;70(18):1630-5.

13. Finnerup NB, Haroutounian S, Kamerman P, Baron R, Bennett DL, Bouhassira D, et al. Neuropathic pain: an updated grading system for research and clinical practice. Pain. 2016;157(8):1599-606.

14. Torrance N, Smith BH, Bennett MI, Lee AJ. The epidemiology of chronic pain of predominantly neuropathic origin. Results from a general population survey. J Pain. 2006;7(4):281-9.

15. Sorensen L, Siddall PJ, Trenell MI, Yue DK. Differences in metabolites in pain-processing brain regions in patients with diabetes and painful neuropathy. Diabetes Care. 2008;31(5):980-1.

16. Scott FT, Leedham-Green ME, Barrett-Muir WY, Hawrami K, Gallagher WJ, Johnson R, et al. A study of shingles and the development of postherpetic neuralgia in East London. J Med Virol. 2003;70 Suppl 1:S24-30.

17. Schmader KE. Epidemiology and impact on quality of life of postherpetic neuralgia and painful diabetic neuropathy. Clin J Pain. 2002;18(6):350-4.

18. van den Beuken-van Everdingen MH, de Rijke JM, Kessels AG, Schouten HC, van Kleef M, Patijn J. Prevalence of pain in patients

with cancer: a systematic review of the past 40 years. *Ann Oncol.* 2007;18(9):1437-49.

19. Jambart S, Ammache Z, Haddad F, Younes A, Hassoun A, Abdalla K, et al. Prevalence of painful diabetic peripheral neuropathy among patients with diabetes mellitus in the Middle East region. *J Int Med Res.* 2011;39(2):366-77.

20. Campbell JN, Meyer RA. Mechanisms of neuropathic pain. *Neuron.* 2006;52(1):77-92.

21. Baranauskas G, Nistri A. Sensitization of pain pathways in the spinal cord: cellular mechanisms. *Prog Neurobiol.* 1998;54(3):349-65.

22. Loeser JD, Treede RD. The Kyoto protocol of IASP Basic Pain Terminology. *Pain.* 2008;137(3):473-7.

23. Latremoliere A, Woolf CJ. Central sensitization: a generator of pain hypersensitivity by central neural plasticity. *J Pain.* 2009;10(9):895-926.

24. Li J, Simone DA, Larson AA. Windup leads to characteristics of central sensitization. *Pain.* 1999;79(1):75-82.

25. Liu X, Sandkuhler J. Characterization of long-term potentiation of C-fiber-evoked potentials in spinal dorsal horn of adult rat: essential role of NK1 and NK2 receptors. *J Neurophysiol.* 1997;78(4):1973-82.

26. Jongen JL, Pederzani T, Koekkoek SK, Shapiro J, van der Burg J, De Zeeuw CI, et al. Autofluorescent flavoprotein imaging of spinal nociceptive activity. *J Neurosci.* 2010;30(11):4081-7.

27. Bennett MI, Rayment C, Hjermstad M, Aass N, Caraceni A, Kaasa S. Prevalence and aetiology of neuropathic pain in cancer patients: a systematic review. *Pain.* 2012;153(2):359-65.

28. Ma C, LaMotte RH. Multiple sites for generation of ectopic spontaneous activity in neurons of the chronically compressed dorsal root ganglion. *J Neurosci.* 2007;27(51):14059-68.

29. D'Mello R, Dickenson AH. Spinal cord mechanisms of pain. *Br J Anaesth*. 2008;101(1):8-16.
30. Melzack R, Wall PD. On the nature of cutaneous sensory mechanisms. *Brain*. 1962;85:331-56.
31. Jongen JL, Smits H, Pederzani T, Bechakra M, Hossaini M, Koekkoek SK, et al. Spinal autofluorescent flavoprotein imaging in a rat model of nerve injury-induced pain and the effect of spinal cord stimulation. *PLoS One*. 2014;9(10):e109029.
32. Besson JM, Oliveras JL, Chaouch A, Rivot JP. Role of the raphe nuclei in stimulation producing analgesia. *Adv Exp Med Biol*. 1981;133:153-76.
33. Bennett CL, Shirk AJ, Huynh HM, Street VA, Nelis E, Van Maldergem L, et al. SIMPLE mutation in demyelinating neuropathy and distribution in sciatic nerve. *Ann Neurol*. 2004;55(5):713-20.
34. Seltzer Z, Dubner R, Shir Y. A novel behavioral model of neuropathic pain disorders produced in rats by partial sciatic nerve injury. *Pain*. 1990;43(2):205-18.
35. Horie Y, Decosterd L, Suzuki R, Ishikawa Y, Wada K. Emission wave-length tuning by mechanical stressing of GaAs/Ge/Si microbeams. *Opt Express*. 2011;19(17):15732-8.
36. Kim SH, Chung JM. An experimental model for peripheral neuropathy produced by segmental spinal nerve ligation in the rat. *Pain*. 1992;50(3):355-63.
37. Bennett GJ, Xie YK. A peripheral mononeuropathy in rat that produces disorders of pain sensation like those seen in man. *Pain*. 1988;33(1):87-107.
38. Langford DJ, Bailey AL, Chanda ML, Clarke SE, Drummond TE, Echols S, et al. Coding of facial expressions of pain in the laboratory mouse. *Nat Methods*. 2010;7(6):447-9.
39. Roytta M, Raine CS. Taxol-induced neuropathy: chronic effects of local injection. *J Neurocytol*. 1986;15(4):483-96.

40. Cavaletti G, Gilardini A, Canta A, Rigamonti L, Rodriguez-Mendez V, Ceresa C, et al. Bortezomib-induced peripheral neurotoxicity: a neurophysiological and pathological study in the rat. *Exp Neurol*. 2007;204(1):317-25.
41. Persohn E, Canta A, Schoepfer S, Traebert M, Mueller L, Gilardini A, et al. Morphological and morphometric analysis of paclitaxel and docetaxel-induced peripheral neuropathy in rats. *Eur J Cancer*. 2005;41(10):1460-6.
42. Polomano RC, Mannes AJ, Clark US, Bennett GJ. A painful peripheral neuropathy in the rat produced by the chemotherapeutic drug, paclitaxel. *Pain*. 2001;94(3):293-304.
43. Flatters SJ, Bennett GJ. Studies of peripheral sensory nerves in paclitaxel-induced painful peripheral neuropathy: evidence for mitochondrial dysfunction. *Pain*. 2006;122(3):245-57.
44. Bechakra M, Schuttenhelm BN, Pederzani T, van Doorn PA, de Zeeuw CI, Jongen JLM. The reduction of intraepidermal P2X3 nerve fiber density correlates with behavioral hyperalgesia in a rat model of nerve injury-induced pain. *J Comp Neurol*. 2017;525(17):3757-68.
45. Themistocleous AC, Ramirez JD, Serra J, Bennett DL. The clinical approach to small fibre neuropathy and painful channelopathy. *Pract Neurol*. 2014;14(6):368-79.
46. Haanpaa M, Attal N, Backonja M, Baron R, Bennett M, Bouhassira D, et al. NeuPSIG guidelines on neuropathic pain assessment. *Pain*. 2011;152(1):14-27.
47. Walsh J, Rabey MI, Hall TM. Agreement and correlation between the self-report Leeds assessment of neuropathic symptoms and signs and Douleur Neuropathique 4 Questions neuropathic pain screening tools in subjects with low back-related leg pain. *J Manipulative Physiol Ther*. 2012;35(3):196-202.

48. Freynhagen R, Baron R, Gockel U, Tolle TR. painDETECT: a new screening questionnaire to identify neuropathic components in patients with back pain. *Curr Med Res Opin.* 2006;22(10):1911-20.
49. Bennett M. The LANSS Pain Scale: the Leeds assessment of neuropathic symptoms and signs. *Pain.* 2001;92(1-2):147-57.
50. Mathieson S, Maher CG, Terwee CB, Folly de Campos T, Lin CW. Neuropathic pain screening questionnaires have limited measurement properties. A systematic review. *J Clin Epidemiol.* 2015;68(8):957-66.
51. Staud R, Weyl EE, Riley JL, 3rd, Fillingim RB. Slow temporal summation of pain for assessment of central pain sensitivity and clinical pain of fibromyalgia patients. *PLoS One.* 2014;9(2):e89086.
52. Verdugo RJ, Ochoa JL. Use and misuse of conventional electrodiagnosis, quantitative sensory testing, thermography, and nerve blocks in the evaluation of painful neuropathic syndromes. *Muscle Nerve.* 1993;16(10):1056-62.
53. Dyck PJ, Dyck PJ, Kennedy WR, Kesserwani H, Melanson M, Ochoa J, et al. Limitations of quantitative sensory testing when patients are biased toward a bad outcome. *Neurology.* 1998;50(5):1213.
54. Maier C, Baron R, Tolle TR, Binder A, Birbaumer N, Birklein F, et al. Quantitative sensory testing in the German Research Network on Neuropathic Pain (DFNS): somatosensory abnormalities in 1236 patients with different neuropathic pain syndromes. *Pain.* 2010;150(3):439-50.
55. Demant DT, Lund K, Vollert J, Maier C, Segerdahl M, Finnerup NB, et al. The effect of oxcarbazepine in peripheral neuropathic pain depends on pain phenotype: a randomised, double-blind, placebo-controlled phenotype-stratified study. *Pain.* 2014;155(11):2263-73.
56. Savage SR, Kirsh KL, Passik SD. Challenges in using opioids to treat pain in persons with substance use disorders. *Addict Sci Clin Pract.* 2008;4(2):4-25.

57. Stander S, Weisshaar E, Mettang T, Szepietowski JC, Carstens E, Ikkoma A, et al. Clinical classification of itch: a position paper of the International Forum for the Study of Itch. *Acta Derm Venereol.* 2007;87(4):291-4.
58. Wahlgren CF. Measurement of itch. *Semin Dermatol.* 1995;14(4):277-84.
59. Cancer pain relief and palliative care. Report of a WHO Expert Committee. *World Health Organ Tech Rep Ser.* 1990;804:1-75.
60. Finnerup NB, Attal N, Haroutounian S, McNicol E, Baron R, Dworkin RH, et al. Pharmacotherapy for neuropathic pain in adults: a systematic review and meta-analysis. *Lancet Neurol.* 2015;14(2):162-73.
61. Colloca L, Ludman T, Bouhassira D, Baron R, Dickenson AH, Yarnitsky D, et al. Neuropathic pain. *Nat Rev Dis Primers.* 2017;3:17002.
62. Kemler MA, De Vet HC, Barendse GA, Van Den Wildenberg FA, Van Kleef M. The effect of spinal cord stimulation in patients with chronic reflex sympathetic dystrophy: two years' follow-up of the randomized controlled trial. *Ann Neurol.* 2004;55(1):13-8.
63. Kemler MA, Barendse GA, van Kleef M, de Vet HC, Rijks CP, Furnee CA, et al. Spinal cord stimulation in patients with chronic reflex sympathetic dystrophy. *N Engl J Med.* 2000;343(9):618-24.
64. Kumar K, Taylor RS, Jacques L, Eldabe S, Meglio M, Molet J, et al. Spinal cord stimulation versus conventional medical management for neuropathic pain: a multicentre randomised controlled trial in patients with failed back surgery syndrome. *Pain.* 2007;132(1-2):179-88.
65. Kumar K, Taylor RS, Jacques L, Eldabe S, Meglio M, Molet J, et al. The effects of spinal cord stimulation in neuropathic pain are sustained: a 24-month follow-up of the prospective randomized controlled multicenter trial of the effectiveness of spinal cord stimulation. *Neurosurgery.* 2008;63(4):762-70; discussion 70.
66. Manca A, Kumar K, Taylor RS, Jacques L, Eldabe S, Meglio M, et al. Quality of life, resource consumption and costs of spinal cord stimula-

tion versus conventional medical management in neuropathic pain patients with failed back surgery syndrome (PROCESS trial). *Eur J Pain*. 2008;12(8):1047-58.

67. Slangen R, Schaper NC, Faber CG, Joosten EA, Dirksen CD, van Dongen RT, et al. Spinal cord stimulation and pain relief in painful diabetic peripheral neuropathy: a prospective two-center randomized controlled trial. *Diabetes Care*. 2014;37(11):3016-24.

68. Slangen R, Pluijms WA, Faber CG, Dirksen CD, Kessels AG, van Kleef M. Sustained effect of spinal cord stimulation on pain and quality of life in painful diabetic peripheral neuropathy. *Br J Anaesth*. 2013;111(6):1030-1.

69. Tesfaye S, Watt J, Benbow SJ, Pang KA, Miles J, MacFarlane IA. Electrical spinal-cord stimulation for painful diabetic peripheral neuropathy. *Lancet*. 1996;348(9043):1698-701.

70. Moayedi M, Davis KD. Theories of pain: from specificity to gate control. *J Neurophysiol*. 2013;109(1):5-12.

71. Bushnell MC, Ceko M, Low LA. Cognitive and emotional control of pain and its disruption in chronic pain. *Nat Rev Neurosci*. 2013;14(7):502-11.

72. Jongen JL, Holstege JC. Propagation of spinal nociceptive activity in the spatial and temporal domains. *Neuroscientist*. 2012;18(1):8-14.

73. Wang F, Belanger E, Paquet ME, Cote DC, De Koninck Y. Probing pain pathways with light. *Neuroscience*. 2016;338:248-71.

74. Liu Z, Wang F, Fischer G, Hogan QH, Yu H. Peripheral nerve injury induces loss of nociceptive neuron-specific Galphai-interacting protein in neuropathic pain rat. *Mol Pain*. 2016;12.

75. Gold MS, Gebhart GF. Nociceptor sensitization in pain pathogenesis. *Nat Med*. 2010;16(11):1248-57.

76. Auvray M, Myin E, Spence C. The sensory-discriminative and affective-motivational aspects of pain. *Neurosci Biobehav Rev.* 2010;34(2):214-23.
77. Melzack R, Eisenberg H. Skin sensory afterglows. *Science.* 1968;159(3813):445-7.
78. Albe-Fessard D, Berkley KJ, Kruger L, Ralston HJ, 3rd, Willis WD, Jr. Diencephalic mechanisms of pain sensation. *Brain Res.* 1985;356(3):217-96.
79. Klepstad P, Rakvag TT, Kaasa S, Holthe M, Dale O, Borchgrevink PC, et al. The 118 A > G polymorphism in the human mu-opioid receptor gene may increase morphine requirements in patients with pain caused by malignant disease. *Acta Anaesthesiol Scand.* 2004;48(10):1232-9.
80. Campa D, Gioia A, Tomei A, Poli P, Barale R. Association of ABCB1/MDR1 and OPRM1 gene polymorphisms with morphine pain relief. *Clin Pharmacol Ther.* 2008;83(4):559-66.
81. Mace E, Montaldo G, Cohen I, Baulac M, Fink M, Tanter M. Functional ultrasound imaging of the brain. *Nat Methods.* 2011;8(8):662-4.
82. Mosher V, Swain M, Pang J, Kaplan G, Sharkey K, MacQueen G, et al. Primary biliary cholangitis patients exhibit MRI changes in structure and function of interoceptive brain regions. *PLoS One.* 2019;14(2):e0211906.
83. Osmanski BF, Pezet S, Ricobaraza A, Lenkei Z, Tanter M. Functional ultrasound imaging of intrinsic connectivity in the living rat brain with high spatiotemporal resolution. *Nat Commun.* 2014;5:5023.
84. Kulkarni B, Bentley DE, Elliott R, Youell P, Watson A, Derbyshire SW, et al. Attention to pain localization and unpleasantness discriminates the functions of the medial and lateral pain systems. *Eur J Neurosci.* 2005;21(11):3133-42.
85. McCracken LM, Vowles KE. Acceptance and commitment therapy and mindfulness for chronic pain: model, process, and progress. *Am Psychol.* 2014;69(2):178-87.

86. Thomas EM, Weiss SM. Nonpharmacological interventions with chronic cancer pain in adults. *Cancer Control*. 2000;7(2):157-64.
87. Strouse TB, Bursch B. Psychological Treatment. *Hematol Oncol Clin North Am*. 2018;32(3):483-91.

PhD portfolio

Information

Student' name: Malik Bechakra
Degrees: BSc. in Life Science and
MSc in Neuroscience and Neuropsychopharmacology
University: Erasmus University Rotterdam
Faculty: Neuroscience
Research school: Mol Med
Supervisor: Dr Joost Jongen

General courses

Integrity in Science
Biomedical English writing and communication
Presenting Skills
NIHES Regression analysis
Mol Med SNP and Human Diseases
Mol Med Microscopic Image Analysis
Mol Med Biomedical Research techniques
Mol Med Cancer Institute Research Day
Mol Med Workshop on Photoshop and Illustrator
Mol Med Course on R
OIC Functional Imaging and Super Resolution Microscopy
ONWAR Neuropsychopharmacology
ONWAR Clinical Neuroscience

Attended conferences

2013 SFN Meeting (San Diego, USA)
2014 World Congress of Pain (Buenos Aires, Argentina)
2015 SFN Meeting (Chicago, USA)
2016 World Congress of Pain (Yokohama, Japan)

List of publications

Jongen JL, Smits H, Pederzani T, **Bechakra M**, Hossaini M, Koekkoek SK, Huygen FJ, De Zeeuw CI, Holstege JC, Joosten EA. Spinal autofluorescent flavoprotein imaging in a rat model of nerve injury-induced pain and the effect of spinal cord stimulation. *PLoS One*. 2014 Oct 3;9(10):e109029.

Bechakra M, Schüttenhelm BN, Pederzani T, van Doorn PA, de Zeeuw CI, Jongen JLM. The reduction of intraepidermal P2X3 nerve fiber density correlates with behavioral hyperalgesia in a rat model of nerve injury-induced pain. *J Comp Neurol*. 2017 Dec 1;525(17):3757-3768.

Bechakra M, Nieuwenhoff MD, van Rosmalen J, Groeneveld GJ, Scheltens-de Boer M, Sonneveld P, van Doorn PA, de Zeeuw CI, Jongen JL. Clinical, electrophysiological, and cutaneous innervation changes in patients with bortezomib-induced peripheral neuropathy reveal insight into mechanisms of neuropathic pain. *Mol Pain*. 2018 Jan-Dec;14:1744806918797042.

Wijntjes J, **Bechakra M**, Schreurs MWJ, Jongen JLM, Koppenaal A, Titulaer MJ. Pruritus in anti-DPPX encephalitis. *Neurol Neuroimmunol Neuroinflamm*. 2018 Apr 2;5(3):e455.

Bechakra M, Moerdijk F, van Rosmalen J, Koch BCP, van der Rijt CCD, Sillevius Smitt PAE, Jongen JLM. Opioid responsiveness of nociceptive versus mixed pain in clinical cancer patients. *Eur J Cancer*. 2018 Dec;105:79-87.

Bechakra M, Nieuwenhoff MD, Rosmalen JV, Jan Groeneveld G, J P M Huygen F, Zeeuw CI, Doorn PAV, Jongen JLM. Pain-related changes in cutaneous innervation of patients suffering from bortezomib-induced, diabetic or chronic idiopathic axonal polyneuropathy. *Brain Res*. 2020 Mar 1;1730:146621.

Acknowledgements

C'est FINI! I am grateful for all the opportunities and support I've been given: I would like to thank all the people who contributed to the accomplishment of my thesis.

I would first like to thank my co-promotor, Dr. J. L. M. Jongen. Thank you for all these years of research, discussion and collaboration. It has been a great experience to work in the lab. Thank you for your constant motivation and encouragement. It has been a privilege to have you as a mentor. I would not have come to this point in my career without your help.

I would like to thank my promotors, Prof. dr. P. A. van Doorn and Prof. dr. C. I. de Zeeuw for their support. Thank you for being available and encouraging.

I would like also to thank all members of my thesis committee: Prof dr. C. G. Faber, Prof.dr. F. J. P. M. Huygen, Prof.dr. P. Sonneveld, Dr. G. J. Groeneveld, Dr. J. C. Holstege, Dr. D. Jaarsma. I appreciate your participation and your valuable comments on this thesis.

Elize and Erika, thank you for your help and for all you taught me during all these years. Elise, thank you for guiding me through the graduation procedure..

I want to thank all colleagues and friends from all those years at the Erasmus MC whether still around or moved on: (in alphabetic order) Aaron, Abigail, Anna, Anne, Annette, Arthur, Bin, Catarina, Christos, Daphne, Dorothee, Edwin, Erik, Farnaz, Femke, Gao, Gerard, Geeske, Georgios, Gosia, Guy, Hana, Jessica, Jolet, Jos, Kees, Laura, Laurens, Mafer, Malou, Mani, Marcel, Mario, Mariska, Marlou, Marteen, Martijn, Martina, Mattijs, Melika, Milly, Monica, Myrthe, Patrick, Petra, Sasa, Shoista, Thomas, Marten, Martijn, Linda, Robert, Rosa, Sara, Sjoert, Tom, Vera, Yarmo, Yvonne, and anyone I may have forgotten.

I want to express my special thanks to my paranymphe to be beside me during my PhD defense: Sandra, Danke für deine Freundschaft and for reminding me to sing "Pam pam paa Lampam" and to always drink dark beers! François, ma poule, merci pour ton humour noir à la française qui fait des fois piquer des yeux et pleurer Luc!

Merci à toute ma famille et ma tribu pour votre soutien indéniabie pendant les moments agréables mais aussi difficiles: Bernard, Christelle, David, Jean, Michael, Nicolas, Sandrine, Sebastien. Ça fait plaisir!

I would like also to thank my friends from Rotterdam for reminding me to stop and have a good time every once in a while. Allison, Amelie, Anne-Marie, Erik, Laura, Olivia, Otto, Ricky, Sadaf, Sara, Thomas, Tina, thank you all for the entertaining parties, pub crawls, festivals and dinners before the current cheerless time due to Covid-19. I hope this time will come back very soon!

Last but not least, I would like to thank especially Mylene, who has always supported me during all this years and to whom this thesis is dedicated to. Without you, I would have never made it this far.

To all the people that I mentioned, and to many more that I did not, I am immensely thankful: to properly acknowledge you all much more needs to be said. It will be said - privately.

Curriculum Vitae

Malik Bechakra was born on January 18th 1985 in Metz, France where he grew up. After secondary school, he studied medicine at the Faculty of Medicine in Nancy. He obtained his Master degree in Neuroscience at the University Segalen in Bordeaux. In 2010, he moved in Rotterdam and was involved in research projects to develop biomarkers of neuropathic pain. In 2014, he enrolled in the PhD program at the Erasmus MC under the supervision of Dr Joost Jongen. The project, focusing on investigating the mechanism of neuropathic and cancer pain, as resulted in the current thesis.

